New roles for Hox and Wnt in Cell Migration

By

Matthew Paul Josephson

Submitted to the graduate degree program in Molecular Biosciences and the Graduate Faculty of the University of Kansas in partial fulfillment of the requirements for the degree of Doctor of Philosophy.

_____
Chairperson Dr. Erik Lundquist

_____
Dr. Brian Ackley

_____
Dr. Stuart Macdonald

_____
Dr. Rob Ward

_____
Dr. Eli Michaelis

Date Defended: 04/29/2016

The Dissertation Committee for Matthew Paul Josephson
certifies that this is the approved version of the following dissertation:

New roles for Hox and Wnt in Cell Migration

_____
Chairperson Dr. Erik Lundquist

Date approved: 04/29/2016

Abstract

Neuron migration is a critical process during central nervous system development. In the dissertation below I report new roles for established genes such as Wnt and Hox, and describe roles for several new genes in neuron migration.

To study migrating neurons I use the model organism nematode worm *Caenorhabditis elegans.* With only 302 neurons, *C. elegans* is an excellent model to examine migration of individual neurons. The QR and QL neuroblasts are two bilaterally symmetric neural progenitor cells born in the posterior region of the worm. Although born in the same area, these cells undergo opposite directions of migration. QR migrates anteriorly, and QL migrates posteriorly. In QL, detection of extracellular EGL-20/Wnt results in trasncription of *mab-5/Antennapedia/Hox* through canonical Wnt signalling. MAB-5 is a posterior migration determinant of the QL lineage, and expression of *mab-5* is necessary and sufficient for posterior migration. *lin-39/Sex combs reduced/Hox* is activated through unknown mechanisms in QR and promotes anterior migration of that lineage. *lin-39* and *mab-5* are well studied genes than have been implicated in cell-autonomous control of Q migrations.

After an introduction to Q cell migration in chapter I, chapter II describes new roles for Hox gene in Q descendant migration that may change the way we think about how Hox genes work. I show that *lin-39, mab-5* and a third Hox gene *egl-5/Abdominal-B/Hox* act in parallel to promote migration of the Q cells, and in their absence almost no migration occurs. This in contrast to the typical opposing roles of Hox genes whereby *lin-39* promotes anterior migration of QR lineage, and *mab-5* promotes posterior migration of the QL lineage. I also find that *mab-5,* and *egl-5* are able to promote Q migration through their expression in posterior body wall muscles, a non-autonomous role in migration. Again this shifts how Hox genes should be

considered, as they are often thought to act solely as autonomous drivers of cell fate and to have opposing roles in differentiation.

As a Hox factor *mab-5* regulates many genes, but few *mab-5* targets have been identified. Results in this dissertation show that *mab-5* may regulate the secreted *F-spondin* homolog *spon-1* to control migration. I demonstrate that the *spon-1* promoter can be driven by MAB-5 in the body wall muscles, and that *spon-1* is important in Q cell direction and extent of migration.

Chapter III presents new roles for *egl-20/Wnt* and *mab-5/Hox* in inhibiting anterior migration. Detailed analysis of the timing of Q descendant migration reveals that *egl-20/Wnt* can act in two steps to inhibit anterior migration and promote posterior migration of the QL linage. (i) Through an acute non-canonical Wnt mechanism EGL-20 inhibits anterior migration, and (ii) later, through canonical Wnt pathway activates transcription of *mab-5* which can further inhibit anterior migration and promote further migration of the QL lineage.

The first characterization of the *C. elegans Neurofibromatosis Type II(NF2)/Merlin* homolog *nfm-1* is detailed in chapter IV. Previously in the Lundquist lab an unbiased forward genetic screen identified an allele of *nfm-1* is required for Q descendant migration. I show that *nfm-1* promotes migration of QR and QL lineages through non-autonomous mechanisms, and can act genetically, possibly in the same pathway with the guidance cue *slt-1/Slit,* to promote complete migration of the QR and QL lineages.

The results contained below use new techniques to study established and novel genes in nervous system development, highlighting the intricacies of developmental genetics. Many genes play multiple roles in development, demonstrated here by new roles for Hox and Wnt in Q cell migration.

Acknowledgments

Although this dissertation bears my name, it would not be possible without the help of many people. Here it is my pleasure to acknowledge them. Firstly, the support of my family has been excellent. Being far from home is stressful, and my family has provided much needed escapes. My parents Ron and Jeanne Josephson have been great leaders to me, especially in times of trouble, and to help me return home. They have always supported me in my meandering career path, never pushing me in any direction, offering only guidance along the way. My aunt Mary Ann Josephson has been of great assistance as well, by being unwaveringly available, and a welcome host to me on many holidays.

Although we never met, Madison and Lila Self have changed my life. Their endowment began the Madison and Lila Self Graduate Fellowship, which provided an excellent opportunity to pursue my doctoral studies at the University of Kansas. Additionally the opportunities, training, and friendship the fellowship provided were unparalleled in professional advice and comradery. If not for the enormous generosity of the Self's, I would not have attended The University of Kansas, and would not have been trained by my exceptional mentor Dr. Erik Lundquist.

Completion of a doctoral degree requires a great deal of commitment, perseverance through adversity, and in my opinion, more importantly an excellent mentor. Dr. Erik Lundquist is an amazing mentor who guided me from knowing very little about science to where I am today. I am doubtful that I would have found a better mentor anywhere in the country. He was able to turn me into a true scientist and knew exactly when I needed guidance (a lot in the beginning), and when I was able to function independently. I sincerely regret that I was unable to secure a mentorship award for Erik during my tenure at KU, and hope that he will soon be

rewarded for his mentorship. Not only this, but I consider Erik a friend who I can come to with any manner of question, and his door was always open, not once can I remember a moment when he was not available to help me with a problem in science or otherwise.

Erik, and all the members of my committee have been great mentors during my time at KU. In mechanisms of development, Dr. Rob Ward would at least pretend like my theories were reasonable before offering a more parsimonious explanation. As I have prepared for a shift to a more genomics-based career, Dr. Stuart Macdonald has provided useful guidance. He also taught me a valuable lesson in punctuality during grant writing class. He gave a zero for one assignment that I turned in 10 minutes late, but I still ended up passing. In many situations I turned to Dr. Brian Ackley for advice, and much of his advised experiments are present in this dissertation. His willingness to spend hours talking about science over beer has taught me much, and I always left these conversations feeling smarter. Dr. Eli Michaelis provided perspective on my project from his background in neuroscience, and for that I am grateful.

Although not on my committee, my collaborator Dr. Guangshuo Ou played a pivotal role in my doctoral education. He graciously hosted me on a research visit to his lab at Tsinghua University in Beijing to learn how to live image neuron migration. In addition to the valuable data I collected I also gained an unmeasurable scientific and cultural experience that I deeply cherish. Dr. Ou and all the lab members were incredible hosts during my six weeks in Beijing, and I will not forget their generosity.

Not only is a good mentor and committee instrumental in the PhD process, but a good environment is also required. The Lundquist lab and my colleagues were superb. Initially I need to thank Dr. Rafael Demarco for convincing me to rotate in the Lundquist lab, where I would thrive. In the lab I was guided initially by Dr. Jamie Alan and Dr. Dyan Morgan. The number of

times I annoyed them with simple questions about simple *C. elegans* questions is beyond count. Dr. Lakshmi Sundararajan was able to guide me through my formative years as a researcher and assisted in many genetic questions which were easy for her, but difficult for me. Future Dr. Mahekta Gujar has been a great colleague, and ear to listen to my woes, and I am infinitely glad she has been there with me. Without the patience and organizational skills of Eric Struckhoff I would have surely misplaced a critical strain or clone, and I am very thankful for his insights on many issues. The Ackley lab has also been of great assistance, between constructive criticisms at lab meetings, to being true friends, they have helped immensely along the way. In particular Dr. Raymond Caylor has become a great friend and guided me through the doctoral process.

I also would like to thank the KU Swim Club, and KU Recreation Services for providing an environment to escape the stress of the PhD grind. Through this I have made lasting friendships, in particular Jared Auten, Rachel Schmidt, and Dalton Munk have been great comrades who have shown me much of Kansas I would have never experienced.

Table of Contents

List of Figures

List of Tables

Chapter I:

Introduction

The human brain is arguably the most complex organ on the planet, with around 86 billion neurons connecting with each other to create the networks that allow for higher thought and consciousness (Azevedo, Carvalho et al. 2009). Many of these neurons must migrate on specific paths in order to make precise connections with other neurons. Neurons born in proliferative zones migrate radially outward to populate what will become the cortical plate (Berry and Rogers 1965, Rakic 1972). Interneurons have more complex migratory routes, and their destination is specified by expression of certain transcription factors, which regulate how they respond to specific extracellular cues (reviewed by Guo and Anton (2014)). Here we use genetic analysis to reveal new ways of thinking about transcription factors, extracellular cues, and the cellular responses they may invoke to control directed cell migration.

To finely examine how cells are able to undergo complex migrations is not currently possible in humans, and therefore must be studied in a model system. In particular, the nematode *Caenorhabditis elegans* is an attractive system to study migration *in vivo. C. elegans* is an established genetic organism which has been used to study many aspects of development. The transparent nature, completely characterized cell lineage, and well-studied genome are several benefits of using the nematode. Specifically, the *C. elegans* Q neuroblasts provide a unique opportunity to precisely examine the gene networks that regulate direction, timing, and ability of cells to migrate. QR and QL are bilaterally symmetric neural progenitor cells born in the posterior region of the *C. elegans* L1 larva (Sulston and Horvitz 1977). After being born in the same region of the animal QR and QL migrate in opposite directions, QR to the anterior, and QL to the posterior. QR migrates a short distance anteriorly on to the seam cell V4. Once on V4, QR divides and its daughters migrate long distances anteriorly, undergoing two more rounds of cell division and cell death to give rise to three neurons, AQR, AVM, and SDQR (Honigberg and

Kenyon 2000). Of the QR descendants AQR migrates the furthest, with a final position near the posterior pharyngeal bulb. QL undergoes an identical pattern of cell divisions and cell death, giving rise to PQR, PVM, and SDQL (Sulston and Horvitz 1977, White, Southgate et al. 1986). Of the QL daughters, PQR migrates the furthest posterior, ending migration near the anus and the phasmids.

One reason the Q neuroblasts are interesting, is their opposing directions of migration. They are born into a similar extracellular environment, but respond differently to that environment and migrate in opposite directions along the anteroposterior axis, the QR lineage migrates anteriorly, and QL posteriorly. This directed migration has been well studied, and the extracellular EGL-20/Wnt ligand is known to be required for posterior migration of the QL lineage. Wnts are established guidance molecules that can affect migration in various ways. In the canonical Wnt pathway, Wnt is detected by a Frizzled receptor, causing a signaling cascade that stabilizes the transcriptional co-factor β-catenin, resulting in transcription of target genes (Smalley and Dale 1999). Many non-canonical Wnt pathways have been discovered in various aspects of development, highlighting the importance of this molecule (Korswagen 2002). In Q neuroblast migration, QL detects the posteriorly derived EGL-20/Wnt ligand, which through the canonical Wnt pathway upregulates the Hox transcription factor *mab-5/Hox* (Kenyon 1986, Salser and Kenyon 1992, Harris, Honigberg et al. 1996, Maloof, Whangbo et al. 1999, Whangbo and Kenyon 1999, Korswagen, Herman et al. 2000, Ji, Middelkoop et al. 2013). In QL, expression of *mab-5/Hox* destines the QL lineage to migrate posteriorly (Whangbo and Kenyon 1999). Interestingly, QR does not appear as sensitive as QL to extracellular EGL-20/Wnt, and does not express *mab-5/Hox* (Whangbo and Kenyon 1999). *mab-5* mutants have anteriorly misdirected QL descendants, and ectopic expression of *mab-5* in QR leads to posterior migration

of that lineage, demonstrating that *mab-5* is necessary and sufficient for posterior Q neuroblast migration (Maloof, Whangbo et al. 1999, Whangbo and Kenyon 1999). Further studies have found that the role of MAB-5 in direction of migration is a cell-autonomous process (Shen, Zhang et al. 2014, Josephson, Chai et al. 2016). Despite much work with MAB-5, very few genes have been implicated downstream of MAB-5 in cell migration.

In addition to *mab-5/Hox,* two other *C. elegans* Hox genes are known to regulate Q descendant migration, *lin-39/Deformed,* and *egl-5/Abdominal-B* (Desai and Horvitz 1989, Chisholm 1991, Maloof, Whangbo et al. 1999, Gleason, Korswagen et al. 2002). *egl-5* has not been well studied, but is reported as having weak QL defects, and no reports have seen *egl-5* expression in Q cells, suggesting a non-autonomous role, but this has not been characterized (Desai and Horvitz 1989, Chisholm 1991, Ferreira, Zhang et al. 1999). *lin-39* is known to be important in cell-autonomously promoting the anterior migration of the Q lineage (Clark, Chisholm et al. 1993, Wang, Muller-Immergluck et al. 1993). Unlike *mab-5*, a positive target of *lin-39* for Q cell migration has been identified; the transmembrane gene *mig-13* is upregulated in QR lineage in response to *lin-39* (Wang, Zhou et al. 2013). Although initial reports demonstrated *mig-13* acted non-autonomously, recent studies have shown *mig-13* promotes anterior migration cell-autonomously (Yang, Sym et al. 2005, Wang, Zhou et al. 2013). It is unclear what activates expression of *egl-5* and *lin-39,* but for *lin-39* it does not appear to be a canonical Wnt signaling cascade (Yang, Sym et al. 2005, Middelkoop and Korswagen 2014). *lin-39, mab-5,* and *egl-5* resemble an abbreviated Hox cluster, in that they are present on the same chromosome, and their position on the chromosome relates to their region of expression.

In this dissertation I begin by describing a new role for Hox genes in cell migration. I show the three *Hox* genes *lin-39, mab-5,* and *egl-5* act in parallel to promote migration. Demonstrated most notably by the *lin-39 mab-5 egl-5* triple mutant, where very little if any Q descendant migration occurs. This is quite unusual for *Hox* genes, as typically they act in opposing roles. For example, within the Q cells, LIN-39 promotes anterior migration, and MAB-5 directs posterior migration in a cell autonomous manner (Clark, Chisholm et al. 1993, Wang, Muller-Immergluck et al. 1993, Shen, Zhang et al. 2014, Josephson, Chai et al. 2016). I further characterize the parallel role as occurring non-autonomously through expression in muscle for *mab-5, egl-5,* and likely *lin-39*. I postulate that that these posterior *Hox* genes have dual roles in migration. They can pattern the posterior region through expression of secreted and transmemebrane genes, to create an environment that allows for Q migration, a cell non-autonomous role. Secondly, the *Hox* genes *lin-39* and *mab-5* can regulate the response to that environment through their expression within QR and QL, respectively, a cell-autonomous role.

A whole organism RNA-sequencing experiment designed to find targets of MAB-5 in posterior Q cell migration identified *spon-1* as being upregulated by *mab-5* (Tamayo, Gujar et al. 2013). The vertebrate homolog of *spon-1*, *F-spondin* encodes a secreted cell adhesion molecule, important in many aspects of the nervous system (Woo, Berry et al. 2008). In vertebrate development, F-spondin is secreted from the floor plate, and provides important guidance cues to developing axons (Klar, Baldassare et al. 1992, Ruiz i Altaba, Cox et al. 1993, Zisman, Marom et al. 2007). *F-spondin* is also required for neuronal survival, and overexpression of *F-spondin* in Alzheimer's disease model mice brains can delay the onset of disease symptoms (Peterziel, Sackmann et al. 2011, Hafez, Huang et al. 2012). Here we describe *spon-1* and it's relationship to MAB-5/Hox in cell migration. We show *spon-1* is required in the muscle cells for proper

direction, and extent of Q descendant migration. We present several lines of evidence that suggest MAB-5 can positively regulate the *spon-1* promoter, likely increasing the amount of *spon-1* and that this regulation is important for cell migration.

MAB-5/Hox and Wnts are clearly important in determining posterior migration of the QL lineage, but also are important in QR anterior migration (this report and (Mentink, Middelkoop et al. 2014)). To further examine how EGL-20 and MAB-5 regulate posterior migration of QL lineage, but do not induce posterior migration of QR descendants I detailed the early migrations of QR.a/p and QL.a/p in *mab-5* and *egl-20* mutants. When QR and QL divide they are still in close proximity. After division their descendants begin long-range migration in opposite directions. I found that QR.a/p began migration immediately after QR division, but QL.a/p experience about a one-hour delay before beginning migration. In *egl-20/Wnt* mutants QL.a/p migrate anteriorly immediately after QL division similar to QR., demonstrating EGL-20 inhibits anterior migration. In QL, EGL-20 induces posterior migration by stimulating *mab-5/Hox* expression in a *bar-1/β-catenin* dependent manner(Kenyon 1986, Harris, Honigberg et al. 1996, Whangbo and Kenyon 1999, Korswagen, Herman et al. 2000). QL.a/p in *mab-5/Hox* and *bar-1/β-catenin* mutants also migrate anteriorly as expected, but this migration is delayed similar to wild-type QL.a/p. This demonstrates a dual role of posterior Q neuroblast migration by EGL-20/Wnt. EGL-20/Wnt acutely inhibits anterior migration of QL.a/p in a non-canonical *β-catenin* independent manner, and later promotes posterior migration through canonical *β-catenin* dependent transcription of the posterior migration determinant, *mab-5/Hox*. The *C. elegans* genome encodes several Wnt homologs that can act in parallel for Q descendant migration (Zinovyeva, Yamamoto et al. 2008). The *C. elegans* Wnt homologs include *egl-20, cwn-1, cwn-2, lin-44,* and *mom-2*. I also find redundancy for Wnts in migration, and find an interesting role

of *lin-44/Wnt* in inhibiting posterior migration of both QR and QL descendants. This highlights the complexity of Wnts in development, EGL-20 inhibits anterior migration, and LIN-44 can inhibit posterior migration.

To elucidate new genes in Q cell migration a forward genetic screen to identify mutations that caused defects in Q descendant migration was performed previously. This screen identified an allele of *nfm-1/NF2/Merlin,* which primarily has defects in anterior migration of the QR descendant, AQR. In vertebrates *NF2* gene acts as a classic tumor suppressor, and can regulate many pathways. Mutations in *NF2* lead to the disease Neurofibromatosis type II (NF II), which causes benign tumors in the glial tissue of affected patients. NF2/Merlin has been examined in many organisms, but *nfm-1* has not been studied in *C. elegans*. Here I report the first detailed characterization of *nfm-1,* and demonstrate that it is required non-autonomously to promote anterior migration of AQR. I tried to determine if *nfm-1* interacts with other pathways as it does in vertebrates, and found a genetic interaction between *nfm-1* and a secreted guidance cue *slt-1/Slit*, that will be investigated in future studies.

Overall the results contained herein demonstrate new roles for Hox genes and Wnt molecules that are conserved from *C. elegans* to humans. We find several genes (MAB-5, EGL-5, SPON-1, NFM-1) that control migration in a non-autonomous fashion, likely by patterning the environment to provide appropriate substrates and cues for migration. The non-autonomous roles for Hox genes and their cooperativity in patterning an environment for cell migration represent novel fundamental insights into the roles of Hox genes and their targets in development.

Chapter II:

Non-autonomous Roles of MAB-5/Hox and SPON-1/F-spondin in Neuronal Migration in *C. elegans*

2.1 Abstract

Nervous system development and circuit formation requires neurons to migrate from their birthplaces to specific destinations. Migrating neurons detect extracellular cues that provide guidance information. In *Caenorhabditis elegans,* the QR and QL neuroblast descendants migrate long distances in opposite directions. The Hox gene *lin-39* cell-autonomously promotes anterior QR descendant migration, and *mab-5/Hox* cell-autonomously promotes posterior QL descendant migration. Here we describe a non-autonomous role of *mab-5* in regulating both QR and QL descendant migrations, a role masked by redundancy with *lin-39*. A third Hox gene, *egl-5/Abdominal-B*, also likely non-autonomously regulates Q descendant migrations. In the *lin-39 mab-5 egl-5* triple mutant, little if any QR and QL descendant migration occurs. In addition to well-described roles of *lin-39* and *mab-5* in the Q descendants, our results suggest that *lin-39, mab-5* and *egl-5* might also pattern the posterior region of the animal for Q descendant migration. Previous studies showed that the *spon-1* gene might be a target of MAB-5 in Q descendant migration. *spon-1* encodes a secreted basement membrane molecule similar to vertebrate F-spondin. Here we show that *spon-1* acts non-autonomously to control Q descendant migration, and might function as a permissive rather than instructive signal for cell migration. We find that increased levels of MAB-5 in body wall muscle can drive *spon-1* promoter adjacent to the Q cells, and loss of *spon-1* suppresses *mab-5* gain-of-function. Thus, MAB-5 might non-autonomously control Q descendant migrations by patterning the posterior region of the animal to which Q cells respond. *spon-1* expression from body wall muscles might be part of the posterior patterning necessary for directed Q descendant migration.

2.2 Introduction

Hox transcription factors are principal regulators of cell fate and control major aspects of development including nervous system development. Hox factors regulate nervous system development in part through cell-autonomous specification of cell fate, axon guidance, and regulation of migratory neural progenitors (Studer, Lumsden et al. 1996, Gavalas, Davenne et al. 1997, Arenkiel, Tvrdik et al. 2004). Additionally there is evidence that Hox genes in the developing brain can cell non-autonomously control axon guidance (Gavalas, Davenne et al. 1997). Neuron migration is an important aspect of nervous system development and many neurons and neuroblasts migrate from their initial birthplace to specific regions of the periphery (neural crest) or cortex. The Q neuroblasts of *C. elegans* represent a tractable and well-studied model for Hox gene controlled neuroblast migration (Chapman, Li et al. 2008, Middelkoop and Korswagen 2014). The Q neuroblasts QR and QL are bilaterally symmetric cells that undergo identical patterns of division, migration, and apoptosis to produce three neurons each (Sulston and Horvitz 1977). QR on the right side of the animal migrates anteriorly, undergoing cell division and migration giving rise to three neurons, with AQR migrating the furthest residing near the posterior pharyngeal bulb (Sulston and Horvitz 1977, Chapman, Li et al. 2008). QL migrates posteriorly undergoing identical cell divisions giving rise to three neurons, of which PQR migrates the furthest to reside posterior to the anus, near the phasmid ganglion (Chalfie, Thomson et al. 1983, Kenyon 1986, Salser and Kenyon 1992, Whangbo and Kenyon 1999, Korswagen, Herman et al. 2000, Chapman, Li et al. 2008).

Hox transcription factors govern QR and QL descendant migrations. Canonical Wnt signaling through detection of extracellular EGL-20/Wnt induces transcription of *antennapedia*-like Hox gene *mab-5* in the Q cells (Maloof, Whangbo et al. 1999). MAB-5 is necessary in the

QL lineage for posterior migration, and in the absence of MAB-5 all QL daughters migrate anteriorly (Harris, Honigberg et al. 1996). MAB-5 is also sufficient for posterior Q cell migrations, as expression of MAB-5 in QR causes posterior migration of the entire QR lineage (Salser and Kenyon 1992). Levels of MAB-5 appear to be tightly controlled, as MAB-5 is able to both activate and inhibit its own expression to ensure a specific level of MAB-5 (Mentink, Middelkoop et al. 2014). There is strong evidence that the directional control of MAB-5 is cell-autonomous. Q cell specific knockdown of *mab-5* causes complete anterior migration of PQR, and specific induction of MAB-5 in anterior migrating Q descendants causes them to reverse direction of migration (Cowing and Kenyon 1992, Harris, Honigberg et al. 1996, Shen, Zhang et al. 2014). The genes that MAB-5 controls to drive posterior migration are largely unknown. A recent study used whole organism RNA-seq of *mab-5* mutants paired with functional analysis to determine genes regulated by MAB-5 in migration (Tamayo, Gujar et al. 2013). This study found enrichment for secreted and transmembrane molecules regulated by MAB-5, suggesting that MAB-5 might directly regulate a cell's interaction with its environment.

The *Deformed*-like Hox gene *lin-39* is required in QR descendants for anterior migration. Both QL and QR initial express *lin-39*, but *mab*-5 inhibits *lin-39* expression in QL when it is expressed in response to Wnt signaling (Clark, Chisholm et al. 1993, Salser, Loer et al. 1993, Wang, Zhou et al. 2013). *lin-39* drives expression of the MIG-13 transmembrane receptor molecule in QL descendants which, along with SDN-1/syndecan, mediates anterior migration (Wang, Zhou et al. 2013, Sundararajan, Norris et al. 2015).

The *C. elegans* genome contains an abbreviated Hox cluster on linkage group III containing, among other Hox genes, *lin-39, mab-5,* and the *Abdominal-B*-like Hox gene *egl-5*. These genes control posterior body regions that represent their order on the chromosome

(Kenyon 1986, Chisholm 1991, Clark, Chisholm et al. 1993, Van Auken, Weaver et al. 2000). The most anterior gene *lin-39* is expressed in QR and transiently in QL, but also in the P3-P8 cells, hyp7 hypodermis, ventral cord neurons, and sex myoblasts (Clandinin, Katz et al. 1997, Maloof, Whangbo et al. 1999, Yang, Sym et al. 2005, Wagmaister, Gleason et al. 2006, Wagmaister, Miley et al. 2006, Kalis, Kissiov et al. 2014). *lin-39* mutants show improper development of P3-8.p cells which results in vulvaless animals (Clark, Chisholm et al. 1993, Salser, Loer et al. 1993). Next, *mab-5* is expressed in QL, but also in posterior body wall muscles (BWM), P7-P12, and the V5 and V6 hypodermal seam cells (Kenyon 1986, Salser and Kenyon 1996, Ji, Middelkoop et al. 2013). MAB-5 and LIN-39 can act in parallel in the P cells where they are both expressed, or play opposing roles in Q neuroblast migration where MAB-5 directs posterior migration, and LIN-39 promotes anterior migration (Salser and Kenyon 1992, Clark, Chisholm et al. 1993, Wang, Zhou et al. 2013). MAB-5 also interacts genetically with the more posteriorly-expressed Hox gene *egl-5* (Chisholm 1991, Ferreira, Zhang et al. 1999). *egl-5* is expressed in the tail region of the animal including BWMs, P11-P12, V6 descendants, HSN, PVM, PVC, and rectal epithelial cells, but not the Q cells (Ferreira, Zhang et al. 1999). *mab-5* and *egl-5* interact in different ways depending on the cell. In P10-P11, MAB-5 inhibits *egl-5* expression, and in V6 descendants MAB-5 promotes expression of *egl-5* (Chisholm 1991, Ferreira, Zhang et al. 1999, Li, Kulkarni et al. 2009). These three *C. elegans* Hox genes have complex cell-specific interactions controlling development of mid-body and posterior regions. All functions of these Hox genes described to date appear to be cell-autonomous roles, including the roles of LIN-39 and MAB-5 in Q descendant migration.

Previous studies show that MAB-5 acts in the Q descendants themselves to control direction of migration. In this work, we describe a new, non-autonomous role of *mab-5* in the

ability of Q descendants to migrate, but not direction. We show that *lin-39* and *mab-5* act in parallel in both AQR and PQR migration, and that transgenic expression of *mab-5* in posterior body wall muscles rescues AQR and PQR defects in *lin-39 mab-5* double mutants. Further, we describe AQR and PQR migration defects in *egl-5* mutants, expression of which is not detectable in Q lineages. Together, these results point to a non-autonomous role of *mab-5* and possibly *lin-39* and *egl-5* in Q migrations. Expression of these genes might pattern the posterior of the animal, providing migration information to the Q descendants. Thus, MAB-5 and LIN-39 might both establish an anterior-posterior Q descendant guidance system (non-autonomous role), and control how the Q descendants respond to this guidance system (autonomous role).

A previous RNA-seq study identified *spon-1* as a potential transcriptional target of MAB-5 (Tamayo, Gujar et al. 2013). The *mab-5(e1751)* gain-of-function (gof) mutation causes ectopic expression of *mab-5* in many cells including QR, and drives posterior migration of the QR descendant AQR (Salser, Loer et al. 1993, Chapman, Li et al. 2008). RNAi knockdown of *spon-1* partially suppressed posterior AQR migration in *mab-5(gof)*, suggesting that *spon-1* mediates the effects of *mab-5(gof)* in posterior migration (Tamayo, Gujar et al. 2013). *spon-1* encodes a secreted basement membrane molecule similar to vertebrate F-spondin (Woo, Berry et al. 2008). In vertebrates, F-spondin is secreted by the floor plate of the neural tube and has multiple roles in neural adhesion, neural crest migration, and axon guidance (Klar, Baldassare et al. 1992, Burstyn-Cohen, Tzarfaty et al. 1999, Debby-Brafman, Burstyn-Cohen et al. 1999, Zisman, Marom et al. 2007). F-spondin becomes processed into three peptides that can both attract and repel developing axons (Tzarfaty-Majar, Lopez-Alemany et al. 2001, Zisman, Marom et al. 2007). F-spondin has been implicated in Alzheimers disease as a binding partner to Amyloid Precursor Protein, with F-spondin treatment improving memory and β amyloid levels in AD

model mice (Ho and Sudhof 2004, Hoe, Wessner et al. 2005, Hafez, Huang et al. 2012). In addition to its role in disease F-spondin is conserved in many species including and has domain similarity to the established nervous system development molecule Reeler (Klar, Baldassare et al. 1992, Higashijima, Nose et al. 1997, Burstyn-Cohen, Tzarfaty et al. 1999, Hu, Xin et al. 2016). In *C. elegans,* SPON-1/F-spondin plays a role in neural adhesion and development (Woo, Berry et al. 2008). *spon-1* is required for muscle cell adhesion, and null or strong loss of function mutants are embryonic lethal (Woo, Berry et al. 2008). Despite being an important nervous system development molecule little is known about the regulation of F-spondin expression. Here we show that *spon-1* itself is required for AQR and PQR migration. Furthermore, we show that *spon-1* promoter activity in body wall muscles can be driven by MAB-5, and that *spon-1* phenotypes are rescued by body wall muscle derived SPON-1. Finally, we present evidence that *spon-1* acts in body wall muscle to mediate the effects of *mab-5(gof)*. Taken together, our results suggest that *mab-5* has a non-autonomous role in Q descendant migration, possibly by patterning the posterior region of the animal for proper Q migration. Further, they suggest that the *spon-1/F-spondin* gene might be a target of MAB-5 in posterior BWMs, which in part provides information for Q descendant migration.

2.3 Materials and Methods

Genetics

All experiments were carried out using standard *C. elegans* technique at 20°C (Brenner 1974). Mutations used were: LGX: *lqIs2[Posm-6::gfp];* LGI: *lrp-1(ku156).* LGII: *spon-1(e2623*, *ju430ts, ju402), hlh-1(cc561), muIs16(mab-5::gfp).* LGIII: *mab-5(e1239, e2088,* and *e1751), lin-39(n1760), egl-5(n945), rdvIs1(Pegl-17::mCherry.* LGIV: *lqIs80 [Pscm::gfp::caax].* LGV: *sid-1(pk3321), lqIs58[Pgcy-32::cfp], wgIs54 [egl-5::TY1::egfp::3xFLAG, UNC-119+].* Unknown chromosomal location *lqIs227, lqIs228* [*Pspon-1::gfp],* and *lqIs271*[*Pmyo-3::MAB-5*], were created by integration of *juEx592* [*lqIs227* + *lqIs228*] (Woo, Berry et al. 2008), and *lqEx808* [*lqIs271*]. Extrachromosomal arrays were generated using standard gonadal injection (Mello and Fire 1995) and include: *lqEx708, lqEx709* [*Pscm::spon-1(RNA+)* 25ng/µL*, Pscm::spon-1(RNA-)* 25ng/µL, *Pgcy-32::cfp* 50ng/µL], *lqEx732, lqEx937* [*Pegl-17::spon-1(RNA+)* 25ng/µL*, Pegl-17::spon-1(RNA-)* 25ng/µL, *Pgcy-32::cfp* 50ng/µL]*, lqEx808* [*Pmyo-3::MAB-5* 25ng/µL, *Pgcy-32::cfp 25*ng/µL], *lqEx834* [*Pegl-17::myr-mCherry* 20ng/µL, *Pegl-17::mCherry::HIS-24* 20ng/µL], *lqEx849* [*Pegl-17::REELER 20ng/*µL, *Pgcy-32::yfp* 20 *ng/*µL], *lqEx854* [*Pegl-17::REELER::gfp 25 ng/*µL *, Pgcy-32::cfp 30 ng/*µL] *lqEx855, lqEx856, lqEx858* [*Pegl-17::TSR1-5 20 ng/*µL] *, Pgcy-32::cfp 25 ng/*µL], *lqEx859, lqEx860* [*Pmyo-3::spon-1 25 ng/*µL, *Pgcy-32::cfp 30 ng/*µL]*, lqEx897, lqEx898* [*Pspon-1::mab-5::cfp* 10 ng/µL, *Pgcy-32::yfp* 20 ng/µL], *lqEx759* [*Pegl-17::spon-1*] *lqEx938, lqEx940, lqEx941* [*Pmyo-3::spon-1(RNA-)*10ng/µL, *Pmyo-3::spon-1(RNA+)*10ng/µL, *Pscm::gfp 20ng/µL, Pgcy-32::mCherry 25ng/µL*], *lqEx942* [*Pgcy-32::yfp 25ng/µL,* into *lin-39(n1760) egl-5(n945)*], *lqEx930, lqEx943* [*Pspon-1::EGL-5::cfp 10ng/µL, Pgcy-32::yfp 25ng/µL*]

Transgene construction

Details about transgene construction are available by request. The entire *spon-1* genomic region was amplified by PCR and placed behind *myo-3* and *egl-17* promoters. *Pegl-17::SP::TSR1-5* contained the *spon-1* endogenous signal peptide, first 29 residues, followed by the 5 thrombospondin repeats; 431-819. *Pegl-17::Reeler* was made by using the first 430 residues which contain both the Reeler and Spondin domains. *Pmyo-3::mab-5* was using a *mab-5* cDNA with the first endogenous *mab-5* intron (the *mab-5* mini-gene). *Pspon-1::mab-5::cfp* was made fusing the *mab-5* minigene to *cfp* at the C-terminus. *Pspon-1::egl-5::cfp* was made using the entire *egl-5* genomic region.

Scoring AQR and PQR migration

Scoring was done using *Pgcy-32,* which is expressed exclusively in AQR, PQR and URXl/r (Chapman, Li et al. 2008). The position of AQR and PQR was scored as previously described using a compound fluorescent microscope (Chapman, Li et al. 2008, Dyer, Demarco et al. 2010). *Ju430ts* animals were allowed to lay eggs for 3 hours at 15°C, then plates were shifted to 20°C. Some animals exhibited *pat* phenotype, viable animals were scored for AQR and PQR as described above. The triple mutant *lin-39 mab-5 egl-5* was maintained over the *hT2* balancer, and scored progeny had wild-type maternal contribution for each gene. Some *Hox* single and double mutant combinations were balanced by *hT2*. Positions 4a and 4b were separated by the PDE neuron marked by *Posm-6::gfp*, which represents the region of Q cell birth. Neurons directly over the PDE were marked as position 4a. Significance of difference was determined by Fisher's Exact test.

Line scan analysis of *Pspon-1::gfp* expression

Animals were synchronized to 4-4.5 hours post-hatching using previous published techniques (Honigberg and Kenyon 2000, Chapman, Li et al. 2008). Animals were mounted on a 2%(w/v) agarose pad in M9 containing 5mM sodium azide. Fluorescent micrographs were acquired for 100ms at 100x using a Qimaging Rolera EMCCD Camera and Metamorph software. Intensity of GFP was measured using ImageJ. Lines were drawn 1 pixel wide from the center of the posterior pharyngeal bulb to the posterior end of the anus on both dorsal and ventral body wall muscle segments. Segmented lines were drawn through body wall muscle nuclei, with pixels set at the anterior, posterior, and center of each muscle cell. Only animals that had both left and right muscle quadrants aligned were scored. To account for animal curvature, we averaged pixel intensity over each percentage of each line measured. This gives a percentage referring to the percent distance from anterior to posterior of the animal. This gave similar results to artificial straightening using ImageJ and was less cumbersome. Twenty animals were imaged on both dorsal and ventral segments for each genotype yielding 40 scans per genotype. In our analysis, dorsal and ventral data were combined for each animal, and any dorsal-ventral differences were not included. Standard deviations were calculated for each percentage position (error bars), and a two-tailed Student's T test with unequal variance was used to determine significance of difference at each percentage position using a bonferroni correction for multiple comparisons (100 in each genotype, $q<0.05$, $p<0.0005$). Transgenes *lqIs227* and *lqIs228* showed similar posterior bias and *lqIs227* was chosen for subsequent analysis due to chromosomal location (*lqIs228* is on the region of LG I balanced by hT2).

2.4 Results

Hox genes *mab-5, lin-39* and *egl-5* control QR and QL descendant migrations

The bilateral neuroblasts QR and QL, born in the posterior between the vulva and anus, give rise to the AQR and PQR neurons respectively (Sulston and Horvitz 1977) (Fig.1A). In wild-type animals, AQR migrates anteriorly to a region near the anterior deirid, and PQR migrates posteriorly to a position posterior to the anus in the phasmid ganglion (White, Southgate et al. 1986, Chapman, Li et al. 2008) (Fig. 1A). The Hox transcription factors *lin-39, mab-5,* and *egl-5* are expressed in specific regions ranging from anterior to posterior, and resemble a Hox cluster on chromosome III (Kenyon 1986, Chisholm 1991, Clark, Chisholm et al. 1993, Salser, Loer et al. 1993, Wang, Muller-Immergluck et al. 1993, Van Auken, Weaver et al. 2000) (Fig.1B,C). MAB-5 is required in QL to direct QL descendant migrations including PQR (Salser and Kenyon 1992) (Fig.1A,E). LIN-39 has been shown to cell-autonomously promote anterior migration of QR descendants, and *lin-39* is normally inhibited by MAB-5 in QL.a/p to allow for posterior migration (Fig.1A,F) (Harris, Honigberg et al. 1996, Wang, Zhou et al. 2013).

We scored AQR and PQR position using *Pgcy-32::cfp* along 5 positions in the animal as previously described (see Methods and Fig. 2A) (Chapman, Li et al. 2008). As expected, *lin-39* mutants showed shortened anterior migration of the QR descendant AQR (Figs 1F, 2B). *lin-39* displayed minor (4%), but significant defects in PQR migration (Fig.2C). *mab-5* mutants affected only PQR migration, with 100% of PQR misdirected, mostly residing in the normal anterior position of AQR (Figs 1E, 2B,C). *egl-5* mutants were reported to have weak QL defects (Desai and Horvitz 1989, Chisholm 1991). We found that *egl-5* affected both AQR and PQR

migration: 2% of AQR failed to migrate fully; and 16% of PQR failed to migrate, or migrated anteriorly (Figs 1G, 2B,C).

Previous studies found that *lin-39* and *mab-5* act in parallel in QR descendant migration (Clark, Chisholm et al. 1993, Wang, Muller-Immergluck et al. 1993). In a *lin-39 mab-5* double mutant, AQR migration defects were significantly stronger compared to *lin-39* alone, and misdirected PQRs failed in their anterior migration (Figs 1H, 2B,C). These data suggest that MAB-5 acts in parallel with LIN-39 in anterior migration.

mab-5 egl-5 double mutants showed no significant difference in AQR migration from *egl-5* alone (Fig.2B). Most PQR were directed anteriorly in the *mab-5 egl-5* double, but some failed in their anterior migration, consistent with the weak anterior AQR migration defects in *egl-5* single mutants. *lin-39 egl-5* double mutants had AQR defects similar to an additive effect of *lin-39* and *egl-5* single mutants (Figs 1I, 2B,C). PQR defects in *lin-39 egl-5* animals were significantly increased compared to an additive effect of both single mutants, suggesting they act in parallel (Fig. 2B,C). Similarly, The *lin-39 mab-5 egl-5* triple mutant showed significantly more severe AQR and PQR migration defects compared to any double *Hox* mutant (Figs 1J, 2B,C). Most AQR and PQR remained near their birth positions with minimal anterior or posterior migration. These results suggest that *lin-39, mab-5,* and *egl-5* are required in parallel for both anterior and posterior migration of QL and QR descendants AQR and PQR, and in their absence, very little migration occurs.

mab-5 and _egl-5_ can act in body wall muscle to control AQR and PQR migration

These data suggest that the Hox genes LIN-39, MAB-5, and EGL-5 act in parallel pathways to promote both anterior and posterior migration of QR and QL descendants AQR and

PQR. *mab-5* is not expressed in QR descendants (Salser, Loer et al. 1993, Harris, Honigberg et al. 1996, Salser and Kenyon 1996), and *lin-39* autonomously drives anterior QR descendant migration and is repressed in QL by *mab-5* (Harris, Honigberg et al. 1996, Wang, Zhou et al. 2013). However, both are expressed in other posterior cells including P cells, and MAB-5 in posterior body wall muscles and seam cells. (Salser, Loer et al. 1993, Wang, Muller-Immergluck et al. 1993, Clandinin, Katz et al. 1997, Maloof, Whangbo et al. 1999, Yang, Sym et al. 2005, Wagmaister, Gleason et al. 2006, Wagmaister, Miley et al. 2006) (Fig.1C). Thus, the effects of *mab-5* on AQR migration and *lin-39* on PQR migration might be due to their roles in cells other than Q descendants. However *lin-39* is expressed briefly in QL lineage, which could be important for initial migration (Wang, Muller-Immergluck et al. 1993).

MAB-5 is expressed in posterior body wall muscles (Salser, Loer et al. 1993) (Fig. 1C). We drove expression of MAB-5 specifically in body wall muscles using the promoter of the *spon-1* gene (Woo, Berry et al. 2008). At the time of Q descendant migration, *Pspon-1::gfp* was expressed most strongly in posterior body wall muscles in the region of the Q cells, but not in the Q cells themselves (Fig. 3). *Pspon-1::mab-5* significantly rescued the AQR and PQR defects seen in the *lin-39 mab-5* double mutant (e.g. 4% to 44% of AQR in position 1, and 2% to 19% of PQR in position 1 ($p < 0.05$)) (Fig. 2B,C). These results show that MAB-5 can have a role in AQR and PQR migration through activity in body wall muscles. Importantly, direction of PQR migration was not rescued by *Pspon-1::mab-5* (e.g. PQRs still migrated anteriorly). Direction of migration is an established cell-autonomous role of *mab-5* and not expected to be rescued by muscle-specific *Pspon-1::mab-5*. These data argue that *mab-5* has a non-autonomous role in anterior AQR and PQR migration.

egl-5 is expressed in posterior cells, but not in the Q cells (Ferreira, Zhang et al. 1999). We examined expression of the full-length *egl-5::gfp* (*wgIs54)* transgene from the modENCODE project (Niu, Lu et al. 2011). This transgene rescued PQR migration defects of *egl-5(n945)* (Fig. 4), but showed no detectable expression in the Q cells. *egl-5::gfp* was expressed in other posterior cells, consistent with previously-described expression (Fig. 4) (Ferreira, Zhang et al. 1999). Similar to above we tested the non-autonomous role of EGL-5 by expressing it from the *spon-1* promoter. *Pspon-1::egl-5::cfp* weakly affected PQR migration on its own, and rescued the stronger PQR migration defects of *egl-5* (Fig. 4) but did not rescue the coiler phenotype of *egl-5* (Data not shown). These data are consistent with a non-autonomous role of EGL-5 in Q descendant migration, likely in posterior body wall muscle.

SPON-1 is required for proper Q descendant migration.

Potential MAB-5 transcriptional targets in Q descendant migration were identified previously by whole-animal RNA seq on *wild-type* and *mab-5* mutants coupled with functional suppression of *mab-5(e1751)* gain-of-function (gof) (Tamayo, Gujar et al. 2013). *spon-1* transcripts were over-represented in *mab-5(gof)*, and reduction of *spon-1* function partially suppressed posterior AQR migration in *mab-5(gof)* (Tamayo, Gujar et al. 2013). These results indicate that *spon-1* expression is regulated by MAB-5 and that SPON-1 is required for posterior AQR migration in *mab-5(gof)*. *spon-1* encodes a molecule similar to vertebrate F-spondin, a secreted basement membrane molecule, and is required for proper muscle cell attachment and neural development (Woo, Berry et al. 2008) (Fig. 5A).

spon-1 null mutation results in embryonic lethality due to muscle cell detachment (Woo, Berry et al. 2008). We first used the viable hypomorphic alleles *e2623* and *ju430ts,* and the

embryonic lethal putative null *ju402* to analyze AQR and PQR migration (Woo, Berry et al. 2008) (Fig. 5A). Both hypomorphic mutants displayed AQR and PQR migration defects (Fig. 5B-D). To our surprise, AQR and PQR continued to develop in these animals as evidenced by *Pgcy-32* expression, and we were able to score their positions (Fig. 5E). Arrested *ju402* L1 larvae showed AQR and PQR migration defects (45% and 60%, respectively), with directional migration defects observed for both (Fig. 5E-G). This shows that SPON-1 function is required for the ability to migrate, as well as direction of migration in the A/P axis.

SPON-1 can act in body wall muscles to control Q descendant migration.

spon-1(+) expression driven in all body wall muscles using the *myo-3* promoter rescued AQR and PQR defects of hypomorphic *e2623* and *ju430* mutants (Fig. 6). It also rescued the lethality and AQR and PQR defects of the null *ju402* mutant (Fig. 6). This suggests that SPON-1 can function in body wall muscles to control AQR and PQR migration. The *myo-3* promoter does not show the posterior body wall muscle expression bias observed with the *spon-1* promoter (Fig. 3), yet *Pmyo-3::spon-1* efficiently rescued directional AQR and PQR defects in *spon-1(ju402)*. This suggests that *spon-1* might play a permissive rather than instructive role in migration, but an instructive role cannot be excluded.

In a wild-type background, expression of SPON-1 in body wall muscles by *Pmyo-3::spon-1* caused weak but significant defects (Table 2.1), suggesting that ectopic SPON-1 expression might perturb cell migration. While *Pspon-1::gfp* expression is not normally observed in the Q lineages (Fig. 3), expression of *spon-1* in the Q neuroblasts using the Q-cell specific *Pegl-17* promoter (Branda and Stern 2000, Cordes, Frank et al. 2006) caused defects in AQR

(3%) and PQR (19%) migration in a *wild-type* background (Fig 1, Table 2.1). We used this transgenic construct to test which parts of the SPON-1 molecule can perturb AQR and PQR migration. Vertebrate F-spondin is cleaved, forming multiple fragments (Zisman, Marom et al. 2007). The fragment containing thrombospondin repeats (TSR)1-4 binds to a lipoprotein receptor-related protein (LRP), which repels axons, while the TSR5-6 fragment, and the Reeler fragment both serve as attractants to developing axons. Weak and variable defects were observed with both fragments (Table 2.1), suggesting that both the TSR repeats and the Reeler/Spondin domain might participate in perturbing AQR and PQR migration. The *C. elegans* LRP molecule LRP-1 was not required for the effects of full-length *spon-1* expression, as *lrp-1(ku156)* had no affect on AQR/PQR migration and did not modify the *Pegl-17::spon-1* phenotype (data not shown).

MAB-5 promotes *spon-1* expression in body wall muscles.

spon-1 transcripts were overrepresented in the transcriptome of *mab-5* gain-of-function animals, indicating that MAB-5 stimulates *spon-1* expression (Tamayo, Gujar et al. 2013). Previous reports indicated that *Pspon-1::gfp* was expressed in body wall muscle cells (Woo, Berry et al. 2008). We analyzed *Pspon-1::gfp* expression at the time when the Q descendants are beginning their migrations in early L1 larvae 4-4.5 hours post-hatching. Expression was observed in posterior body wall muscles cells (Fig. 3), but not in the Q cells as determined by the Q-cell specific marker *rdvIs1 (Pegl-17::mCherry)* (Branda and Stern 2000, Ou, Stuurman et al. 2010) (Fig. 3). *Pspon-1::gfp* expression was in body wall muscle cells adjacent to the Q neuroblasts, with expression extending posteriorly to the tail, but only a short distance anteriorly (Fig. 3).

The gain-of-function *mab-5(e1751)* allele causes ectopic expression of *mab-5* in several tissues including the QR lineage (Salser and Kenyon 1992, Salser, Loer et al. 1993). We found an increase in expression of the *Pspon-1::gfp* transgene in *mab-5(gof)* (Fig. 7). While no expression was observed outside of body wall muscles, the extent of *Pspon-1::gfp* expression was increased anteriorly, with robust expression frequently present in anterior body wall muscles, sometimes reaching into the head (Fig.7C,D). We quantified pixel intensity along line scans through the body wall muscles from anterior to posterior to quantify GFP intensity along the A/P axis (Figs 7, 8) (see Methods). *Wild-type* animals had little detectable expression along the first anterior 20%, after which GFP intensity rose steadily with the region of highest GFP intensity also correlated to the location of Q birth (Figs 3, 8A). *mab-5(gof)* had a significant increase in *Pspon-1::gfp* expression along the entire animal but still maintained the highest intensity around the Q cell birthplace (Figs 7C,D, 8A). These results indicate that *mab-5(gof)* increased *Pspon-1::gfp* in body wall muscles. This result is consistent with the RNA-seq results showing *spon-1* overrepresentation in *mab-5(e1751)gof* animals (Tamayo, Gujar et al. 2013). A whole-organism RNA seq strategy was used in this study, so the sum of expression in all cells of the animal, including body wall muscles, was assayed. *mab-5* is expressed in QL and descendants as well as in other cells in the posterior, including posterior body wall muscles (Salser, Loer et al. 1993). We confirmed posterior body wall muscle expression of the full-length *mab-5::gfp* transgene *muIs16* in early L1 animals at the time when Q descendants begin migration (Hunter, Harris et al. 1999) (Fig. 9).

We drove *mab-5* expression in all body wall muscles using the *myo-3* promoter. *Pmyo-3::mab-5* animals were grossly misshapen and could not be reliably quantified with line scans. However, in early L1 larvae, *Pmyo-3::mab-5* caused uniform expression of *Pspon-1::gfp* in all

body wall muscle cells from head to tail (Figs 7E, F). These results show that in the body wall muscles, MAB-5 can activate *Pspon-1::gfp* expression. Together with the previous RNA seq results (Tamayo, Gujar et al. 2013), these data suggest that MAB-5 drives endogenous *spon-1* expression in posterior body wall muscles adjacent to the Q cells.

MAB-5 is not required for *spon-1* expression in body wall muscles

Consistent with the previous RNA-seq study that showed no effect on *spon-1* transcript levels in *mab-5(lof),* two *lof* alleles *mab-5(e1239),* and *mab-5(e2088)* had generally the same *Pspon-1::gfp* expression pattern as *wild-type* (Fig. 8B) (Tamayo, Gujar et al. 2013). Thus, While MAB-5 was sufficient to drive *spon-1* expression in body wall muscles; it was not required for *spon-1* expression.

Because *spon-1* expression persisted in *mab-5(lof)* animals we speculated that other Hox genes *egl-5* and *lin-39* might act in parallel with *mab-5* to activate *spon-1* expression, especially given the parallel roles in AQR and PQR migration noted here (Fig. 2). We tested *egl-5* single mutants, *mab-5 egl-5* double mutants, and a triple hox *lin-39 mab-5 egl-5* mutant on *Pspon-1::gfp* expression. None had any notable differences from *wild-type* animals (Figs. 10A, 11). The triple Hox mutants were unable to be quantified using line scan analysis because of grossly misshapen body, but maintained a *wild-type* expression pattern (Fig. 11). An *hlh-1* binding site predicted by ChIP-Seq is upstream of *spon-1* (Lei, Fukushige et al. 2010, Niu, Lu et al. 2011). *hlh-1* is the *C. elegans myoD* homolog and is required for body wall muscle formation (Chen, Krause et al. 1992, Chen, Krause et al. 1994). We tested the hypomorphic *hlh-1(cc561)* (Harfe, Branda et al. 1998) allele on *Pspon-1::gfp* expression and found no significant difference from

wild-type (Fig. 10B). Taken together this suggests other factors might cooperate with MAB-5 to promote *spon-1* expression.

In double mutants of the *spon-1(e2623)* hypomorphic allele and *mab-5(null)* alleles *e2088* and *e1239*, AQR migration defects generally resembled *spon-1* alone (Table 2.2). Doubles with hypomorphic *mab-5* alleles *mu114* and *bx54* displayed significantly more AQR migration failure (Table 2.2). Misdirected PQR anterior migration also failed in double mutants, with hypomorphic *mab-5* alleles having the stronger effect (Table 2.2). The lack of strong genetic interaction between *mab-5* and *spon-1* loss-of-function mutations is consistent with our finding that *mab-5* is not required for *spon-1* expression. While we do not understand the nature of the genetic interactions with the *mab-5* hypomorphs, the results suggest that residual *mab-5* activity in *spon-1(e2623)* antagonizes anterior AQR and PQR migration.

SPON-1 suppresses *mab-5* gain-of-function

The gain-of-function *mab-5(e1751)* allele causes posterior migration of both AQR and PQR (Fig. 12A,B) (Chapman, Li et al. 2008, Tamayo, Gujar et al. 2013). Previously, SPON-1 was shown to be required for the full effect of *mab-5(gof)*, as *spon-1* knock-down with feeding RNAi partially suppressed posterior AQR migration in *mab-5(gof)* (Tamayo, Gujar et al. 2013). The *spon-1(e2623)* mutation also significantly suppressed posterior AQR migration in *mab-5* gain-of-function (Fig. 12D): *mab-5(e1751)* displayed 78% of AQR neurons migrating posterior to the anus to the normal position of PQR, whereas *mab-5(e1751); spon-1(e2623)* displayed 56% ($p < 0.05$).

We used transgenic RNAi of *spon-1* driven from the *myo-3, egl-17* and *scm* promoters to knock down *spon-1* (Esposito, Di Schiavi et al. 2007, Sundararajan and Lundquist 2012). Alone,

Pmyo-3:: spon-1(RNAi) weakly affected AQR (1% defective) migration (Table 2.1). Because SPON-1 synthesis occurs in body wall muscle and is required for embryogenesis, viable *Pmyo-3::spon-1(RNAi)* transgenes likely cause weak disruption of body wall muscle derived SPON-1 (i.e. too weak to cause lethality). However, each RNAi construct suppressed *mab-5(gof)* (Fig. 12C,D). *mab-5(e1751)* rarely displayed AQR that were positioned anterior to the PDE neurons, the place of Q cell birth. In *mab-5(e1751); Pegl-17::spon-1(RNAi)* animals, AQR neurons were observed anterior to the PDE neuron (Fig. 12C), illustrating suppression of *mab-5(e1751)gof*. In *C. elegans*, RNAi can spread from one cell to another via the double-stranded RNA channel SID-1, which has been used as tool for cell-specific RNAi (Winston, Molodowitch et al. 2002, Calixto, Chelur et al. 2010). Suppression caused by the Q-cell-specific *Pegl-17::spon-1(RNAi)* transgene was abolished by *sid-1* mutation (Fig. 12D). This suggests that suppression was due to RNAi spreading from the Q cells (likely to body wall muscle), and that restriction of RNAi to the Q cells did not perturb *spon-1* function. In sum, these data indicate that SPON-1, likely from the body wall muscles, is partially required for posterior AQR migration observed in *mab-5(gof)*.

2.5 Discussion

Two main themes emerge from this work. First, our data indicate that the Hox factors MAB-5, EGL-5, and possibly LIN-39 have non-autonomous parallel roles in Q descendant migrations. For MAB-5, this role is in contrast to the well-described autonomous function in QL. The non-autonomous roles of LIN-39 and MAB-5 are not apparent in single mutants due to redundancy, although *lin-39* mutants show some PQR migration defects. Second, this work shows that the secreted basement membrane molecule SPON-1, similar to vertebrate F-spondin, might be a transcriptional target of MAB-5 in the body wall muscle cells that non-autonomously influences Q cell migrations.

A non-autonomous role of MAB-5 in Q descendant migration

Here we report a previously-undescribed role of the Hox gene *mab-5* in the migration of the QR and QL descendants AQR and PQR. Previous studies showed that MAB-5 autonomously regulates posterior migration of QL descendants (Salser and Kenyon 1992), and that LIN-39 is autonomously required for anterior migration of QR descendants (Harris, Honigberg et al. 1996, Wang, Zhou et al. 2013). We found that *lin-39 mab-5* double mutants displayed enhanced AQR anterior migration defects compared to *lin-39*, suggesting that *mab-5* and *lin-39* act in parallel pathways for anterior AQR migration. Furthermore, *lin-39* mutants alone displayed posterior PQR migration defects. MAB-5 expression is not observed in the QR/AQR lineage (Salser, Loer et al. 1993), and when expressed in this lineage, drives posterior migration. Additionally, *lin-39* is transiently expressed in QL/PQR lineage but is inhibited by MAB-5 expression in this lineage when QL descendant migration occurs (Wang, Zhou et al. 2013). These data suggest that LIN-39 and MAB-5 might have roles outside of the Q cells to regulate anterior AQR and posterior PQR migration. *lin-39* and *mab-5* are expressed in other

posterior cells, including *mab-5* in posterior and mid-body body wall muscle (Salser, Loer et al. 1993, Clandinin, Katz et al. 1997, Maloof, Whangbo et al. 1999, Yang, Sym et al. 2005, Wagmaister, Gleason et al. 2006, Wagmaister, Miley et al. 2006). Expression of *mab-5* in posterior body wall muscles rescued AQR migration defects in the *lin-39 mab-5* double mutant to resemble *lin-39* alone. It also rescued anterior migration defects of PQR in the *lin-39 mab-5* double. Of note, body wall muscle expression of *mab-5* did not rescue the directional defects of PQR in the *lin-39 mab-5* double mutant, as all PQR still migrated anteriorly. Posterior migration of PQR is a cell-autonomous role of *mab-5*, and body wall muscle expression of *mab-5* would not be expected to rescue directional defects. Together, these data point to a non-autonomous role of MAB-5 in anterior AQR and PQR migration. The posterior PQR defects of *lin-39* could be due to a non-autonomous role, or could be due to transient *lin-39* expression in the QL lineage (which is known to occur in *mab-5* mutants). This non-autonomous role for MAB-5 on cell migration is in contrast to much of the work done with Hox genes that primarily has focused on cell-autonomous roles of these genes, but there is precedence for Hox genes in vertebrates non cell-autonomously controlling axon guidance (Gavalas, Davenne et al. 1997).

The *lin-39 mab-5 egl-5* triple mutant shows little or no Q descendant migration

egl-5 mutants displayed PQR migration defects and weak AQR migration defects, consistent with previous reports of Q lineage defects in *egl-5* (Chisholm 1991). Functional full length *egl-5::gfp* expression was not observed in the Q lineages, and expressing EGL-5 specifically in posterior body wall muscles rescued *egl-5* defects. This suggests that *egl-5* might also non-autonomously regulate PQR migration, although expression in the Q lineages cannot be excluded as a possibility. The posterior PQR migration defects might be stronger in *egl-5* mutants, because the QL descendants migrate posteriorly through the region that expresses *egl-5*.

egl-5 did not enhance *mab-5* or *lin-39* defects, but did enhance AQR defects in the *lin-39 mab-5 egl-5* triple, which showed minimal migration of AQR and PQR away from the Q cell birthplace. This suggests that these three Hox genes act together to promote migration of the Q descendants, and in their absence, little or no anterior or posterior migration away from the Q cell birthplace occurs. In light of evidence presented here of a non-autonomous role of MAB-5, the nearly-complete lack of AQR and PQR migration in the *lin-39 egl-5 mab-5* triple is likely due to failure of both autonomous and non-autonomous roles of these molecules in AQR and PQR migration.

SPON-1/F-spondin controls Q descendant migration

Previously, RNA-seq identified *spon-1/F-spondin* as being positively regulated by MAB-5 in Q descendant migration (Tamayo, Gujar et al. 2013). We found that mutations in *spon-1* caused AQR and PQR incomplete migration, and directional defects. *spon-1* mutant*s* partially suppressed *mab-5(gof),* consistent with previous results using RNAi against *spon-1* (Tamayo, Gujar et al. 2013). Restriction of *spon-1* RNAi to the Q lineages was insufficient for suppression, whereas RNAi in surrounding tissues and/or body wall muscle resulted in suppression. This result suggests that *spon-1* acts non-autonomously in suppression of *mab-5(gof)*. This is consistent with *Pspon-1::gfp* expression, which we observed in posterior body wall muscles adjacent to the Q cells but not in the Q cells themselves.

spon-1 was expressed in posterior body wall muscles adjacent to the Q neuroblasts, and *spon-1* mutants displayed directional AQR and PQR migration defects. These results suggest that SPON-1 might provide directional guidance information for Q descendant migration. However, expression of SPON-1 from all body wall muscles cells, from anterior to posterior, efficiently rescued AQR and PQR defects, a result not expected of a cue providing directional

information. Therefore, SPON-1 might generally promote the ability of cells to migrate. The localized expression of *spon-1* adjacent to the Q cells in early L1 might represent a need for high levels of SPON-1 or newly-synthesized SPON-1 to generally stimulate cell migration at that time. While *Pmyo-3::spon-1* does not provide localized expression, it might provide high levels of expression throughout larval development, when it is needed for cell migration. However, this does not explain the directional migration defects in *spon-1* mutants. *Pmyo-3::spon-1* expression caused weak AQR and PQR defects alone, consistent with a potential role in directed guidance. However, the preponderance of evidence suggests a permissive role of SPON-1 in cell migration, which differs from F-spondin in vertebrates, where it acts as a repellent to migrating neural crest cells (Debby-Brafman, Burstyn-Cohen et al. 1999). However, there are also cases where F-spondin serves as an attractant and permissive signal to developing axons (Burstyn-Cohen, Frumkin et al. 1998, Burstyn-Cohen, Tzarfaty et al. 1999, Zisman, Marom et al. 2007).

Increased levels of MAB-5 stimulates *Pspon-1::gfp* expression in body wall muscle

We have shown that a *Pspon-1::gfp* transcriptional reporter was expressed at higher levels and more broadly in *mab-5(gof)*, consistent with previous RNA seq showing that endogenous *spon-1* transcripts are overrepresented in mab-5(gof) animals (Tamayo, Gujar et al. 2013). Expression of *mab-5* in all body wall muscles resulted in robust *Pspon-1::gfp* expression in all body wall muscles, even those in the anterior. These experiments indicate that increased MAB-5 activity in the body wall muscles can drive *Pspon-1:gfp* expression. A ChIP seq study using MAB-5 (Niu, Lu et al. 2011) did not identify the *spon-1* locus as a potential MAB-5 target. Thus, MAB-5 might indirectly regulate *spon-1* expression in body wall muscle. However, this ChIP seq study was done with L3 larvae, long after Q migration, so any transient interaction at the *spon-1* promoter in L1 would have been missed. The ability of MAB-5 to drive *Pspon-1::gfp*

in gain-of-function *mab-5* animals might reflect an endogenous role of MAB-5 in *spon-1* regulation. It is also possible that gain-of-function *mab-5* has an ectopic effect on *spon-1* expression. Future studies aimed at isolating factors necessary for *spon-1* expression will resolve this issue.

Complete loss of SPON-1 function causes embryonic lethality, and *mab-5* mutants are not lethal, suggesting that MAB-5 is not the only factor that regulates *spon-1* expression. Indeed, *mab-5(lof)* mutants did not affect *Pspon-1:gfp,* consistent with RNA seq showing no effect of *mab-5(lof)* on *spon-1* transcript accumulation (Tamayo, Gujar et al. 2013). The *lin-39 mab-5 egl-5* triple mutant also had no effect, indicating that neither LIN-39 nor EGL-5 cooperate with MAB-5 in *Pspon-1::gfp* expression. The *spon-1* locus contains a predicted *hlh-1* binding region (Niu, Lu et al. 2011), but *hlh-1* also did not influence *spon-1* expression. While MAB-5 is sufficient to drive *spon-1* expression, other factors might be required redundantly with *mab-5* in normal *spon-1* expression. Furthermore, LIN-39 and EGL-5 might be required for the expression of factors that act in parallel to factors regulated by *mab-5* (*e.g. spon-1*). This redundancy could be in the same cell, or in distinct cells each expressing factors that influence AQR and PQR migration.

In addition to the well-characterized cell-autonomous function of LIN-39 and MAB-5 in Q migration, we find possible roles outside of the Q lineage to promote migration, roles that have been masked by redundancy of function of these molecules. We show evidence for a novel non-autonomous role of the Hox gene *mab-5* in Q migrations. *lin-39, mab-5,* and *egl-5* have distinct expression patterns, yet appear to have overlapping functions in promoting Q lineage migrations. We speculate that LIN-39, MAB-5, and EGL-5 pattern the posterior region of the animal for use as a substrate for Q migrations (a non-autonomous role), and that LIN-39 and MAB-5 control the

response of the Q descendants to that posterior pattern (an autonomous role). Our data indicate that secreted basement membrane molecule SPON-1/F-spondin might be a target of MAB-5 in body wall muscle and is important for Q descendant migration. In the absence of *lin-39, mab-5,* and *egl-5*, very little Q descendant migration away from the Q cell birthplace occurs, suggesting multiple and parallel pathways are regulated by these Hox factors in Q migrations.

2.6 Figures

Figure 2.1

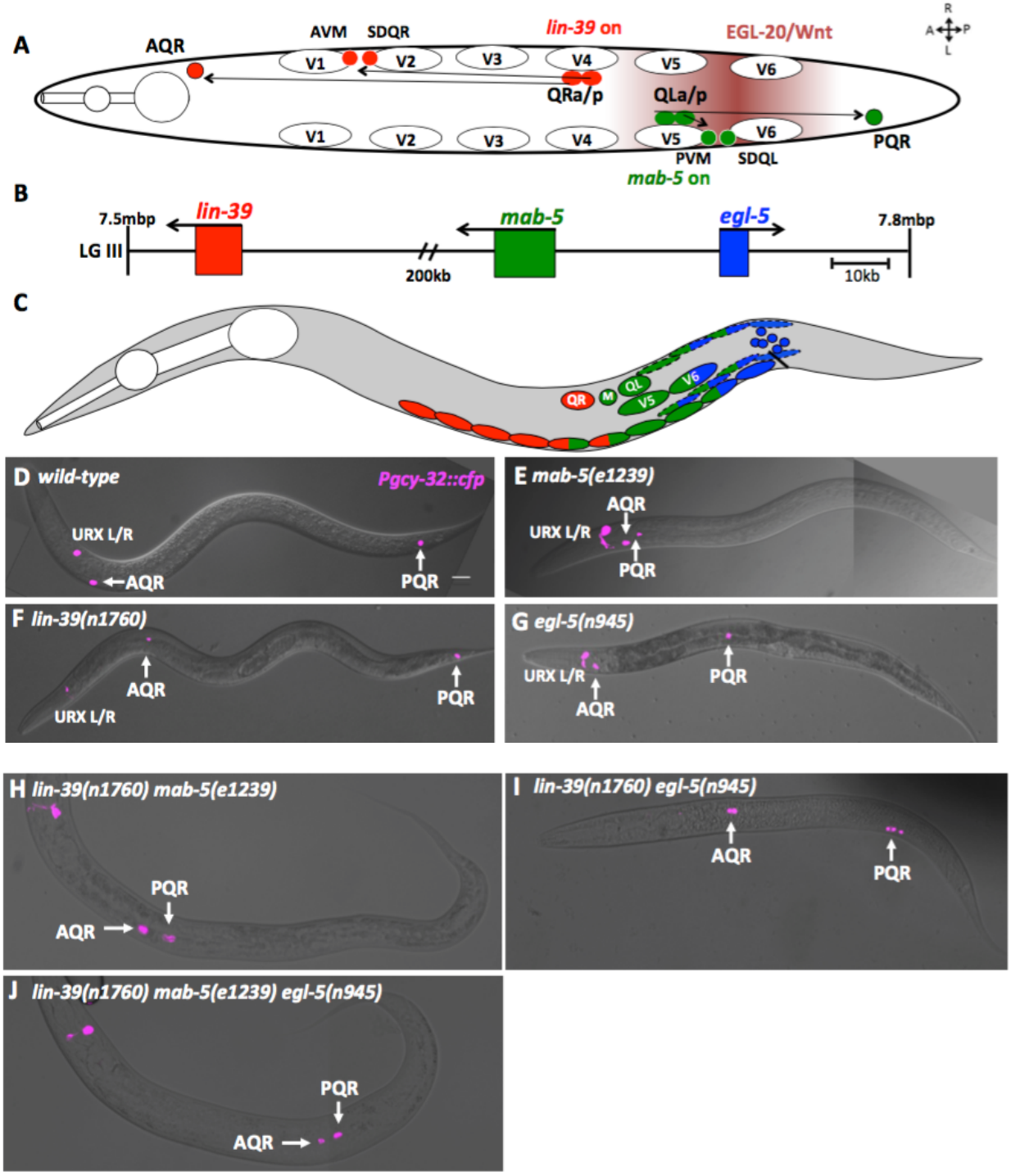

Figure 2.1

***C. elegans* Hox genes *lin-39, mab-5* and *egl-5* affect Q descendant migrations:** A) Diagram of a dorsal view of wild-type Q descendant migration. EGL-20/Wnt (maroon shading) induces MAB-5 in QL and descendants which directs posterior migration. QR and descendants do not respond to EGL-20/Wnt, and express *lin*-39, driving anterior migration. B) Position on LG III (7.5-7.8 mbp) of the three *C. elegans Hox* genes that affect post-embryonic development. C) representation of cells that express *lin-39* (red) *, mab-5* (green) and *egl-5* (blue) during the L1 larval stage. Dashed ovals represent body wall muscles, solid ovals the P cells, and blue circular cells near the anus represent the rectal epithelium where *egl-5* is expressed. D-J) Positions of Q descendants AQR and PQR in L4/young adult animals. *lqIs58[Pgcy-32::cfp]* micrographs were merged with Differential Interference Contrast (DIC) micrographs in wild-type and mutants. In all micrographs unless otherwise noted dorsal is up, anterior is left, and scale bar represents 10μm**.**

Figure 2.2

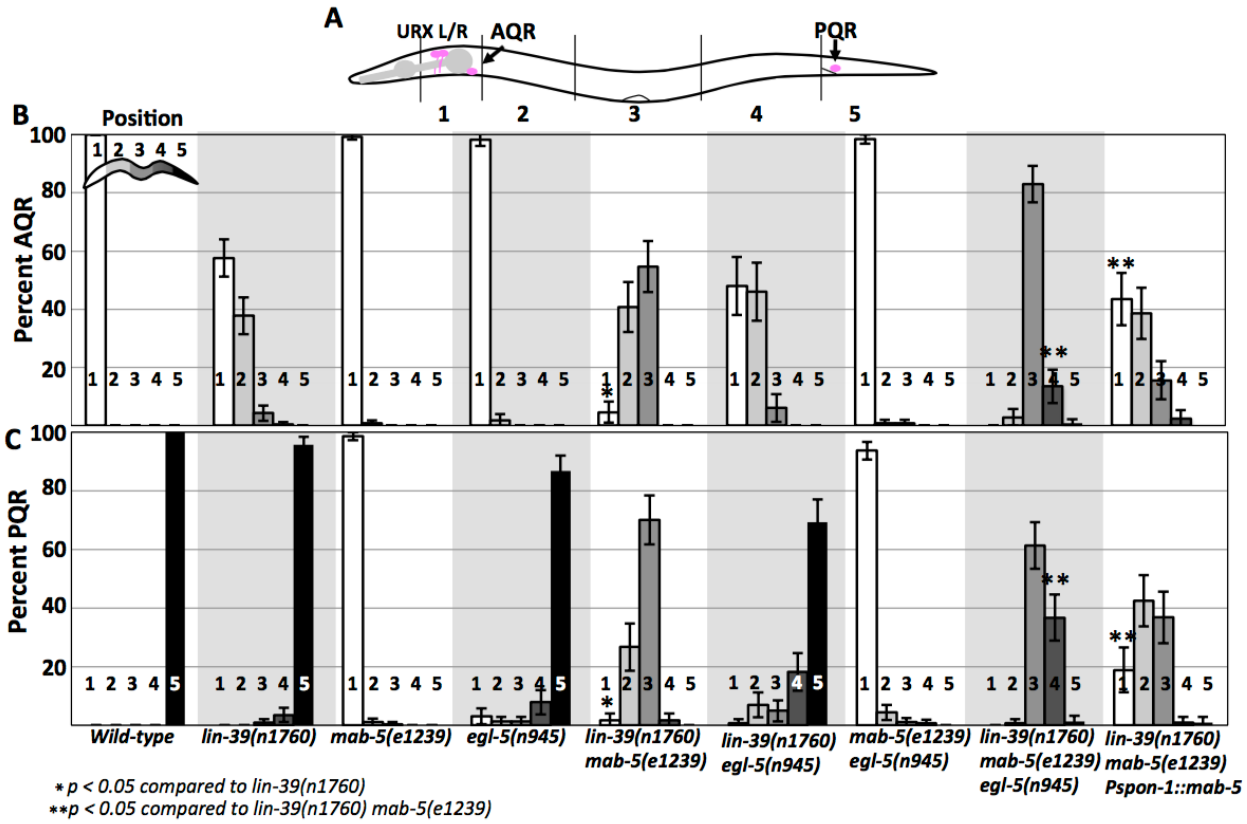
A
URX L/R
AQR
PQR
1
2
3
4
5
B
Position
Percent AQR
C
Percent PQR
Wild-type
lin-39(n1760)
mab-5(e1239)
egl-5(n945)
lin-39(n1760) mab-5(e1239)
lin-39(n1760) egl-5(n945)
mab-5(e1239) egl-5(n945)
lin-39(n1760) mab-5(e1239) egl-5(n945)
lin-39(n1760) mab-5(e1239) Pspon-1::mab-5
* p < 0.05 compared to lin-39(n1760)
** p < 0.05 compared to lin-39(n1760) mab-5(e1239)

Figure 2.2 AQR and PQR migration defects in *lin-39, mab-5,* and *egl-5*. A) Schematic of an animal with scoring zones indicated (see Methods). The wild-type positions of AQR (position 1) and PQR (position 5) are indicated. **B-C)** Percent of AQR and PQR residing at each position in adult animals as visualized by *lqIs58[Pgcy-32::cfp]*. Error bars represent 2x standard error of the proportion. Fisher's Exact test was used to determine significance of difference. Genotypes with *Pspon-1::mab-5* transgene represent combined results from two independently derived arrays with similar effects.

Figure 2.3

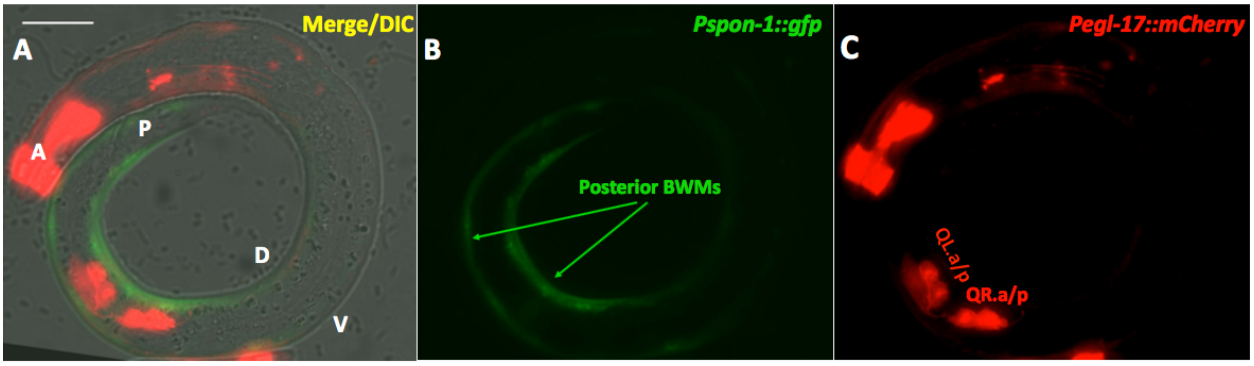
A
Merge/DIC
P
A
D
V
B
Pspon-1::gfp
Posterior BWMs
C
Pegl-17::mCherry
QL.a/p
QR.a/p

Figure 2.3 *Pspon-1::gfp* expression. Micrographs of an L1 larva at 4-4.5h post-hatching are shown. **A)** *Pspon-1::gfp* expression in posterior body wall muscles. **B)** Qx.a/p visualized using *rdvIs1[Pegl-17::mCherry]*. **C)** Merged *Pspon-1::gfp*, *Pegl-17::mCherry,* and DIC images. The animal is coiled such that the anterior (A) is near the posterior (P). Dorsal (D) and ventral (V) are indicated. The scale bar represents 10μm.

Figure 2.4

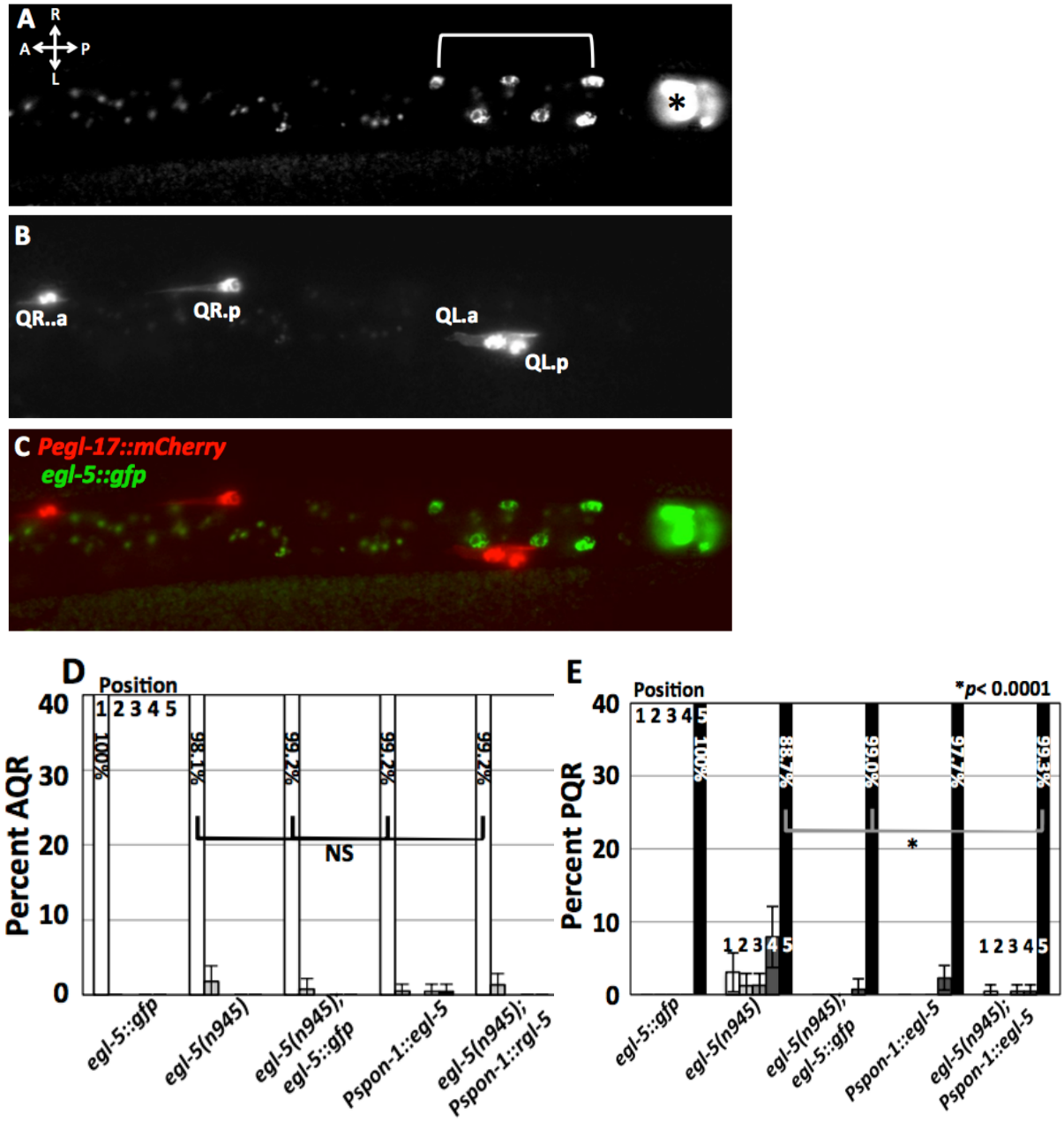
A
R
A
P
L
*
B
QR..a
QR.p
QL.a
QL.p
C Pegl-17::mCherry
egl-5::gfp
D
Position
1 2 3 4 5
Percent AQR
40
30
20
10
0
100%
98.1%
99.2%
99.2%
99.2%
NS
egl-5::gfp
egl-5(n945)
egl-5(n945); egl-5::gfp
Pspon-1::egl-5
egl-5(n945); Pspon-1::rgl-5
E
Position
*p< 0.0001
Percent PQR
*
egl-5::gfp
egl-5(n945)
egl-5(n945); egl-5::gfp
Pspon-1::egl-5
egl-5(n945); Pspon-1::egl-5

Figure 2.4 Full-length *egl-5::gfp* expression. Fluorescent micrographs of posterior region of an L1 larva at 5-5.5h post hatching, dorsal view. Anterior is left. The scale bar represents 5μm. A) *egl-5::gfp (wgIs54).* The asterisk indicates rectal epithelial expression of *egl-5::gfp*, and brackets indicate nuclei of posterior body wall muscles or P cells. The punctate fluorescence anterior to the bracketed nuclei is background autofluorescence of the gut. B) *Pegl-17::mCherry.* C) Merged image. D-E) *egl-5::gfp,* and *Pspon-1::egl-5* transgenic rescue of *egl-5(n945)* as described for Figure 4.2. Represents combined results of two independent *Pspon-1::egl-5* arrays that showed similar effects.

Figure 2.5

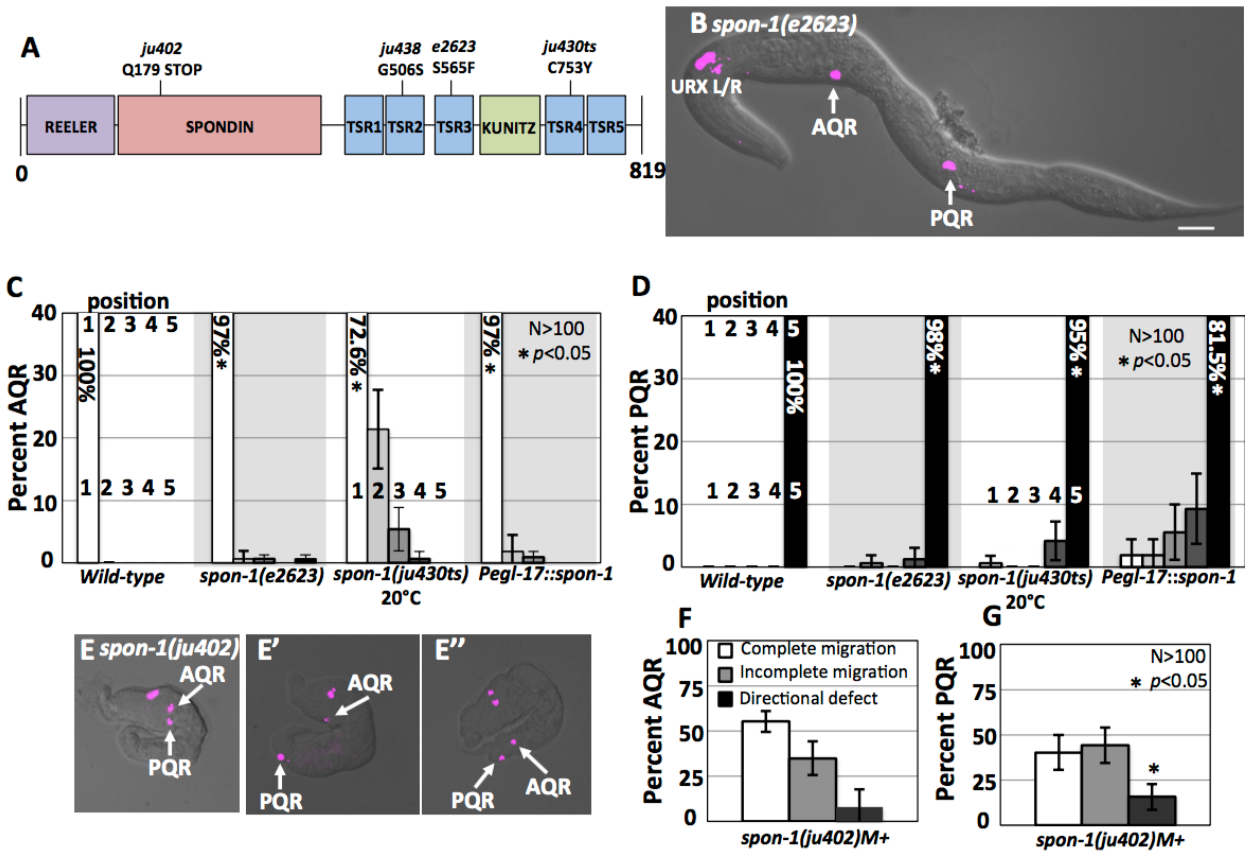
A
ju402
Q179 STOP
ju438
G506S
e2623
S565F
ju430ts
C753Y
REELER
SPONDIN
TSR1
TSR2
TSR3
KUNITZ
TSR4
TSR5
0
819
B spon-1(e2623)
URX L/R
AQR
PQR
C
position
Percent AQR
100%
97%*
72.6%*
97%*
N>100
* p<0.05
Wild-type
spon-1(e2623)
spon-1(ju430ts)
Pegl-17::spon-1
20°C
D
position
Percent PQR
100%
98%*
95%*
81.5%*
N>100
* p<0.05
Wild-type
spon-1(e2623)
spon-1(ju430ts)
Pegl-17::spon-1
20°C
E spon-1(ju402)
AQR
PQR
E'
AQR
PQR
E''
PQR
AQR
F
Percent AQR
Complete migration
Incomplete migration
Directional defect
spon-1(ju402)M+
G
Percent PQR
N>100
* p<0.05
spon-1(ju402)M+

Figure 2.5 AQR and PQR migration defects in *spon-1* mutants. A) A diagram of the predicted 819-residue SPON-1 molecule with Reeler, Spondin, Thrombospondin (TSR), and Kunitz serine protease inhibitor (KUNITZ) domains shown. The positions of mutations are indicated. B) A *spon-1(e2623)* young adult animal with defects in AQR and PQR migration (merged *cfp* and DIC micrographs). The scale bar represents 20μm. C and D) AQR and PQR migration defects in *spon-1* as described in Fig 2. Error bars represent 2x standard error of the proportion. E-E'') *spon-1(ju402)M+* arrested L1 animals with *Pgcy-32::cfp.* E) PQR reversal in migration direction, E') Complete AQR and PQR migration, and E'') AQR directional defect. F-G) Percent of AQR (F), and PQR (G) that show defects in *spon-1(ju402)M+* arrested L1 animals.

Figure 2.6

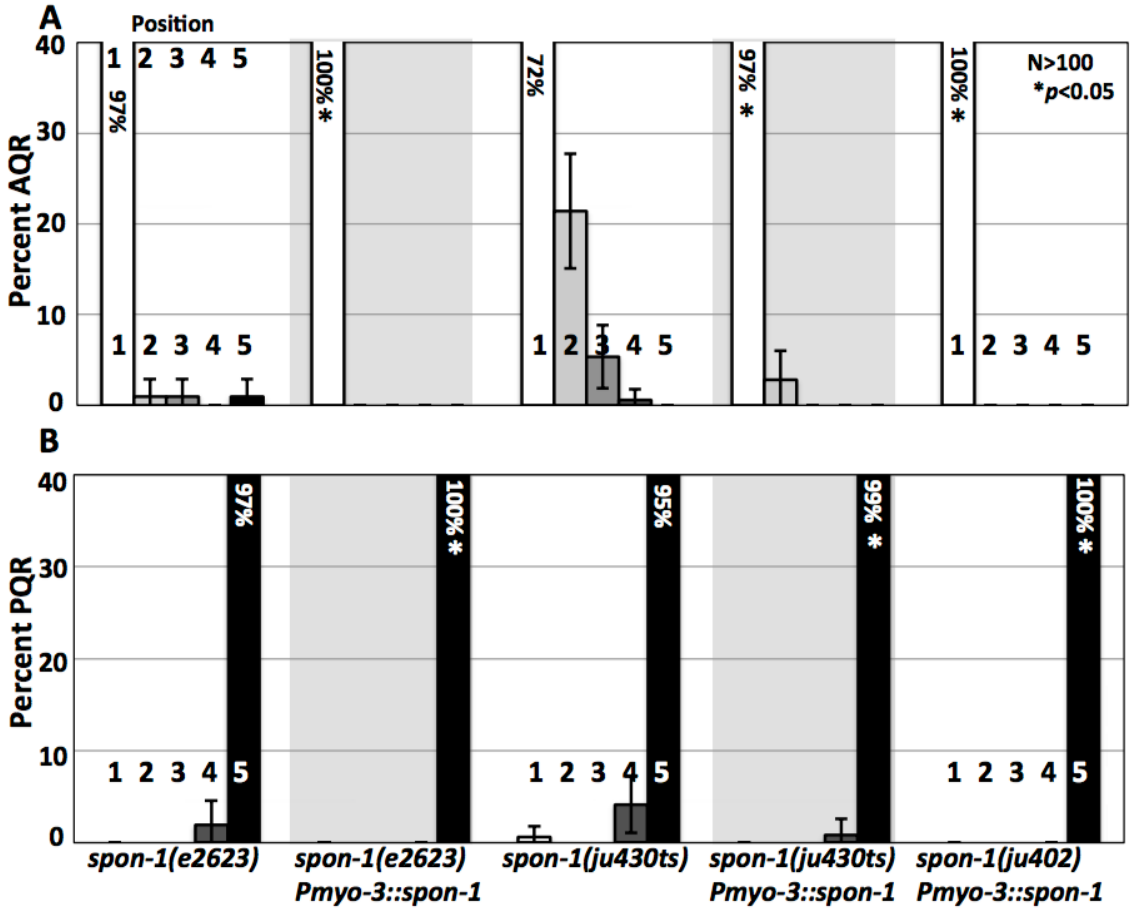
A
Position
Percent AQR
40
30
20
10
0
1 2 3 4 5
97%
100% *
72%
97% *
100% *
N>100
*p<0.05
B
Percent PQR
97%
100% *
95%
99% *
100% *
spon-1(e2623)
spon-1(e2623) Pmyo-3::spon-1
spon-1(ju430ts)
spon-1(ju430ts) Pmyo-3::spon-1
spon-1(ju402) Pmyo-3::spon-1

Figure 2.6 Muscle-derived SPON-1 rescues AQR and PQR migration. A-B) Quantification of AQR(A) and PQR(B) position as in Fig 2.2. *Pmyo-3::spon*-1 represents the transgene expressing SPON-1 in body wall muscle cells. Asterisk indicates significant (n>100, $p<0.05$ Fishers exact test) difference from corresponding *spon-1* mutant (except for *ju402* which is lethal). Genotypes with transgene arrays show results of combined similar results from 2 or more independently derived lines with similar effects.

Figure 2.7

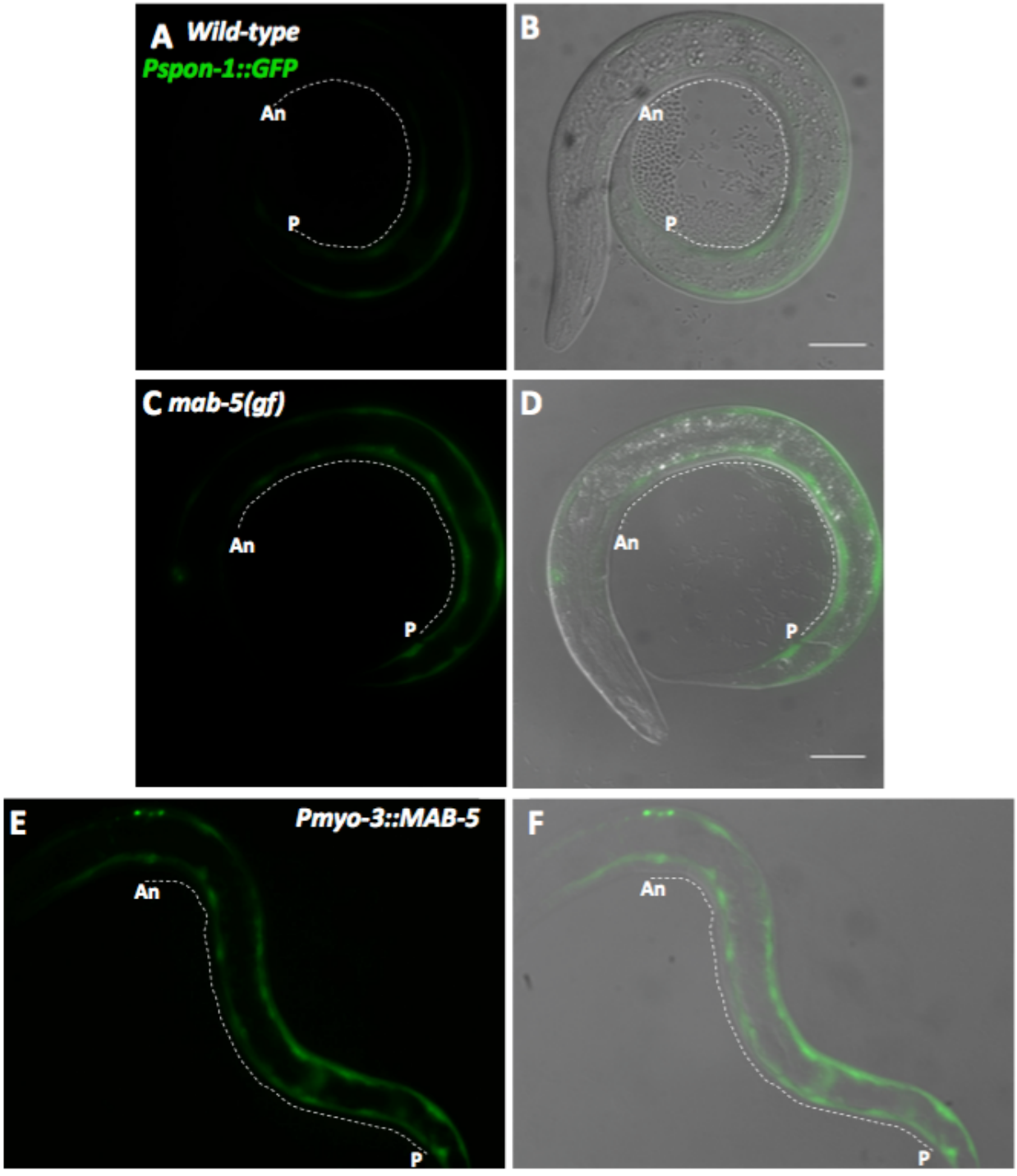
A Wild-type
Pspon-1::GFP
An
P
B
An
P
C mab-5(gf)
An
P
D
An
P
E
Pmyo-3::MAB-5
An
P
F
An
P

Figure 2.7 *Pspon-1::gfp* expression in *mab-5* gain-of-function. Fluorescent micrographs of *Pspon-1::gfp*-expressing L1 larvae 4-4.5h post-hatching. Fluorescent *Pspon-1::gfp* (A,C,E) and merged DIC (B,D,F) micrographs. Dashed lines indicate regions of body wall muscle used in line scans for the analysis in Figure 6 (An, anterior near the posterior pharyngeal bulb; P, posterior near the anus) (see Methods). The scale bar represents 10μm.

Figure 2.8

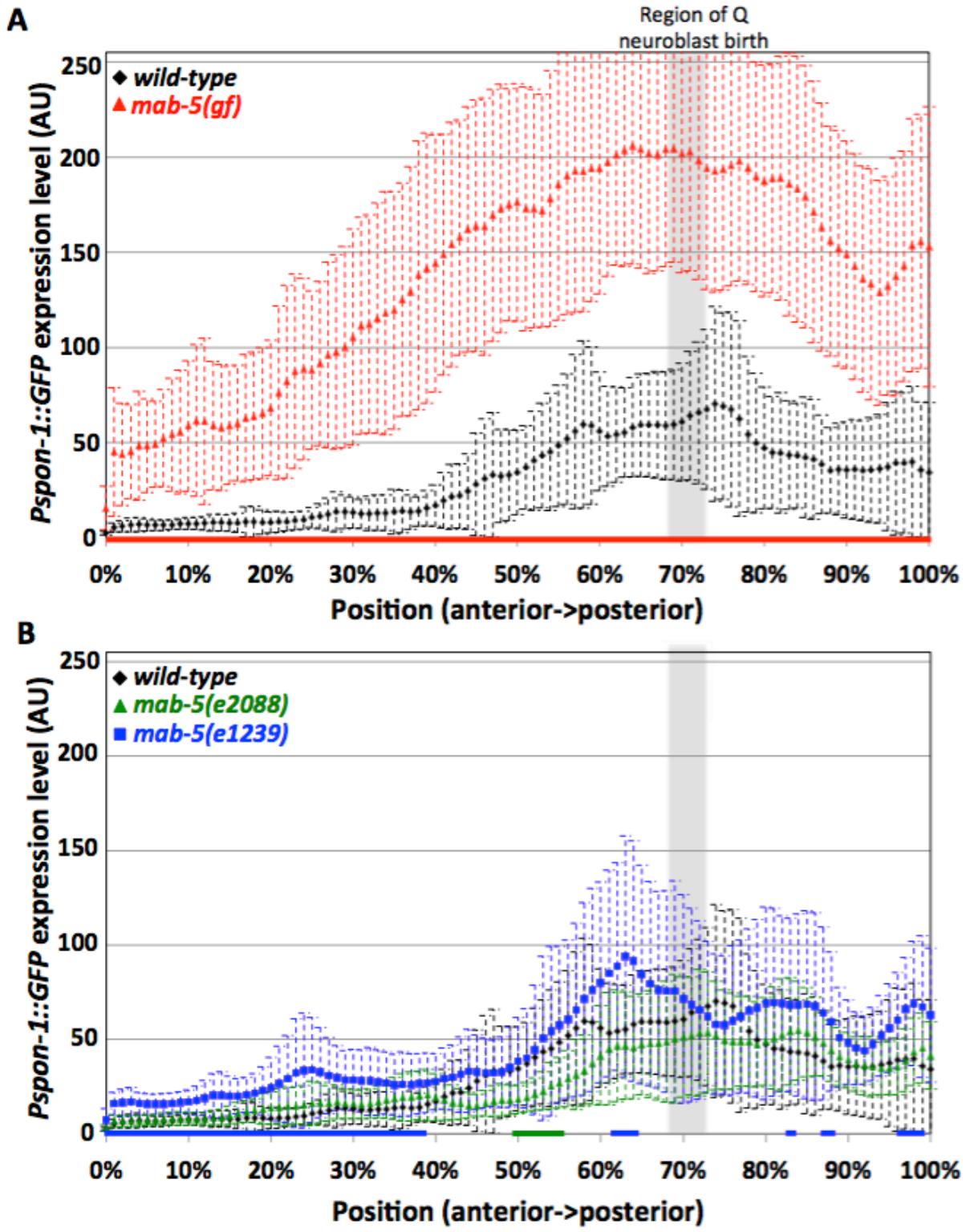
A
Region of Q
neuroblast birth
wild-type
mab-5(gf)
Pspon-1::GFP expression level (AU)
250
200
150
100
50
0
0%
10%
20%
30%
40%
50%
60%
70%
80%
90%
100%
Position (anterior->posterior)
B
wild-type
mab-5(e2088)
mab-5(e1239)
Pspon-1::GFP expression level (AU)
250
200
150
100
50
0
0%
10%
20%
30%
40%
50%
60%
70%
80%
90%
100%
Position (anterior->posterior)

Figure 2.8 Quantification of *Pspon-1::gfp* intensity in body wall muscles. Graphs represent intensities of *Pspon-1::gfp* expression determined by line scans through body wall muscle quadrants in L1 animals 4-4.5h post-hatching (See Methods). The Y-axis represents the intensity of GFP in arbitrary units (AU). The X-axis corresponds to position on the animal (0% is the posterior pharyngeal bulb, 100% is at the anus). The approximate region of Q neuroblast birth is shaded gray. Dashed error bars represent one standard deviation. Colored bars along the X axis correspond to regions of significant difference compared to *wild-type* ($q < 0.05$, multiple comparison corrected Students T-test, n = 40 body wall muscle quadrants (2 per animal, dorsal and ventral combined)). A) *mab-5(e1751)* gain-of-function. B) *mab-5* putative null mutants *e2088* and *e1239***.**

Figure 2.9

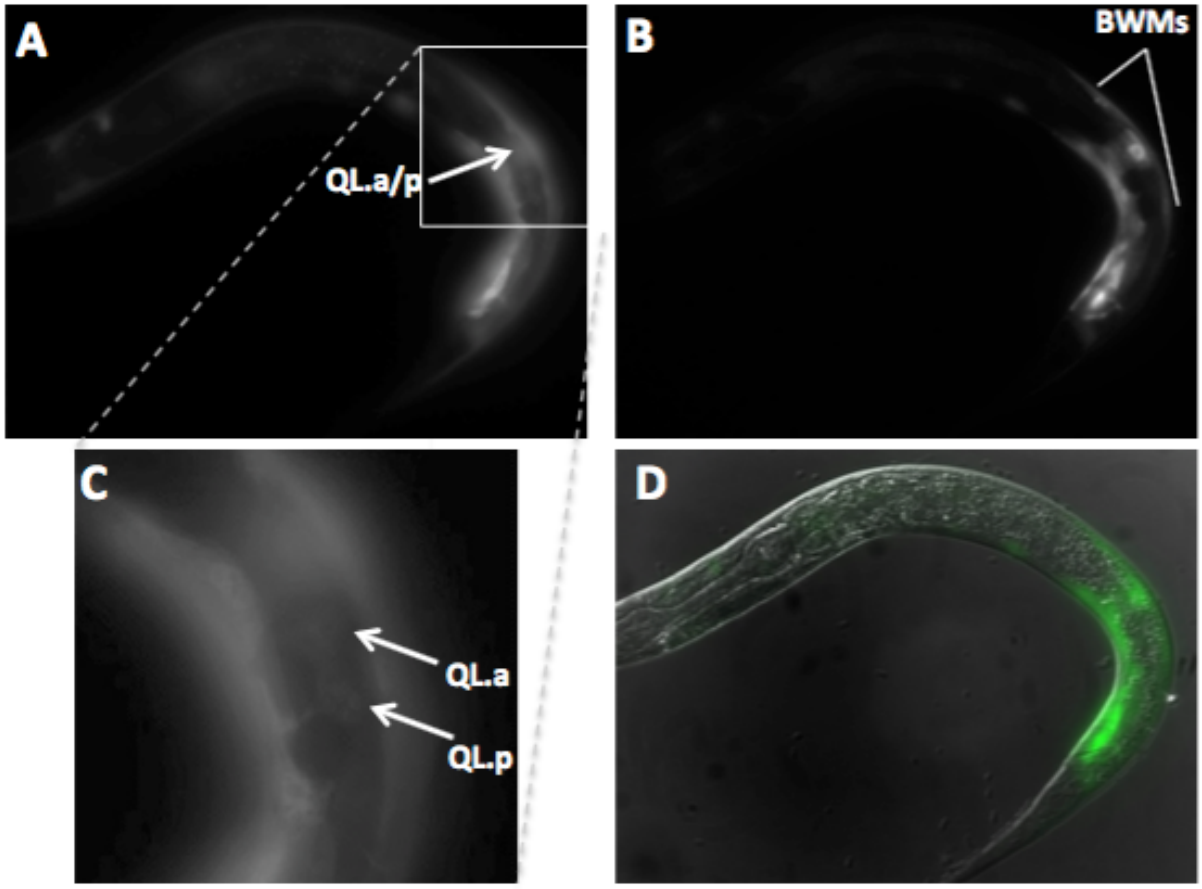

Figure 3.9 Expression of *mab-5::gfp (muIs16)* in wild-type animals. Fluorescent micrographs of *muIs16* animals 4-4.5h post hatching with left (A,C), and right (B) side of animal in focus. C is an enlargement of section in A to show faint expression in QLa/p. D) is merge of A,B, and DIC. Scale bars represent 5μm.

Figure 2.10

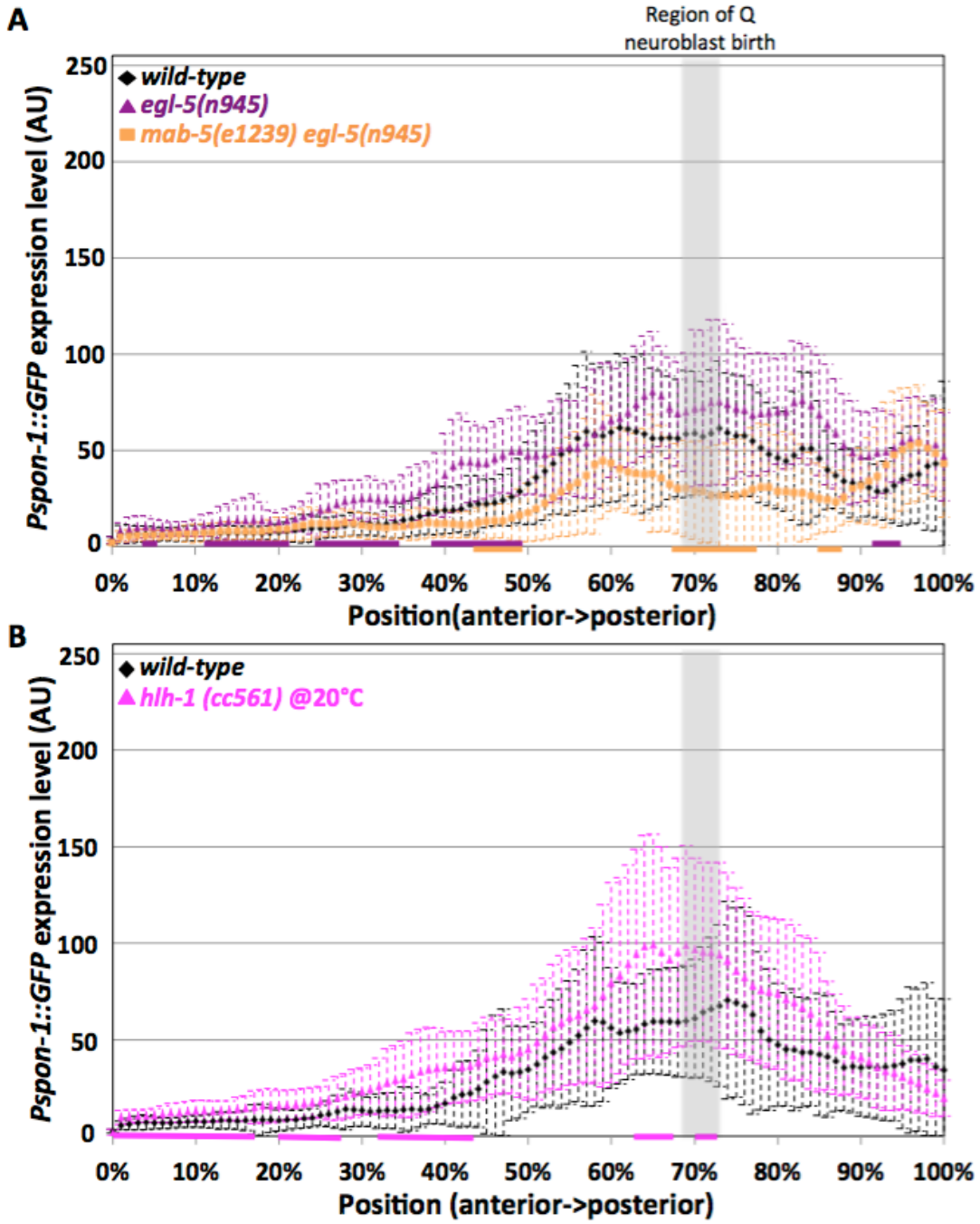
A
Region of Q
neuroblast birth
wild-type
egl-5(n945)
mab-5(e1239) egl-5(n945)
Pspon-1::GFP expression level (AU)
250
200
150
100
50
0
0%
10%
20%
30%
40%
50%
60%
70%
80%
90%
100%
Position(anterior->posterior)
B
wild-type
hlh-1 (cc561) @20°C
Pspon-1::GFP expression level (AU)
250
200
150
100
50
0
0%
10%
20%
30%
40%
50%
60%
70%
80%
90%
100%
Position (anterior->posterior)

Figure 10. *egl-5* and *hlh-1* are not required for body wall expression of *Pspon-1::gfp*. Graphs represent intensities of *Pspon-1::gfp* expression determined by line scans through body wall muscle quadrants in L1 animals 4-4.5h post-hatching (See Methods). The Y-axis represents the intensity of GFP in arbitrary units (AU). The X-axis corresponds to position on the animal (0% is the posterior pharyngeal bulb, 100% is at the anus). The approximate region of Q neuroblast birth is shaded gray. Dashed error bars represent one standard deviation. Colored bars along the X axis correspond to regions of significant difference compared to *wild-type* ($q < 0.05$, multiple comparison corrected Students T-test, $n = 40$ body wall muscle quadrants (2 per animal, dorsal and ventral combined)). A) *wild-type*, *egl-5,* and *mab-5 egl-5* double mutant. B) *wild-type,* and *hlh-1(cc561)* hypomorphic allele.

Figure 2.11

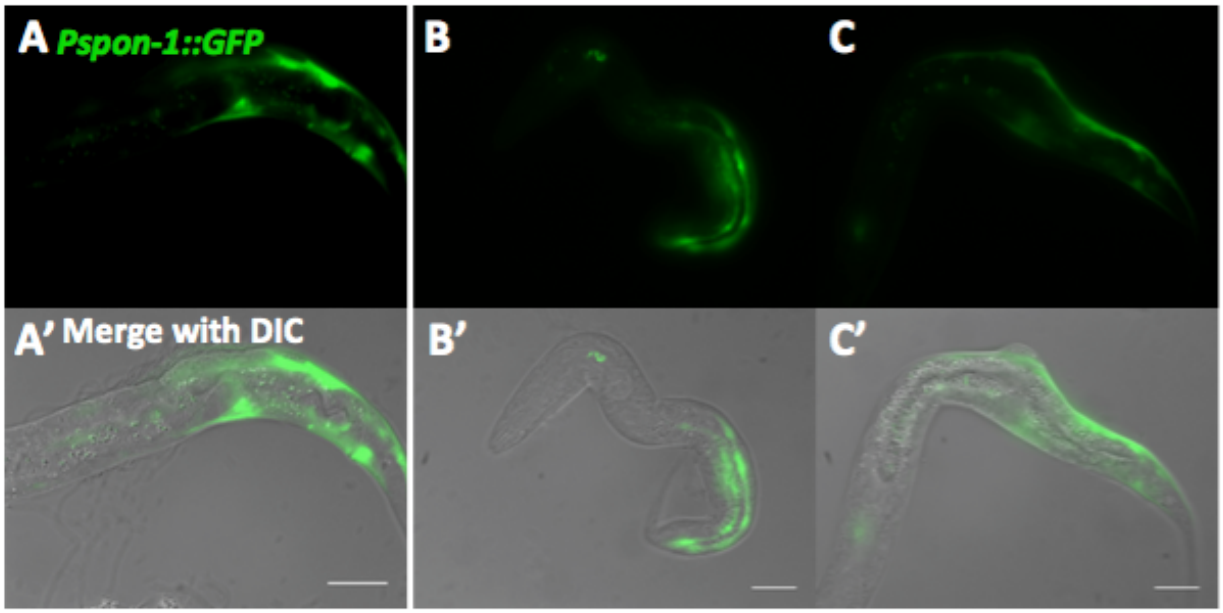

Figure 2.11 *Pspon-1::gfp* in *lin-39 mab-5 egl-5* triple mutant. Fluorescent micrographs (**A-C**) and merged DIC micrographs (**A',B',C'**) of three *lin-39(n1760M+) mab-5(e1239) egl-5(n945)* animals with *Pspon-1::gfp.* Animals are 4-4.5h post hatching, scale bar represents 10μM. Anterior is to the left, and dorsal is up.

Figure 2.12

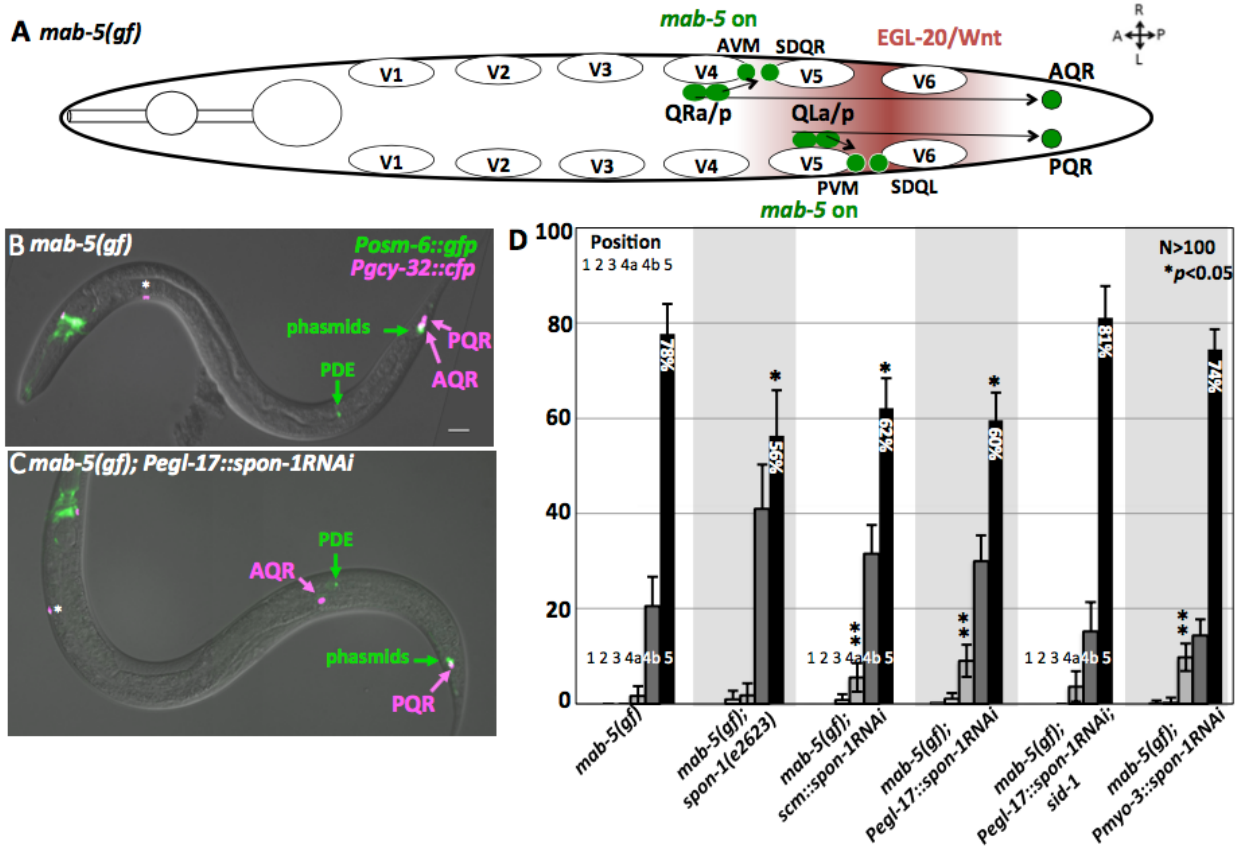
A mab-5(gf)
mab-5 on
AVM
SDQR
EGL-20/Wnt
V1
V2
V3
V4
V5
V6
AQR
QRa/p
QLa/p
PQR
PVM
SDQL
mab-5 on
B mab-5(gf)
Posm-6::gfp
Pgcy-32::cfp
phasmids
PQR
PDE
AQR
C mab-5(gf); Pegl-17::spon-1RNAi
PDE
AQR
phasmids
PQR
D
Position
1 2 3 4a 4b 5
N>100
*p<0.05
100
80
60
40
20
0
74%
55%
62%
60%
81%
74%
mab-5(gf)
mab-5(gf); spon-1(e2623)
mab-5(gf); scm::spon-1RNAi
mab-5(gf); Pegl-17::spon-1RNAi
mab-5(gf); Pegl-17::spon-1RNAi; sid-1
mab-5(gf); Pmyo-3::spon-1RNAi

Figure 2.12 Suppression of *mab-5(gof)* by *spon-1*. A) A diagram of Q descendant migration in *mab-5(e1751)* gain-of-function mutants as described in Fig 1A. *mab-5* is ectopically expressed in QR lineages, causing its descendants including AQR to migrate posteriorly. B-C) Merged DIC and fluorescent micrographs of *mab-5(gof)* animals. *Posm-6::gfp* marks the PDE neuron which serves as landmark for Q birth position. The asterisk indicates an unidentified cell body present in *mab-5(gof)* but not *wild-type* that expresses *Pgcy-32::cfp.* D) Quantification of AQR position in *mab-5(e1751)gof* mutants alone and in double mutant combination (see Fig 2). Asterisks indicate a significant ($p < 0.05$, Fisher's Exact test) reduction in the percentage of AQR residing in position 5 compared to *mab-5(gof)*. Double asterisk refers to genotypes with a significant increase in anterior migration (position 4a or more anterior) compared to *mab-5(gof)* 4a and 4b refer to location within position 4, with 4a anterior to PDE, and 4b posterior to PDE. Error bars represent 2x standard error of the proportion.

Table 2.1

A

Genotype	AQR position (%)						PQR position (%)					
	1	2	3	4	5	N	1	2	3	4	5	N
wildtype	100	0	0	0	0	300	0	0	0	0	100	300
Pegl-17::spon-1	99	1	0	0	0	108	2	2	6	9	81*	108
Pegl-17::SP::TSR1-5	99.5*	0.25	0	0	0.25	386	0.3	0	0	0.5	99.2*	372
Pegl-17::Reeler/spondin	99.5*	0	0	0	0.5	216	0.5	0	0.5	3	96*	265
Pmyo-3::mab-5	97*	3	0	0	0	210	0	0	0	0	100	210
Pspon-1::mab-5	99*	0.3	0.3	0.3	0	277	0	0	0	0	100	277
Pmyo-3::spon-1	99*	0	0.5	0.5	0	289	0	0	0	0	100	303
Pmyo-3::spon-1(RNAi)	99*	1	0	0	0	364	0	0	0	0	100	364

*$p<0.05$ compared to wildtype

B

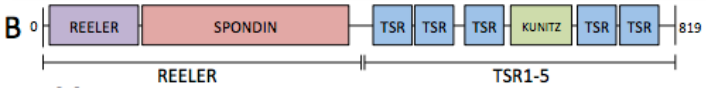

Table 2.1 *mab-5* and *spon*-1 ectopic expression. A) Animals were scored with *Pgcy-32::cfp* marking AQR and PQR. All genotypes with transgenes except *Pmyo-3::mab-5* and *wild-type* were scored as combined results of multiple independently derived extrachromosomal arrays with similar effects. *Pmyo-3::mab-5* is an integrated line. Asterisk indicates significant difference ($p<0.05$**,** Fisher's Exact test) compared to *wildtype.* B) "Reeler" constructs contain the first 430 amino acids of SPON-1, while "SP::TSR-5" constructs contain the endogenous signal peptide (29 residues) followed by residues 431-819.

Table 2.2

Genotype	AQR position (%)						PQR position (%)					
	1	2	3	4	5	N	1	2	3	4	5	N
spon-1(e2623)	98	1	1	0	0	158	0	1	0	1	98	159
mab-5(e2088)	100	0	0	0	0	249	96	2	1	0	1	249
mab-5(e2088); spon-1(e2623)	100	0	0	0	0	146	87	9	2	2	0	249
mab-5(e1239)	99	1	0	0	0	283	99	1	0	0	0	283
mab-5(e1239); spon-1(e2623)	97	2	0	0	1	316	92	3	3	1	1	316
mab-5(bx54)	100	0	0	0	0	161	86	11	2	1	0	161
mab-5(bx54); spon-1(e2623)	88*	7	5	1	0	176	80	13	5	1	2	176
mab-5(mu114)	100	0	0	0	0	202	83	11	4	0	1	202
mab-5(mu114); spon-1(e2623)	89*	9	0	0	0	226	72	20	7	0	0	225

*$p<0.05$ compared to corresponding *mab-5* additive effect (not tested for PQR)

Table 2.2 Genetic interactions of *spon-1* and *mab-5* loss-of-function. In various *mab-5* and *spon-1* hypomorphic alleles AQR and PQR were visualized using an integrated *Pgcy-32::cfp* transgene. Asterisk indicates significance compared to additive effect of *e2623* and corresponding *mab-5(lof)* ($p < 0.05$, Fisher's Exact test).

Chapter III:

EGL-20/Wnt and MAB-5/Hox Act Sequentially to Inhibit Anterior Migration of Neuroblasts in *C. elegans*

3.1 Abstract

Directed neuroblast and neuronal migration is important in the proper development of nervous systems. In *C. elegans* the bilateral Q neuroblasts QR (on the right) and QL (on the left) undergo an identical pattern of cell division and differentiation but migrate in opposite directions (QR and descendants anteriorly and QL and descendants posteriorly). EGL-20/Wnt, via canonical Wnt signaling, drives the expression of MAB-5/Hox in QL but not QR. MAB-5 acts as a determinant of posterior migration, and *mab-5* and *egl-20* mutants display anterior QL descendant migrations. Here we analyze the behaviors of QR and QL descendants as they begin their anterior and posterior migrations, and the effects of EGL-20 and MAB-5 on these behaviors. The anterior and posterior daughters of QR (QR.a/p) after the first division immediately polarize and begin anterior migration, whereas QL.a/p remain rounded and non-migratory. After ~1 hour, QL.a migrates posteriorly over QL.p. We find that in *egl-20/Wnt, bar-1/β-catenin,* and *mab-5/Hox* mutants, QL.a/p polarize and migrate anteriorly, indicating that these molecules normally inhibit anterior migration of QL.a/p. In *egl-20/Wnt* mutants, QL.a/p immediately polarize and begin migration, whereas in *bar-1/β-catenin* and *mab-5/Hox*, the cells transiently retain a rounded, non-migratory morphology before anterior migration. Thus, EGL-20/Wnt mediates an acute inhibition of anterior migration independently of BAR-1/β-catenin and MAB-5/Hox, and a later, possible transcriptional response mediated by BAR-1/β-catenin and MAB-5/Hox. In addition to inhibiting anterior migration, MAB-5/Hox also cell-autonomously promotes posterior migration of QL.a (and QR.a in a *mab-5* gain-of-function).

3.2 Introduction

The directed migration of neurons and neuroblasts is important in nervous system development to establish proper connectivity and circuits. Wnt signaling has been broadly implicated in mammalian cortical and hippocampal neurogenesis (Freese, Pino et al. 2010, Boitard, Bocchi et al. 2015, Schafer, Han et al. 2015). The Q neuroblasts in *C. elegans* have been a useful system in which to dissect the molecular mechanisms of directed neuroblast and neuronal migration (Middelkoop and Korswagen 2014). The Q cells are bilateral neuroblasts in the posterior region of *C. elegans*. The left and right Q cells produce three neurons through an identical pattern of division and programmed cell death (Sulston and Horvitz 1977, Chalfie and Sulston 1981, Middelkoop and Korswagen 2014). Despite these similarities, QR and descendants migrate to the anterior, and QL and descendants migrate to the posterior. The Q neuroblasts are born in embryogenesis as the sister cells of the V5 hypodermal seam cell and reside between the V4 and V5 seam cells in the posterior-lateral region (Sulston and Horvitz 1977, Chalfie and Sulston 1981). At hatching in the L1 larva, the Q neuroblasts undergo an initial protrusion and migration such that by 4h post hatching in the L1, QL has migrated posteriorly atop the V5 seam cell, and QR has migrated anteriorly atop the V4 seam cell (Honigberg and Kenyon 2000, Chapman, Li et al. 2008, Middelkoop and Korswagen 2014). After migrating, the Q neuroblasts undergo their first cell division producing anterior and posterior daughters (QR.a/p and QL.a/p). A posterior EGL-20/Wnt signal induces the expression of the MAB-5 Hox transcription factor in QL.a/p but not QR.a/p via canonical Wnt signaling and BAR-1/β-catenin (Chalfie, Thomson et al. 1983, Kenyon 1986, Salser and Kenyon 1992, Harris, Honigberg et al. 1996, Whangbo and Kenyon 1999, Korswagen, Herman et al. 2000, Herman 2003, Eisenmann 2005, Ji, Middelkoop et al. 2013). MAB-5 is required for the further posterior migration of QL descendants. After this

initial directional decision, Wnts redundantly control both QL and QR descendant migrations (Zinovyeva, Yamamoto et al. 2008).

The QR descendant AQR and QL descendant PQR migrate the longest distances to the anterior and posterior of any of the three Q descendant neurons, with AQR residing near the anterior deirid and posterior pharyngeal bulb and PQR residing among the phasmid ganglia posterior to the anus (Chapman, Li et al. 2008). In *egl-20* and *mab-5* loss-of-function mutants, the initial anterior and posterior migrations of QR and QL are normal (Chapman, Li et al. 2008), but QL descendants fail to migrate posteriorly and instead migrate anteriorly (Tamayo, Gujar et al. 2013). In a *mab-5* gain-of-function mutant, both QR and QL descendants migrate posteriorly despite normal initial migration of QR to the anterior and QL to the posterior (Salser and Kenyon 1992, Chapman, Li et al. 2008, Tamayo, Gujar et al. 2013). Thus, MAB-5 is a determinant of posterior migration and can act in both QL and QR descendants, but normally only acts in QL due to EGL-20/Wnt-induced expression of MAB-5 in QL but not QR. The patterns of cell division and cell death, and the gross differentiation of the three neurons produced from each cell are unaffected by *mab-5* mutation, suggesting that *mab-5* is involved in terminal differentiation to specify direction of migration, and not cell fate or differentiation generally.

While it is clear that EGL-20/Wnt and MAB-5 promote posterior migration, the mechanism by which these molecules alter QL.a/p behavior relative to QR.a/p during posterior versus anterior migration remains unclear. In this study, we analyzed the behavior of the QR.a/p and QL.a/p cells as they migrate in wild-type*, egl-20,* and *mab-5* mutants. We found that in wild-type, QR.a/p began anterior migration shortly after division, whereas QL.a/p retained a rounded, non-migratory morphology. Approximately one hour after QR.a/p migration, QL.a began to migrate posteriorly over QL.p. In *mab-5* and *egl-20* loss-of-function, QL.a/p polarized

and migrated anteriorly, similar to QR.a/p in wild-type, suggesting that both normally inhibit anterior QL.a/p migration. However, in *mab-5*, QL.a/p transiently retained a rounded, non-migratory morphology, whereas in *egl-20*, QL.a/p began migration shortly after division, similar to QR.a/p in wild-type. *bar-1/β*-catenin mutants resembled *mab-5* and displayed the transient non-migratory morphology not seen in *egl-20*. These results suggest that EGL-20 has both an acute MAB-5-independent role and a later MAB-5-dependent role in inhibiting anterior QL.a/p migration, and that the acute role of *egl-20* does not involve BAR-1/β-catenin. The *mab-5* gain-of-function mutant caused QR.a/p posterior migration similar to QL.a/p, including posterior migration of QR.a. Thus, in addition to inhibiting anterior migration, MAB-5 also promoted posterior migration.

3.3 Materials and methods

Genetics. *C. elegans* were cultured by standard techniques and all experiments performed at 20C. The following mutations and transgenes were used: LGI: *lin-44(n1792), mom-5(ne12), lin-17(n761)*; LGII *cwn-1(ok546), ayIs9[Pegl-17::gfp]*, *mig-14(ga62* and *or78*); LGIII *mab-5(gk670, e1239, e2088, mu114, bx54,* and *e1751)*, *lin-39(e1760)*; LGIV *cwn-2(ok895), egl-20(n585, ju105, gk453010, lq42,* and *lq74*); LGV *mom-2(or77), lqIs58[Pgcy-32::cfp]*; LGX: *bar-1(ga80, mu63,* and *mu349);* unmapped *lqIs220[Pegl-17::mab-5::gfp], lqIs221[Pegl-17::mab-5::gfp], casIs330[Pegl-17::gfp, Pegl-17::myr::mCherry*, *Pegl-17::his-24::mCherry, Pegl-17::MOEabd::gfp]* (Shen, Zhang et al. 2014). Genotypes containing M+ indicate that homozygous animals from a heterozygous mother were scored (i.e. had wild-type maternal gene function). In the case of the *Wnt* triple and quadruple mutant, linkage group IV containing *egl-20* and *cwn-2* was balanced by the nT1 balancer chromosome marked with pharyngeal GFP.

The *Pegl-17::mab-5::gfp* transgene was produced by placing a full-length *mab-5* cDNA downstream of the *egl-17* promoter and fused in frame to the *gfp* coding region at the 3' end (C-terminal tag). The sequence of this plasmid, pEL862, is available upon request. Six independent extrachromosomal arrays and two independent integrants (*lqIs220* and *lqIs221)* had a similar effect of causing posterior AQR migration (Fig 3.1).

***egl-20* and *mab-5* allele sequencing.** The lesions associated with *egl-20(lq42* and *lq74)* and *mab-5(mu114)* were determined by whole genome sequencing using Cloudmap (Minevich, Park et al. 2012) and confirmed with Sanger sequencing of the region. *egl-20(lq42)* was a C to T transition at chromosome IV position 9,813,864 (Wormbase release WS249) resulting in an arginine to stop; *egl-20(lq74)* was a G to A transition at 9,814,127 resulting in a cysteine to

tyrosine missense; *egl-20(gk453010)* was a C to T transition at 9,814,137 resulting in an arginine to stop; and *mab-5(mu114)* was a G to A transition at chromosome III position 7,783,349 in the first exon of *mab-5* resulting in a tryptophan to stop. *mab-5(e2088)* was a complex rearrangement involving the second exon of *mab-5* at position 7,782,932. The exact molecular nature of *e2088* could not be determined.

L1 synchronization and Q cell imaging. L1 larvae were synchronized by hatching as previously described. Gravid adults and larvae were washed from plates on which many eggs had been laid. Eggs were allowed to hatch for one hour, and newly hatched larvae, all within an hour's age of one another, were washed off and allowed to develop for specific times: 3.5h for the 3.5-4.5h timepoint; 4h for the 4-5h timepoint; 4.5h for the 4.5-5.5h timepoint; 5h for the 5-6h timepoint; 5.5h for the 5.5-6.5h timepoint; 6h for the 6-7h timepoint; 6.5h for the 6.5-7.5h timepoint; and 7h for the 7-8h timepoint. At the specified timepoint, L1 larvae were mounted for microscopic inspection and imaging of Q cell position and morphology using the *ayIs9[Pegl-17::gfp]* transgene.

Scoring Q cell position. From micrographs of L1 larvae expressing *ayIs9[Pegl-17::gfp]*, the morphology and position of QL.a/p and QR.a/p were determined. QR.a/p cells were scored as migrating if they had assumed an elongated migratory morphology with anterior protrusions and/or if QL.a had separated from QL.p (Figs 3.2 and 3.3). Cells that remained rounded and adjacent to one another were scored as non-migratory. Posterior migration of QL.a in wild type and QL.a and QR.a in *mab-5* gain-of-function was defined by QX.a extending protrusions on top of QX.p, or if QX.a could not be distinguished from QX.p, indicating that QX.a was migrating

behind or in front of QX.p (Figs 3.2 and 3.3). Significance of differences in Fig 3.4 were determined using Fisher's exact test.

For data in Fig 3.10, L1 larvae were synchronized and imaged at the 4.5-5.5h timepoint, when most QR.a/p had migrated anteriorly and QL.a/p remained rounded and non-migratory. The migrations of QL.a/p were scored in those animals with migratory QR.a/p (n = 50 for each genotype). Significances of difference were determined by Fisher's exact test.

Time-lapse imaging of QL and QR. For time-lapse imaging, the *casIs330* transgene was used to visualize QL, QR and descendants. *casIs330* contains the Q-cell promoter *egl-17* driving the expression of *myr::mCherry* (to mark membranes), *his-24::mCherry* (to mark chromatin), and *MOEabd::gfp*, the actin-binding domain of human moesin fused to GFP, to mark F-actin (Shen, Zhang et al. 2014). Images were acquired every 2 minutes using a spinning disk confocal microscope (Zeiss Axio Observer Z1, with Yokogawa CSU-X1 Spinning Disk Unit) using previously-described methods to anesthetize and immobilize animals. Images were analyzed and assembled using ImageJ and Adobe Photoshop. Time-lapse imaging with the *casIs330* transgene delayed migrations and cell divisions by ~2-fold compared to *ayIs9* still images, but the same pattern of QL.a/p and QR.a/p migration as observed with *ayIs9* still images was conserved.

Scoring AQR and PQR migration. AQR and PQR are neuronal descendants of QR and QL, respectively, and migrate the longest distances of Q descendants into the head and tail of the animal. AQR normally migrates anteriorly to a region near the anterior deirid and the posterior pharyngeal bulb, and PQR normally migrates posteriorly near the phasmid ganglia posterior to the anus in the tail. AQR and PQR position was scored as described previously. The animal is

divided into five regions in the anterior-posterior axis: Position 1 is the normal position of AQR; position 2 is posterior to position 1 but anterior to the vulva; position 3 is adjacent to the vulva; position 4 is the position of Q cell birth; and position 5 is the normal position of PQR posterior to the anus. AQR and PQR position was scored in 100 animals of each genotype indicated in Fig 3.1.

3.4 Results

Wnt signaling redundantly controls AQR and PQR migration. A genome-wide screen for new mutations affecting AQR and PQR migration identified two new mutations, *lq42* and *lq74*. Both caused anterior PQR migration, and minor or no defects in AQR migration (Fig 3.1). Genes affected by the mutations were mapped by whole genome single nucleotide polymorphism resequencing using the Cloudmap protocol (Minevich, Park et al. 2012) (data not shown). Both mapped to a region in the center of LG IV, and each harbored a mutation in the *egl-20* gene, which encodes a *C. elegans* Wnt molecule. *egl-20* has been shown previously to affect PQR but not AQR migration (Chapman, Li et al. 2008), consistent with the phenotypes of *lq42* and *lq74*. *lq42* introduced a premature stop codon at arginine 296 (C to T), and *lq74* was a missense mutation changing cysteine 248 to tyrosine (G to A) (see Methods). Both failed to complement *egl-20(n585)* for PQR migration (data not shown). The *egl-20(gk453010)* allele was generated by the Million Mutation Project (present in strain VC40076) (Thompson, Edgley et al. 2013). *gk453010* is a G to A transition resulting in an arginine 245 to opal stop codon mutation. The *egl-20(hu105)* allele also introduces a premature stop codon (Coudreuse, Roel et al. 2006, Penigault and Felix 2011). *lq42, lq74, hu105,* and *gk453010* each displayed nearly completely penetrant anterior PQR migration (Fig 3.1), suggesting that they are all putative null mutations, with the exception of the *lq74* missense mutation which may retain some function (1% PQR did not migrate completely to head).

AQR and PQR migration was analyzed in mutants of the four other *C. elegans Wnt* genes *cwn-1, cwn-2, lin-44,* and *mom-2* (Fig 3.1). Putative null alleles of *cwn-2* and *lin-44* displayed no defects. A null *cwn-1* allele displayed 29% failure of AQR to complete anterior migration. *mom-2*, which has not been previously reported to affect Q descendant migrations, displayed 3% AQR and PQR migration defects in the partial loss of function *or77M+* allele (M+ is used to designate homozygous animals from a heterozygous mother and therefore with a wild-type maternal contribution of gene function). Thus, *egl-20, cwn-1,* and, *mom-2* each affect AQR and PQR migration in distinct ways.

Redundancy among Wnts in Q descendant migrations has been reported previously (Zinovyeva, Yamamoto et al. 2008). The *Wnt* triple mutant *egl-20(n585) cwn-2(ok895); cwn-1(ok546)* displayed highly penetrant PQR anterior migration and a failure of both AQR and PQR migration along the anterior route (Fig 3.1). No AQR or PQR migrated posteriorly in this genotype. Mutation of *lin-44* in the *egl-20(n585M+) cwn-2(ok895M+); cwn-1(ok546); lin-44(n1792)* quadruple mutant resulted in posterior migration of both AQR and PQR (28% and 37%) (Fig 3.1). This indicates that *lin-44* activity inhibits posterior AQR and PQR migration in the absence of *egl-20, cwn-1*, and *cwn-2*, and suggests that *lin-44* can act as a posterior repellant. Previous studies indicated that *lin-44* caused posterior displacement of QL descendants PVM and SDQL (Zinovyeva, Yamamoto et al. 2008), and HSN (Pan, Howell et al. 2006), in certain multiple Wnt mutant combinations, consistent with a posterior repellant activity of *lin-44.* The triple and quadruple Wnt mutants were scored with maternal contribution of both *egl-20* and *cwn-2,* so we cannot be certain that maternal Wnt function remains in these mutants. MIG-14/Wntless is required for Wnt processing and function and affects QL descendant migrations (Yang, Lorenowicz et al. 2008). Two *mig-14* mutants had less severe defects than the *Wnt* triple

and quadruple mutants (Fig 3.1). The likely hypomorph *ga62* had weak effects on both AQR and PQR, and the lethal in-frame deletion mutation *or78*, with wild-type maternal contribution, resembled *egl-20* and only affected PQR migration. These data suggest either that these mutations did not completely eliminate *mig-14* function, or that *mig-14* is not involved in all Wnt-related signaling events.

Wnt signaling might not affect early Q neuroblast migration. The above results, along with previous studies (Zinovyeva, Yamamoto et al. 2008, Sundararajan, Norris et al. 2014), indicate that the five *C. elegans Wnt* genes and four *Frizzled* genes *mig-1, lin-17, cfz-2,* and *mom-5* act redundantly to control Q descendant migration. However, *egl-20* alone and the *egl-20(n585) cwn-2; cwn-1* triple mutant displayed no defects in early Q anterior-posterior protrusion and migration, despite severe AQR and PQR descendant migration defects (Chapman, Li et al. 2008, Sundararajan, Norris et al. 2014) (Fig 3.1). To further investigate the role of Wnts in early Q protrusion and migration, we analyzed early QL and QR protrusion and migration with the *ayIs9[Pegl-17::gfp]* transgene, expressed in the early Q cells (Branda and Stern 2000, Cordes, Frank et al. 2006, Sundararajan and Lundquist 2012). Two additional mutant combinations were tested: the *Wnt* triple mutant *egl-20(lq42M+); mom-2(or77M+); lin-44(n1792)* and the *Frizzled* double mutant *mom-5(ne12M+) lin-17(n761M+)*. Neither displayed defects in direction of initial QL and QR migration (QL divided atop V5 and QR atop V4 ($n \geq 10$)) (data not shown). We have not scored early Q migrations in the absence of all Wnt signaling due to maternal perdurance and/or incomplete knockdown of all Wnt genes at once. However, we have not observed early Q directional migration defects in any Wnt signaling mutant combination tested, despite strong AQR and PQR migration defects. This suggests Wnt signaling might not be

involved in early Q anterior-posterior protrusion and migration, with function restricted to later migrations of the Q descendants.

QR daughters begin migration immediately after QR division. In order to understand how EGL-20/Wnt signaling drives posterior QL descendant migration, the behaviors of QR.a/p and QL.a/p just after division were analyzed. We monitored the position of the Q cell daughters using a *Pegl-17::gfp* transgene *ayIs9* expressed in the Q cells (Fig 3.2). Newly-hatched L1 larvae were synchronized within the same hour-long age range at half-hour timepoints after hatching (e.g. 3.5-4.5h, 4.0-5.0h, 4.5-5.5h, 5.0-6.0h, 5.5-6.5h, 6.0-7.0h) (see Methods for synchronization of L1 larvae). The positions of QR, QL, and their daughters were determined in 20 animals at each timepoint. At 3.5-4.5h, 19/20 of the QR examined had divided, whereas only 13/20 of the QL had divided. This trend held true in all genotypes analyzed, suggesting that QL divides slightly later than QR. Indeed, at 4.0-5.0h, 4/20 QL had not yet divided, but 20/20 of the QRs had divided.

After division, the QR and QL daughters had a rounded morphology with little or no protrusion (Fig 3.2A, B and Fig 3.3). Shortly after division in the 4.0-5.0h timepoint, the QR daughters polarized and begun migrating to the anterior (Fig 3.2C and D). Migrating QR.a/p cells first elongated in the anterior-posterior axis and then extended F-actin-rich lamellipodia-like protrusions in the direction of migration (to the anterior), similar to what has been previously reported (Fig 3.3A and 3.S1 File) (Wang, Zhou et al. 2013, Shen, Zhang et al. 2014, Tian, Diao et al. 2015). The QR.a/p cells maintained this polarized, migratory morphology as they migrated anteriorly until their second round of cell division at approximately 7h post-hatching (Fig 3.2D-I and Fig 3.3A). At 6.0-7.0, QR.a/p cells began to lose the polarized morphology and assumed a

rounded morphology in preparation for the second round of cell division (Fig 3.2I and Fig 3.3A). Time-lapse imaging with the *casIs330* transgene (3.S1 File, 3.S2 File, and Fig 3.3) (Wang, Zhou et al. 2013) resulted in an approximately 2-fold delay in migration and division relative to the *ayIs9* transgene.

To account for variability in the timing of migration, QR.a/p migration was quantified in 20 animals at each time point using *ayIs9* (Fig 3.4). Cells were scored as migratory if they extended protrusions to the anterior, often accompanied by migration from their birthplace and also separation from one another (Fig 3.2E-F and Fig 3.3A). At 4.0-5.0h, 6/20 of the QR daughters had polarized and started migrating to the anterior (Fig 3.4). At 4.5-5.5h, 16/20 were migrating, and at 5.0-6.0, 18/20. By 5.5-6.5h, all (20/20) of the QR.a/p were polarized and migrating to the anterior (Fig 3.4).

QL daughters remain rounded and non-migratory. In contrast to QR.a/p, the QL.a/p daughters did not polarize and migrate anteriorly. From 3.5-5.5h, at a time when QR.a/p had polarized and begun migration, the QL.a/p cells retained a rounded, non-migratory morphology and did not migrate (Fig 3.2 A'-F' and Fig 3.3B). Occasionally, protrusions were observed on non-migratory QL.a/p (e.g. Fig 3.2F'), but they did not assume the elongated morphology and robust anterior protrusion observed in QR.a/p. At 5.0-6.0h, the anterior QL.a daughters began migrating posteriorly over the anterior QL.p daughters, which retained a rounded morphology (Fig 3.2G'-H' and Fig 3.3B) (3.S2 File). QL.p showed no significant migration over this time period, consistent with previous observations (Ou and Vale 2009). Often, QL.a apparently migrated over the top of QL.p (Fig 3.2H' and Fig 3.3B). QL.a was scored as migrating

posteriorly if it was over QL.p, or if it was indistinguishable from QL.p suggesting it was migrating in front of or behind QL.p (data not shown).

Quantification of migration in 20 animals showed that only 1/20 QL.a began posterior migration at the 5.0-6.0h timepoint (Fig 3.4). At 5.5-6.5h, 13/20 of the anterior QL.a cells had migrated. At 6.0-7.0h, all QL.a had migrated posterior to QL.p and began to assume a rounded morphology preceding the second round of cell division (Fig 3.2I'). Posterior QL.p showed little or no polarization or migration in the entire time before the second round of cell division (7.0-8.0h after hatching).

In sum, QR.a/p polarized and began to migrate anteriorly shortly after division. The division of QL was delayed compared to QR, and the QL.a/p daughters remained rounded and non-migratory in the 3.5-5.0h time window while the QR.a/p daughters migrated to the anterior. At 5.0-6.0h, QL.a began migrating posteriorly over QL.p and continued posterior migration. QL.p did not migrate in this time period. A schematic summary of QR.a/p and QL.a/p migratory behavior is shown in Fig 3.5.

EGL-20/Wnt and MAB-5/Hox inhibit QL.a/p anterior polarization and migration. *egl-20* and *mab-5* loss-of-function mutations caused anterior migration of PQR and did not affect AQR migration (Fig 3.1). *mab-5(e1239, gk670,* and *e2088)* all showed nearly completely penetrant PQR anterior migration, suggesting that they are all strong loss-of-function alleles. *mab-5(e2088)* was a complex rearrangement affecting the second exon of *mab-5* (see Methods). *mab-5(bx54)*, a missense mutation in the homeodomain of *mab-5* (Chow and Emmons 1994), and *mab-5(mu114)*, a premature stop codon early in the first exon (see Methods), displayed weaker defects, indicating that they are hypomorphic alleles.

As expected, direction and extent of initial QR and QL migration prior to the first Q cell division was unaffected by *egl-20* and *mab-5* (Figs 3.4, 3.6A, and 3.7A). Furthermore, the QR.a/p anterior and posterior daughters polarized and migrated to the anterior in all cases (Figs 3.4, 3.6, and 3.7). Previous work showed that in *egl-20* mutants, the posterior QR.p daughter displayed variable posterior polarization during migration (Mentink, Middelkoop et al. 2014). We did not follow this phenotype in these studies.

In *egl-20(n585),* QL.a/p polarized and migrated anteriorly shortly after division at the 4.0-5.0h timepoint, similar to QR.a/p (Fig 4). In some cases, QL.a/p polarized and began to migrate before QR.a/p (Fig 3.6B). Upon quantification, 3/20 QL.a/p at the 4.0-5.0 timepoint and 14/20 at the 4.5-5.5h timepoint had polarized and begun anterior migration, similar to QR.a/p (Fig 3.4). QL.a/p resembled QR.a/p in their anterior migrations through the remaining timepoints (Fig 3.6C). Thus, in the absence of EGL-20/Wnt, QL.a/p polarized and migrated anteriorly, indicating that EGL-20 inhibits polarization and anterior migration of QL.a/p.

In *mab-5* mutants, QL.a/p also polarized and migrated to the anterior similar to *egl-20* (Fig 3.7). Upon quantification of two *mab-5* mutants, 2/20 QL.a/p polarized and began migrating to the anterior at the 4.0-5.0h timepoint in both mutants, and 7/20 and 4/20 at the 4.5-5.5h timepoint (Fig 3.4). By 5.5-6.5h, all QL.a/p had migrated anteriorly in both *mab-5* mutants (Fig 3.4). These results suggest that MAB-5/Hox also inhibits QL.a/p anterior polarization and migration.

***mab-5* gain-of-function causes posterior QR.a/p migration.** *mab-5(e1751)* is a gain-of-function variant that results in ectopic expression of *mab-5* in cells, including in QRs which normally do not express it (Salser, Loer et al. 1993). *mab-5(e1751)* mutants display posterior

migration of both QL and QR descendant neurons AQR and PQR, the opposite of *mab-5* loss-of-function (Tamayo, Gujar et al. 2013) (Fig 3.1). We analyzed Q descendant behaviors in *mab-5(e1751)*. Initial Q migrations were normal, as QR migrated anteriorly and QL posteriorly, indicating that *mab-5(e1751)* does not affect initial Q migration (Fig 3.8A). QL.a/p behavior generally resembled what is seen in wild type (persistent rounded and non-migratory morphology until 5.0-6.0h, with QL.a beginning to migrate posteriorly over QL.p at this time) (Fig 3.8).

Strikingly, QR.a/p behaved similarly to QL.a/p in *mab-5(e1751)* (Fig 3.8). Some QR.a/p slightly separated from one another, but did not show the polarized and anterior migratory behavior seen in wild-type QR.a/p from 4h onward. Eventually, QR.a migrated posteriorly over QR.p just as QL.a did, beginning at the 5.5-6.5h timepoint (Figs 3.4 and 3.8). *mab-5(e1751)* resulted in a delay in QR.a/p and QL.a/p posterior migration relative to *wild-type* QL.a/p (Fig 3.4). At the 6.0-7.0h timepoint, all of QL.a had migrated posteriorly in *wild-type* where only 12/20 QR.a and 10/20 QL.a had migrated posteriorly in *mab-5(e1751)*. Together with *mab-5* loss-of-function, these data suggest that MAB-5 normally inhibits anterior migration of QL.a/p and can also inhibit QR.a/p anterior migration in the gain-of-function mutant (Fig 3.5). In addition to inhibiting anterior migration, *mab-5* activity can also induce posterior migration of the QR.a cell, similar to wild-type QL.a.

mab-5 is expressed in QL as well as in other cells surrounding QL in the posterior of the animal. We constructed a transgene driving *mab-5* expression from the *egl-17* promoter expressed in the early Q cells. Q descendant neurons AQR and PQR both migrated posteriorly in animals harboring this transgene, similar to *mab-5(e1751)* (Fig 3.1). Initial QL and QR migration were normal in *Pegl-17::mab-5* animals, but both QL.a/p and QR.a/p resembled *mab-*

5(e1751) (they remained rounded and non-migratory) (Fig 3.9). These data indicate that MAB-5 expression in the Q cells themselves is sufficient to prevent anterior migration of QL.a/p and QR.a/p and drive their posterior migration, consistent with previous results showing autonomy of *mab-5* function in neuronal descendant migrations (Salser and Kenyon 1992).

In *egl-20(n585); mab-5(e1751)* and *egl-20(n585); Pegl-17::mab-5* animals, AQR and PQR both migrated posteriorly similar to *mab-5* gain-of-function alone, consistent with *mab-5* acting downstream of *egl-20*. At the 4.5-5.5h timepoint, QL.a/p and QR.a/p resembled *mab-5(e1751)* alone and had not begun migration to the anterior as in *egl-20(n585)* (data not shown). However, both QL.a/p and QR.a/p showed the transient separation before posterior migration as observed for QR.a/p in *mab-5(e1751)* (2/21 QL.a/p and 4/21 QR.a/p for *egl-20(n585); mab-5(e1751),* and 1/22 QL.a/p and 7/22 QR.a/p for *egl-20(n585); Pegl-17::mab-5*). In sum, these results indicate that the effects of *mab-5* gain-of-function are independent of *egl-20*, and are consistent with MAB-5 acting downstream of EGL-20.

QL.a/p anterior migration is delayed in *mab-5* mutants compared to *egl-20*. Loss of function of *egl-20* or *mab-5* resulted in anterior migration of QL.a/p. While similar to *egl-20*, in *mab-5* mutants we noted a delay in QL.a/p polarization relative to QR.a/p not seen in *egl-20* (Fig 3.4). QL.a/p often remained unpolarized while QR.a/p had begun migration (Fig 3.7B). In *mab-5(e1239)* at 4.5-5.5h, 7/20 QL.a/p had begun migration while 16/20 QR.a/p had (Fig 3.4). The difference was more extreme in *mab-5(gk670)* (4/20 versus 17/20). Meanwhile, 14/20 QL.a/p began migration in *egl-20(n585)* at the same timepoint (significantly more than *mab-5(gk670)* (*$p = 0.004$*)). This delay is also observed in the 5.0-6.0h timepoint (Fig 3.4), where 20/20 QL.a/p

began anterior migration in *egl-20(n585)*, compared to 17/20 and 10/20 ($p = 0.0004$) in two *mab-5* mutants, despite all QR.a/p having begun migration in *mab-5* mutants.

To explore this difference between *mab-5* and *egl-20* further, we determined, at the 4.5-5.5h timepoint, the proportion of QL.a/p that had polarized and begun to migrate anteriorly in animals with migrating QR.a/p (Fig 3.10). In wild type, 4% of QL.a had begun migration (to the posterior), while in *egl-20(n585)* and *egl-20(hu105)*, 78% and 80% of QL.a/p had begun anterior migration ($p < 0.05$). Furthermore, we noted that 8% of QL.a/p polarized and migrated before QR.a/p in *egl-20(n585)* (Fig 3.6B).

In this assay, two *mab*-5 mutants displayed significantly less QL.a/p migration compared *egl-20* (24% and 18% compared to 78% and 80%, $p < 0.05$) (Fig 3.10). These data demonstrate that QL.a/p anterior polarization and migration in *mab-5* mutants is delayed relative to *egl-20*, with QL.a/p in *mab-5* transiently retaining a rounded, non-migratory morphology (Fig 3.7B), a delay not observed in *egl-20* mutants.

***bar-1/β-catenin* QL.a/p migration resembles *mab-5*.** MAB-5 expression in QL.a/p is induced by canonical Wnt signaling involving EGL-20/Wnt and BAR-1/β-catenin (Chalfie, Thomson et al. 1983, Kenyon 1986, Salser and Kenyon 1992, Harris, Honigberg et al. 1996, Whangbo and Kenyon 1999, Korswagen, Herman et al. 2000, Herman 2003, Eisenmann 2005). *bar-1* loss-of-function mutations displayed anterior PQR migration similar to *egl-20* and *mab-5* (Fig 3.1). *bar-1(ga80* and *mu349)* displayed nearly completely-penetrant anterior PQR migration, suggesting they cause strong loss of function, although *mu349* showed a significantly weaker effect (Fig 3.1). *bar-1(mu63)* showed much weaker PQR defects and is likely a hypomorphic allele (Fig 3.1). We analyzed QL.a/p behavior in the strong *bar-1* alleles *ga80* and *mu349*. As in *egl-20*

and *mab-5*, QL.a/p polarized and migrated anteriorly (Fig 3.10). To determine if *bar-1* resembled *egl-20* or displayed the delay of *mab*-5, we scored the percentage of migrating QL.a/p in *bar-1* mutants in which QR.a/p had begun migration at the 4.5-5.5h timepoint (Fig 3.10): 29% of *bar-1(ga80)* and 36% of *bar-1(mu349)* showed QL.a/p migration. This was significantly less than *egl-20* mutants ($p < 0.05$) and was not significantly different from *mab-5* (Fig 3.10). Thus, *bar-1* mutants also displayed a delay in QL.a/p anterior migration similar to *mab-5* and not seen in *egl-20*.

3.5 Discussion

MAB-5/Hox and EGL-20/Wnt inhibit anterior migration. Here we describe the distinct behaviors of QL and QR descendants in response to Wnt signaling. After the first Q cell division, QR.a/p and QL.a/p had a rounded morphology with little or no protrusion. Shortly after division, QR.a/p began to elongate in the anterior-posterior axis by extending F-actin-rich lamellipodial protrusions to the anterior. They then began anterior migration with polarized, migratory morphology for approximately 2h, at which time they stopped migrating, become rounded, and underwent their second round of cell division. In contrast, QL.a/p remain rounded with little or no protrusive morphology and migration. Our results show that EGL-20/Wnt and MAB-5/Hox are required to prevent QL.a/p from polarizing and migrating to the anterior. When MAB-5/Hox was ectopically expressed in QR.a/p via the *mab-5(e1751)* mutation or transgenic expression of *mab-5* in both Q cells, QR.a/p polarization and migration was similarly inhibited.

EGL-20/Wnt has MAB-5-independent and MAB-5-dependent roles. Both *egl-20* and *mab-5* loss-of-function mutants displayed anterior QL.a/p migration. However, we noted a delay in anterior migration in *mab-5* not observed in *egl-20.* QL.a/p in *mab-5* remain rounded and non-migratory for a short time (~0.5-1h) before they polarized and migrated anteriorly. In contrast, QL.a/p in *egl-20* mutants resembled QR.a/p: they immediately polarized and began anterior migration. *mab-5* expression is induced in QL by canonical Wnt signaling via EGL-20/Wnt and BAR-1/ β-catenin. The delay in QL.a/p anterior migration was also observed in *bar-1/β-catenin* mutants, similar to *mab*-5. This suggests that EGL-20/Wnt has at least two distinct roles in inhibiting migration (Fig 3.11). EGL-20/Wnt might acutely inhibit migration in a MAB-5 and BAR-1-independent pathway, and later, via canonical Wnt signaling and MAB-5 expression,

consolidate this inhibition. Consistent with this idea of step-wise regulation of Q descendant migration by EGL-20, previous studies showed that QR descendants display cell-intrinsic temporal responses to Wnt signals that determines their final positions in the anterior-posterior axis (Mentink, Middelkoop et al. 2014).

How might EGL-20 and MAB-5 inhibit QL.a/p anterior migration? EGL-20 could activate an acute response by acting directly on the ability of the cell to polarize and migrate (e.g. e.g. inhibiting cytoskeletal rearrangements and protrusive events necessary for migration). This response does not require BAR-1 or MAB-5, suggesting that it might be a non-canonical Wnt signaling pathway that acts directly on protrusive ability (e.g. the cytoskeleton). There is precedence for BAR-1-independent Wnt signaling in later QR descendant migrations, which are shortened in *Wnt* mutants independent of BAR-1/β-catenin (Zinovyeva, Yamamoto et al. 2008). In addition to the acute role, which is transient, EGL-20 can also activate canonical Wnt signaling via BAR-1/β-catenin resulting in MAB-5 expression. The acute EGL-20 signal might inhibit anterior migration until MAB-5 is expressed, which begins in QL during its initial migration and before division (Ji, Middelkoop et al. 2013). In this scenario, the delay in anterior migration in *mab-5* mutants might indicate the lag time in *mab-5* expression and regulation of target gene expression to inhibit anterior migration. Wnt signaling and *mab-5* expression remain tied in a feedback loop that ensures consistent and continuous levels of *mab-5* expression (Ji, Middelkoop et al. 2013).

MAB-5 might consolidate inhibition of anterior migration by regulating genes involved in polarization and migration and/or genes involved in responding to an A-P guidance cue. Indeed, expression of the Hox factor LIN-39 is inhibited in QL.a/p by MAB-5 (Wang, Zhou et al. 2013). LIN-39 normally promotes anterior migration in QR.a/p by driving the expression of

the transmembrane MIG-13 molecule (Wang, Zhou et al. 2013). In parallel to SDN-1/Syndecan (Sundararajan, Norris et al. 2015), MIG-13 responds to an A-P guidance cue by mediating cytoskeletal rearrangements underlying anterior protrusion and migration (Wang, Zhou et al. 2013). Thus, MAB-5 might inhibit anterior QL.a/p migration in part by inhibiting LIN-39 expression in QL.a/p.

MAB-5 promotes posterior migration. While QL.a/p normally remain rounded and non-migratory while QR.a/p migrate anteriorly, QL.a eventually migrates posteriorly over QL.p. QL.a posterior migration is dependent on MAB-5, as we found that ectopic expression of MAB-5 in both QL and QR resulted in posterior migration of both anterior daughters. Thus, MAB-5 is not simply inhibiting migration. One possibility is that by inhibiting anterior migration, MAB-5 allows QL.a/p to respond to a later *de novo* guidance signal that directs posterior migration. By not migrating anteriorly, QL.a/p are in a position to respond to this new signal. Alternatively, MAB-5 might regulate gene expression in QL.a/p that alters response to a posterior guidance cue, possibly the same A-P cue used by QR.a/p to migrate anteriorly. As Wnts regulate Q descendant migrations, MAB-5 might alter the response of QL.a/p to Wnt signals directing anterior-posterior migrations.

The *Wnt* quadruple mutant *cwn-1; egl-20 cwn-2; lin-44* showed some posterior migration of both AQR and PQR. EGL-20/Wnt is required to activate *mab-5* expression, so it is possible that in the *Wnt* quadruple, posterior migration occurs in the absence of *mab-5*. This indicates that Wnts constitute the anterior-posterior guidance system to which *mab-5* modifies responses. In the absence of Wnts, some cells migrate posteriorly despite not having *mab-5* expression due to a disrupted anterior-posterior guidance system. It is also possible that *mab-5* is activated in

an *egl-20*-independent manner in both AQR and PQR in this quadruple mutant and is responsible for posterior migration.

In sum, our results indicate that both QR.a/p and QL.a/p can both respond to an anterior migration signal. Normally, EGL-20 prevents QL.a/p from responding by first acutely inhibiting migration, likely due to the inherent sensitivity of QL to the EGL-20 signal (Whangbo and Kenyon 1999). EGL-20 also activates *mab-5* expression in QL.a/p via BAR-1/ β-catenin and canonical Wnt signaling, which likely results in changes in gene expression that maintains inhibition of anterior migration. MAB-5-induced gene expression might also then promote posterior migration. However, it is also possible that by inhibiting anterior migration, *mab-5* allows the QL.a/p cells to respond to a later posterior migration signal that is not present early in QL.a/p migration. These results indicate that *egl-20* and *mab-5* mutations do not transform QL into a QR-like fate, but rather discretely modify how these cells differentially respond to anterior-posterior guidance information.

These studies and others are beginning to paint a picture of the early migration events of the Q neuroblasts and descendants. Initial anterior QR and posterior QL migration are regulated by inherent differences in the functions of the transmembrane molecules UNC-40/DCC and PTP-3/LAR in QR versus QL (Sundararajan and Lundquist 2012), and does not appear to involve Wnt signaling. While the signal specifying initial anterior versus posterior migration is unknown, the Fat-like Cadherin CDH-4 non-autonomously controls UNC-40/DCC and PTP-3/LAR function in QR versus QL (Sundararajan, Norris et al. 2014). Due to posterior migration of QL and inherent differences in sensitivity, an EGL-20/Wnt signal acutely inhibits QL.a/p anterior migrations, possibly via a non-canonical mechanism. Via canonical Wnt signaling and BAR-1/β-catenin, EGL-20/Wnt also induces MAB-5 expression in QL.a/p, which inhibits LIN-39/Hox and thus

MIG-13 expression and consolidates inhibition of anterior migration. Additionally, MAB-5 might regulate other genes that inhibit anterior migration and direct posterior migration. It will be important to identify the potential non-canonical mechanism of EGL-20/Wnt inhibition of anterior migration, and to define other genes regulated by MAB-5 to autonomously inhibit anterior migration and promote posterior migration.

3.6 Figures

Figure 3.1

Genotype	AQR position (%)						PQR position (%)					
	1	2	3	4	5	N	1	2	3	4	5	N
wild-type	100	0	0	0	0	>300	0	0	0	0	100	>300
egl-20(n585)	100	0	0	0	0	100	97	2	1	0	0	100
egl-20(gk453010)	100	0	0	0	0	100	98	0	0	0	2	100
egl-20(hu105)	100	0	0	0	0	100	99	0	0	0	1	100
egl-20(lq42)	100	0	0	0	0	100	98	0	0	0	2	100
egl-20(lq74)	99	0	0	1	0	100	98	1	0	0	1	100
cwn-1(ok546)	71	23	6	0	0	100	0	0	0	0	100	100
cwn-2(ok895)	100	0	0	0	0	100	0	0	0	0	100	100
lin-44(n1792)	100	0	0	0	0	100	0	0	0	0	100	100
mom-2(or77M+)	97	2	1	0	0	200	0	0	1	2	97	100
egl-20(n585M+) cwn-2(ok895M+); cwn-1(ok546)	39	49	10	2	0	100	32	55	12	1	0	100
egl-20(n585M+) cwn-2(ok895M+); cwn-1(ok546); lin-44(n1792)	6	18	25	23	28	200	3	16	19	25	37	200
mig-14(ga62)	93	5	0	1	1	116	0	1	0	0	99	116
mig-14(or78M+)	100	0	0	0	0	100	96	0	0	0	4	100
mab-5(e1239)	99	1	0	0	0	283	99	1	0	0	0	283
mab-5(gk670)	100	0	0	0	0	164	99	1	0	0	0	164
mab-5(e2088)	100	0	0	0	0	100	98	2	0	0	0	100
mab-5(mu114)	100	0	0	0	0	100	77*	17	5	1	0	100
mab-5(bx54)	100	0	0	0	0	100	78*	12	7	2	1	100
mab-5(e1751)	0	0	0	10	90	100	0	0	0	0	100	100
lqIs220[Pegl-17::mab-5]	0	0	0	11	89	100	0	0	0	0	100	100
lqIs221[Pegl-17::mab-5]	0	0	0	8	92	100	0	0	0	0	100	100
lqIs220; mab-5(e1239)	0	0	0	4	96	238	0	0	1	2	97	238
lqIs220; egl-20(gk453010)	0	0	1	4	95	194	0	0	0	1	99	194
bar-1(ga80)	100	0	0	0	0	100	98	0	0	0	2	100
bar-1(mu349)	100	0	0	0	0	100	89**	6	4	1	0	100
bar-1(mu63)	100	0	0	0	0	100	6***	4	13	28	49	100

*$p < 0.0001$ compared to *mab-5(e1239, gk670,* and *e2088)*
**$p = 0.0184$ compared to *bar-1(ga80)*
***$p < 0.0001$ compared to *bar-1(ga80)* and *bar-1(mu349)*

Figure 3.1 AQR and PQR migration in Wnt pathway and Hox mutants. The percentages of AQR and PQR in mutants is shown, with respect to positions 1-5 as described in Methods and shown on the diagram. Statistical significance was calculated using Fisher's Exact test.

Figure 3.2

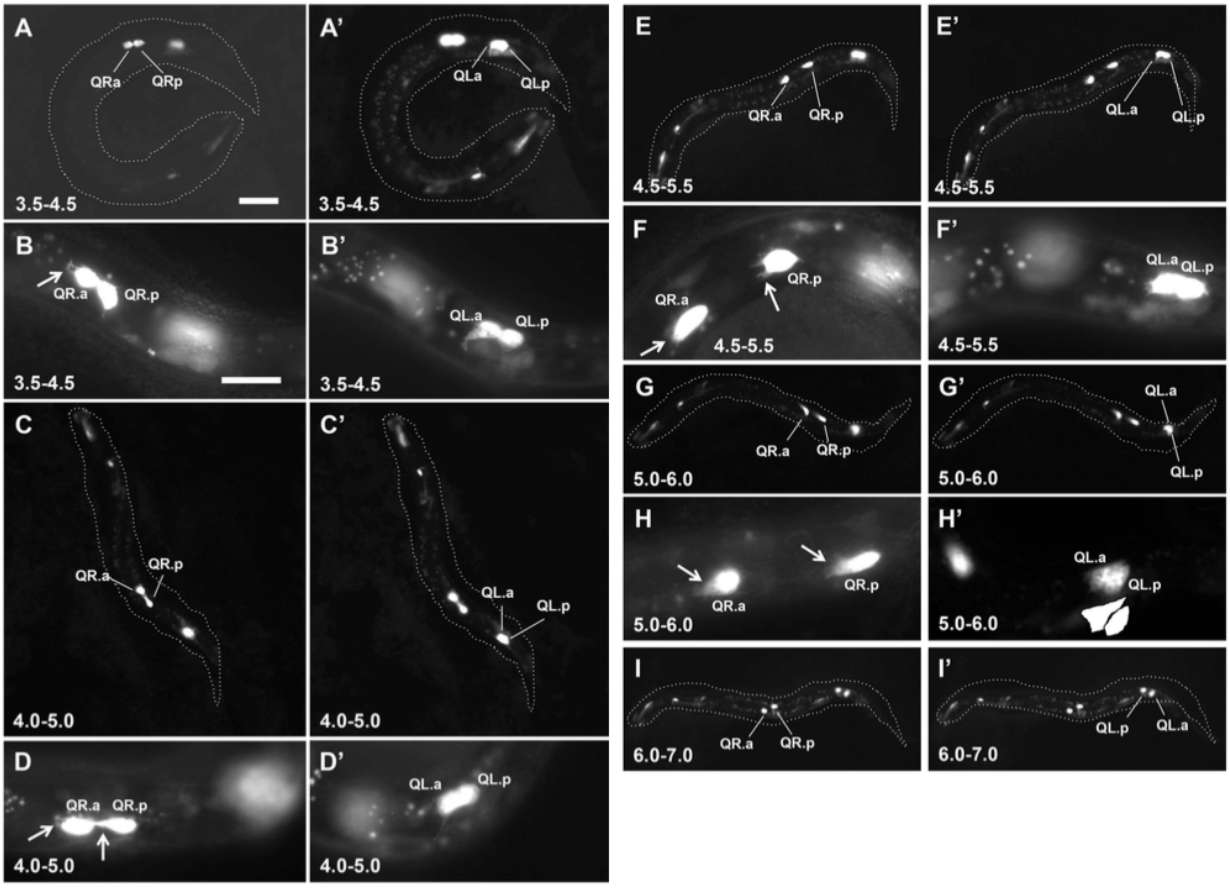
A
QRa
QRp
3.5-4.5
A'
QLa
QLp
3.5-4.5
B
QR.a
QR.p
3.5-4.5
B'
QL.a
QL.p
3.5-4.5
C
QR.a
QR.p
4.0-5.0
C'
QL.a
QL.p
4.0-5.0
D
QR.a QR.p
4.0-5.0
D'
QL.a
QL.p
4.0-5.0
E
QR.a
QR.p
4.5-5.5
E'
QL.a
QL.p
4.5-5.5
F
QR.p
QR.a
4.5-5.5
F'
QL.a QL.p
4.5-5.5
G
QR.a
QR.p
5.0-6.0
G'
QL.a
QL.p
5.0-6.0
H
QR.a
QR.p
5.0-6.0
H'
QL.a
QL.p
5.0-6.0
I
QR.a
QR.p
6.0-7.0
I'
QL.p
QL.a
6.0-7.0

Figure 3.2 Q descendant migrations in *wild-type*. Fluorescent micrographs of *ayIs9[Pegl-17::gfp]* expression in Q descendants are shown in the same animals (QR, A-I; QL, A'-I'). Anterior is to the left. The dashed lines indicate the body of the whole animal in the micrograph. Arrows indicate anterior protrusions characteristic of the QR migratory morphology. The scale bar in A represents 5μm for A, C, E, G, and I; and the scale bar in B represents 5μm for B, D, F, and H.

Figure 3.3

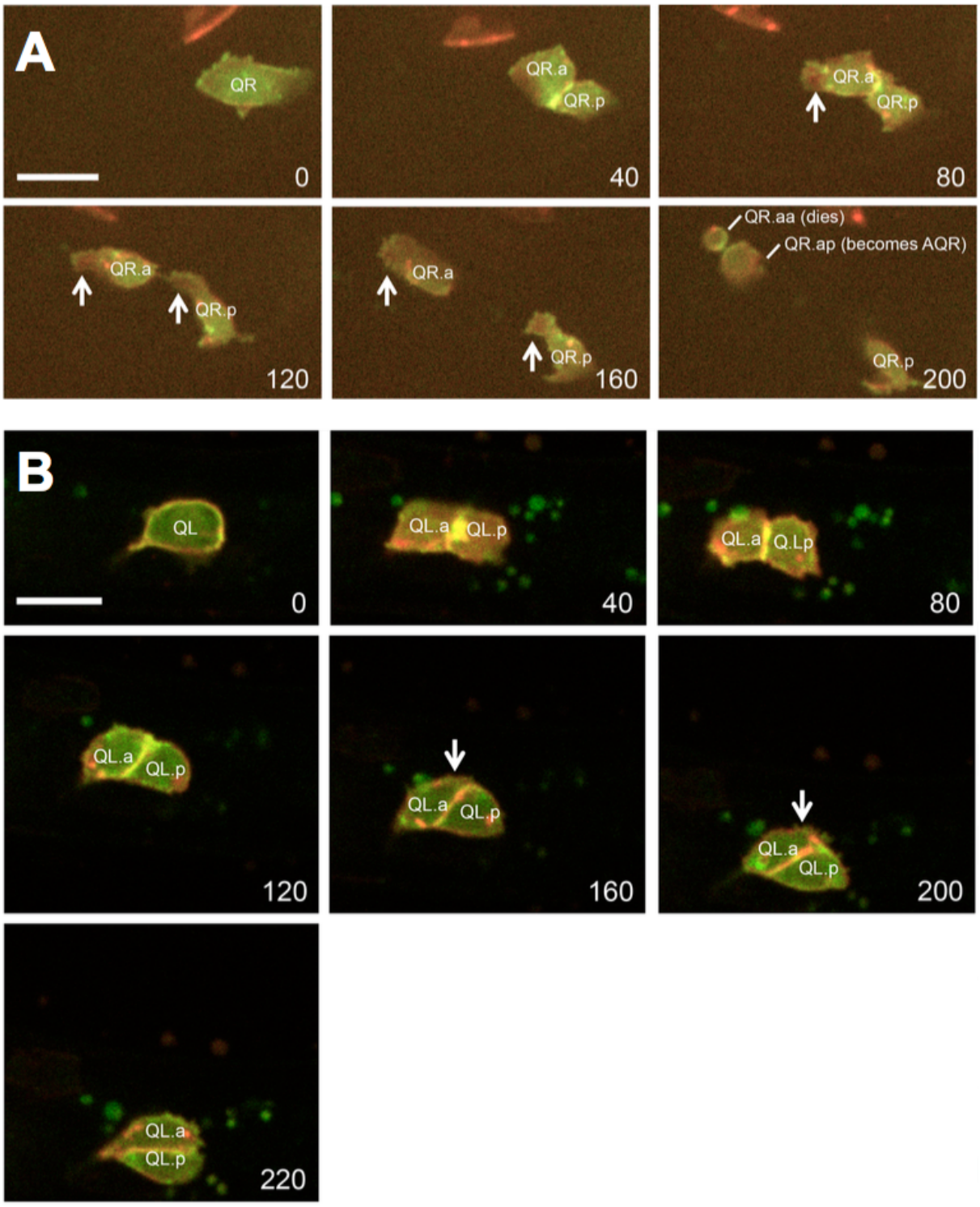
A
QR
0
QR.a
QR.p
40
QR.a
QR.p
80
QR.a
QR.p
120
QR.a
QR.p
160
QR.aa (dies)
QR.ap (becomes AQR)
QR.p
200
B
QL
0
QL.a
QL.p
40
QL.a
Q.Lp
80
QL.a
QL.p
120
QL.a
QL.p
160
QL.a
QL.p
200
QL.a
QL.p
220

Figure 3.3 Time-lapse imaging of QR and QL descendant migrations. Micrographs from time lapse imaging of QR (A) and QL (B) are shown, using the *casIs330* transgene (Shen, Zhang et al. 2014) (see Methods). Individual images were taken from S1 and S2 Files at the timepoints in minutes indicated in the lower right of each micrograph. Red indicates MYR::mCherry at membranes and in chromatin (HIS-24::mCherry), and green represents F-actin (MOEabd::GFP). (A) QR and descendants are indicated. Arrows point to the F-actin-rich lamellipodial protrusions that accompany polarization and anterior migration. F-actin also accumulated at the furrows between dividing cells (e.g. between QR.a and QR.p at 40min, and between QR.aa and QR.ap at 200min). (B) QL and descendant migration. Arrows point to the extensions from QL.a posteriorly over QL.p. In these time-lapse imaging experiments with the *casIs330* transgene, migrations and cell divisions were delayed by ~2-fold compared to *ayIs9* still images, but the same pattern of QL.a/p and QR.a/p migration as observed with *ayIs9* still images was conserved.

Figure 3.4

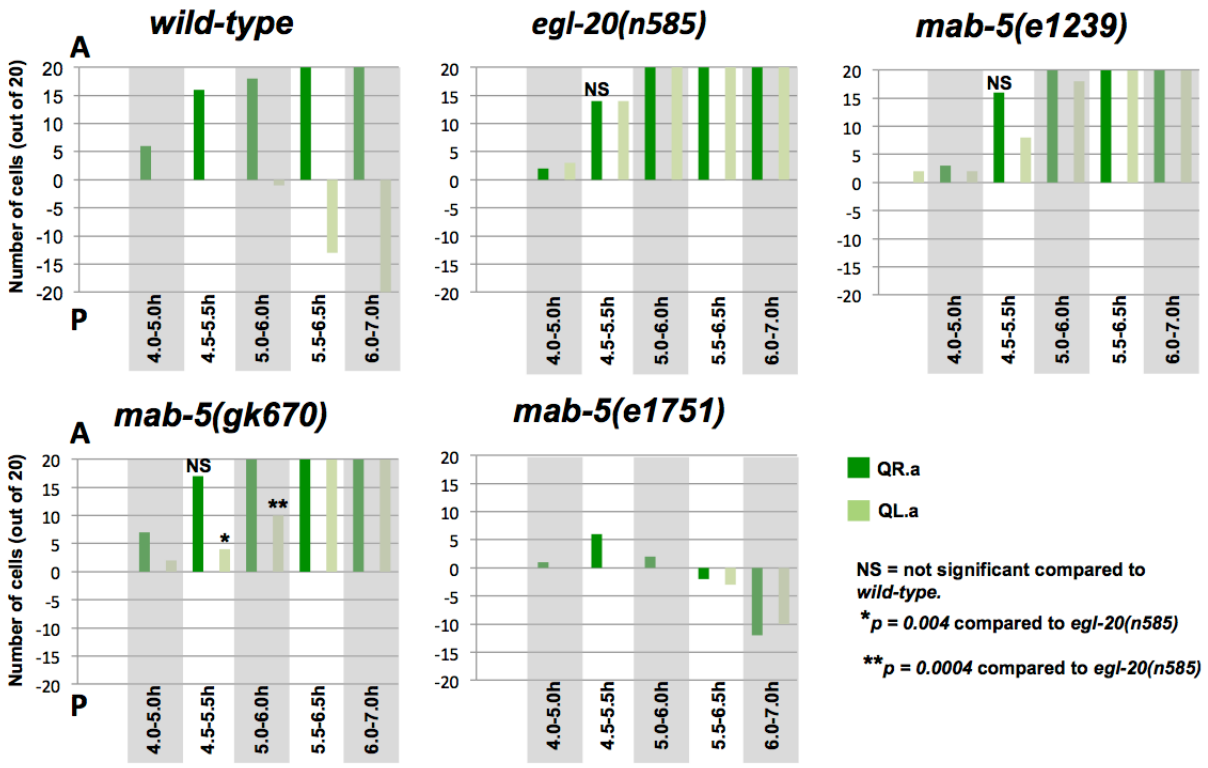
wild-type
egl-20(n585)
mab-5(e1239)
mab-5(gk670)
mab-5(e1751)
A
P
Number of cells (out of 20)
20
15
10
5
0
-5
-10
-15
-20
4.0-5.0h
4.5-5.5h
5.0-6.0h
5.5-6.5h
6.0-7.0h
NS
*
**
QR.a
QL.a
NS = not significant compared to wild-type.
*p = 0.004 compared to egl-20(n585)
**p = 0.0004 compared to egl-20(n585)

Figure 3.4 Quantitative representation of Q descendant migrations. Graphs represent Q migrations in indicated genotypes. The number (out of 20) of QR.a (dark green) and QL.a (light green) that had migrated (Y axis) at each timepoint (X axis) are indicated. Positive numbers on the Y axis represent anterior migration, and negative numbers represent posterior migration. A cell was scored a migratory if it extended an anterior lamellipodial like protrusion and separated from its sister (for anterior migration) or if it extended a posterior protrusion over its sister or migrated behind its sister (for posterior migration).

Figure 3.5

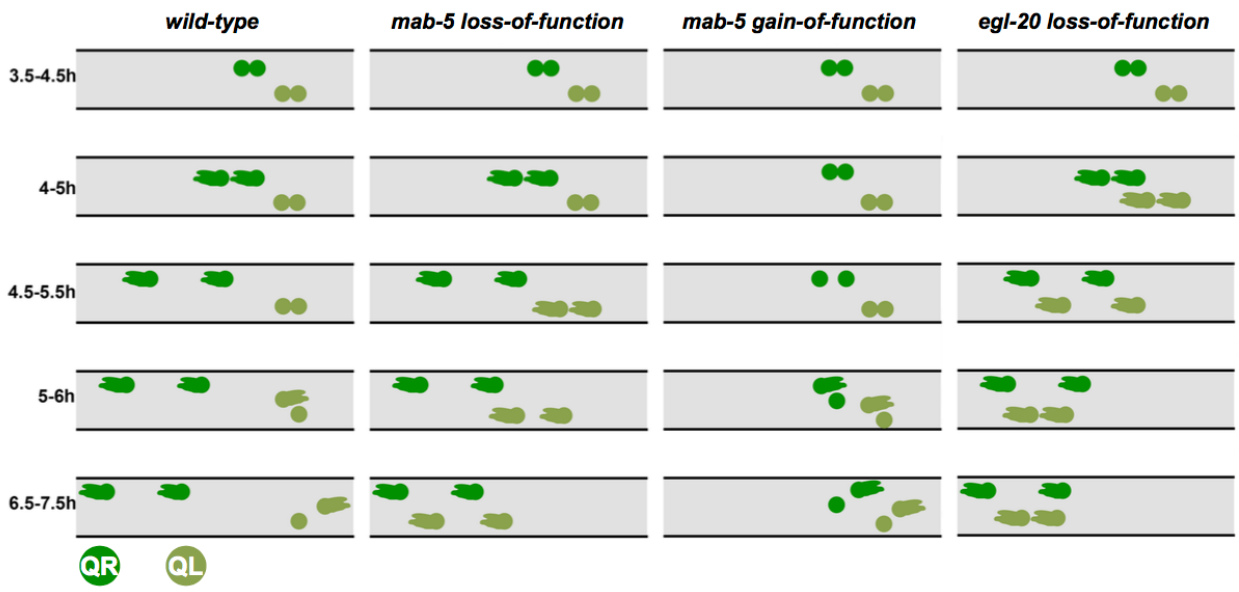
wild-type
mab-5 loss-of-function
mab-5 gain-of-function
egl-20 loss-of-function
3.5-4.5h
4-5h
4.5-5.5h
5-6h
6.5-7.5h
QR
QL

Figure 3.5 Schematic summary QR.a/p and QL.a/p migration behavior. QR.a/p are dark green and QL.a/p are light green. Genotypes and time points using *ayIs9[Pegl-17::gfp]* are indicated. QL.a/p begin anterior migration soon after division in the 4.0-5.0h timepoint, whereas QL.a/p in *mab-5* delay anterior migration until the 4.5-5.5h timepoint. Anterior is to the left.

Figure 3.6

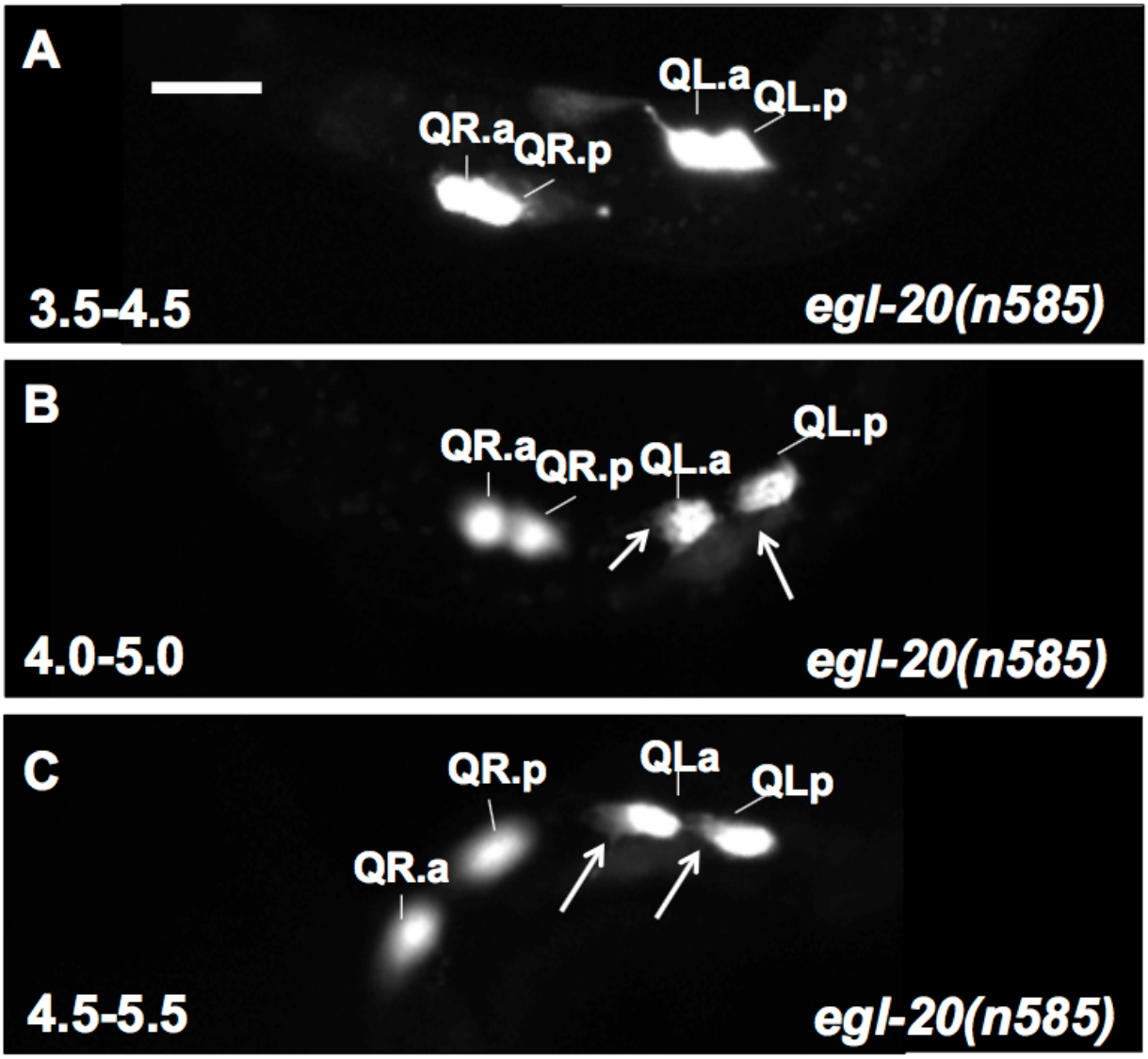
A
QL.a
QL.p
QR.a
QR.p
3.5-4.5
egl-20(n585)
B
QR.a
QR.p
QL.a
QL.p
4.0-5.0
egl-20(n585)
C
QR.p
QLa
QLp
QR.a
4.5-5.5
egl-20(n585)

Figure 3.6 Q descendant migrations in *egl-20(n585)* mutants. Fluorescent micrographs of *ayIs9[Pegl-17::gfp]* expression in Q descendants are shown. Anterior is to the left. Arrows indicate anterior protrusions characteristic of migratory morphology. QL.a has begun anterior migration before QR.a in this animal at the 4.0-5.0h timepoint. The scale bar in A represents 5μm.

Figure 3.7

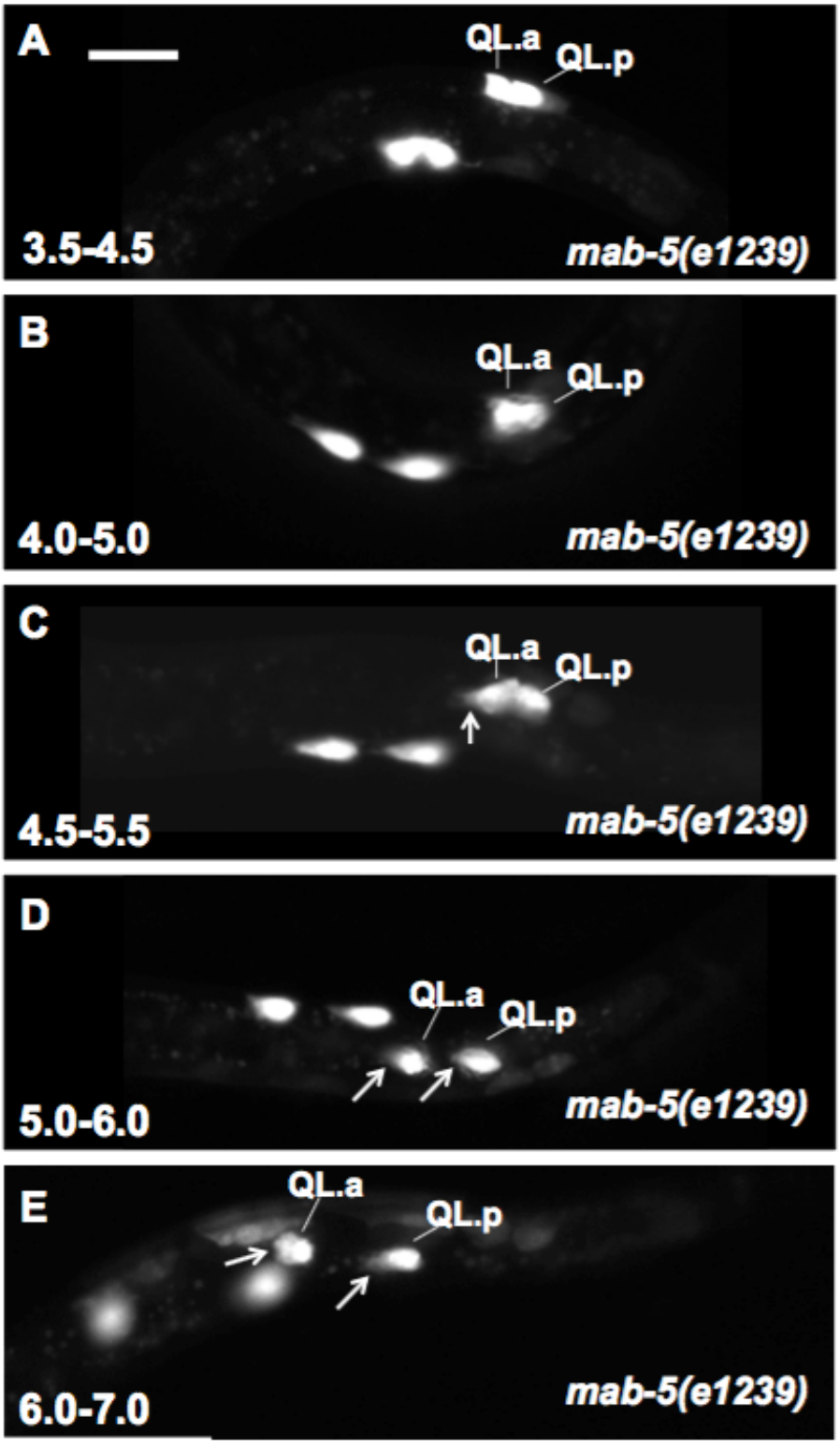
A
QL.a
QL.p
3.5-4.5
mab-5(e1239)
B
QL.a
QL.p
4.0-5.0
mab-5(e1239)
C
QL.a
QL.p
4.5-5.5
mab-5(e1239)
D
QL.a
QL.p
5.0-6.0
mab-5(e1239)
E
QL.a
QL.p
6.0-7.0
mab-5(e1239)

Figure 3.7 Q descendant migrations in *mab-5* loss-of-function. Fluorescent micrographs of *ayIs9[Pegl-17::gfp]* expression in the Q cells of *mab-5(e1239)* loss-of-function mutants are shown. At 4.0-5.0h and 4.5-5.5h, QL.a/p have not migrated, but QL.a is beginning to extend an anterior protrusion (arrow in C). Beginning at the 5.5-6.5h timepoint, both QL.a and QR.a begin posterior migration. Anterior is to the left, and the scale bar in A represents 5μm.

Figure 3.8

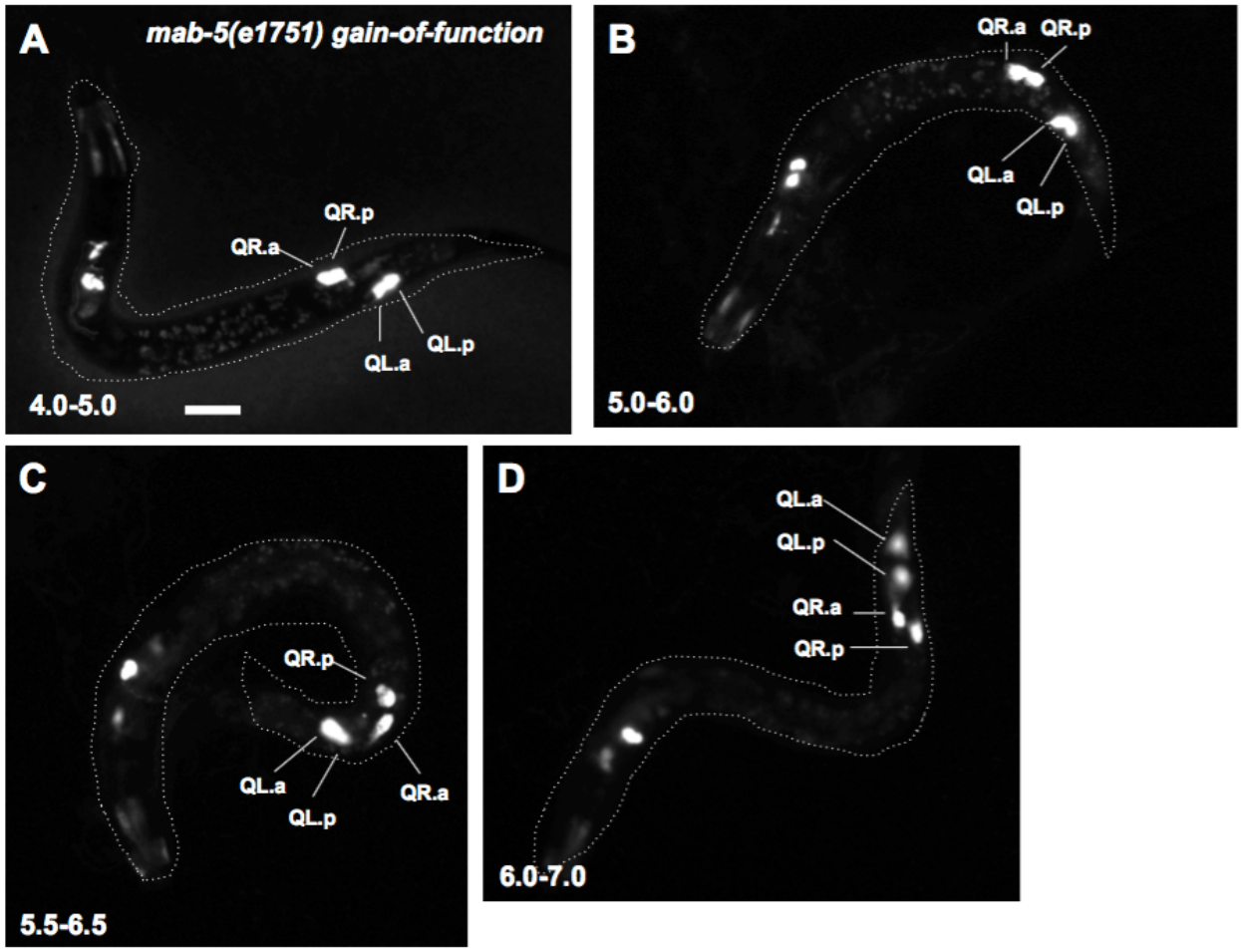
A
mab-5(e1751) gain-of-function
QR.p
QR.a
QL.p
QL.a
4.0-5.0
B
QR.a
QR.p
QL.a
QL.p
5.0-6.0
C
QR.p
QL.a
QR.a
QL.p
5.5-6.5
D
QL.a
QL.p
QR.a
QR.p
6.0-7.0

Figure 3.8 Q descendant migrations in *mab-5(e1751)* gain-of-function. Fluorescent micrographs of *ayIs9[Pegl-17::gfp]* expression in Q descendants are shown. Anterior is to the left. The dashed lines indicate the body of the whole animal in the micrograph. Both QL.a/p and QR.a/p retain a rounded, non-migratory morphology until 5.5-6.5h, when QL.a and QR.a begin posterior migration. At 6.0-7.0h, both anterior daughters have migrated posteriorly to the posterior daughters. The scale bar in A represents 5μm.

Figure 3.9

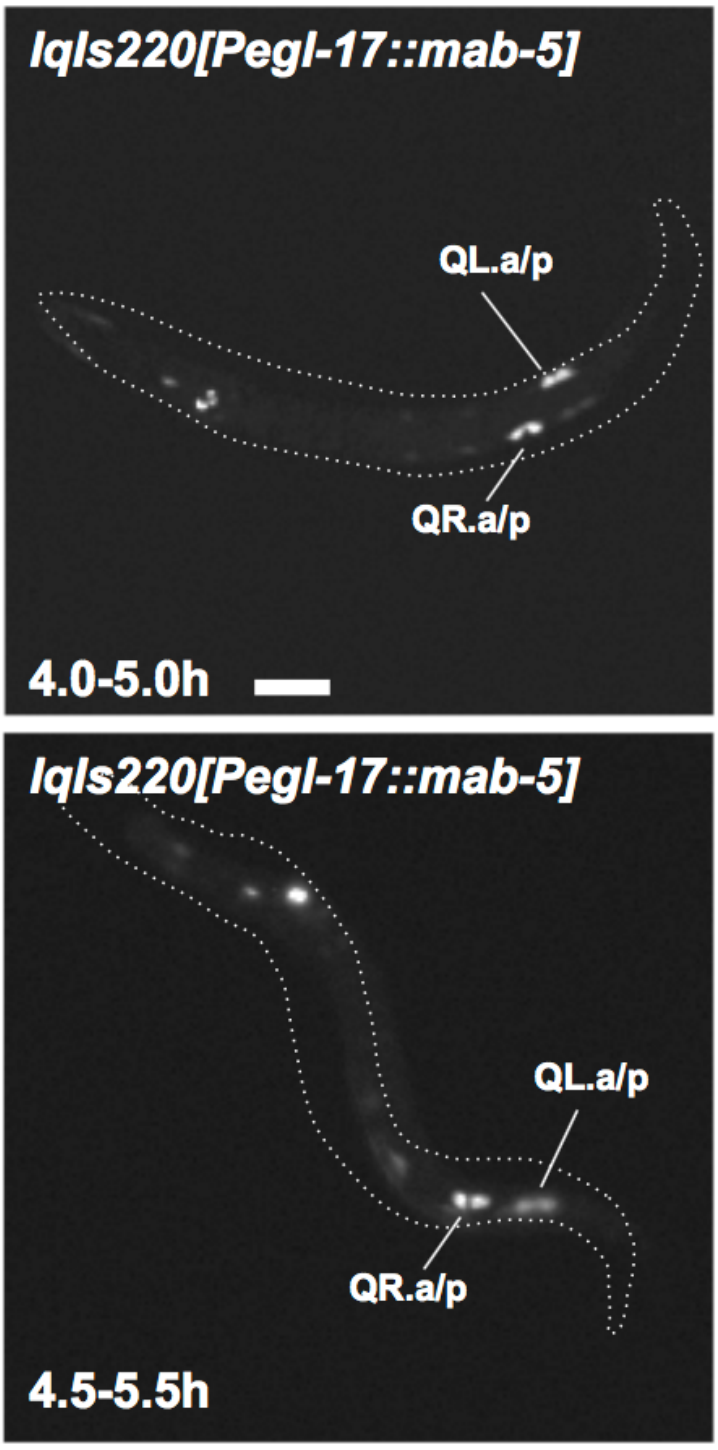
lqIs220[Pegl-17::mab-5]
QL.a/p
QR.a/p
4.0-5.0h
lqIs220[Pegl-17::mab-5]
QL.a/p
QR.a/p
4.5-5.5h

Figure 3.9 Q descendant migration in animals with transgenic *mab-5* expression in QL and QR. Fluorescent micrographs of *Pegl-17::gfp* expression in Q descendants are shown. Anterior is to the left. The dashed lines indicate the body of the whole animal in the micrograph. Both QR.a/p and QL.a/p are non migratory at the 4.5-5.5h timepoint. The scale bar represents 5μm for both micrographs.

Figure 3.10

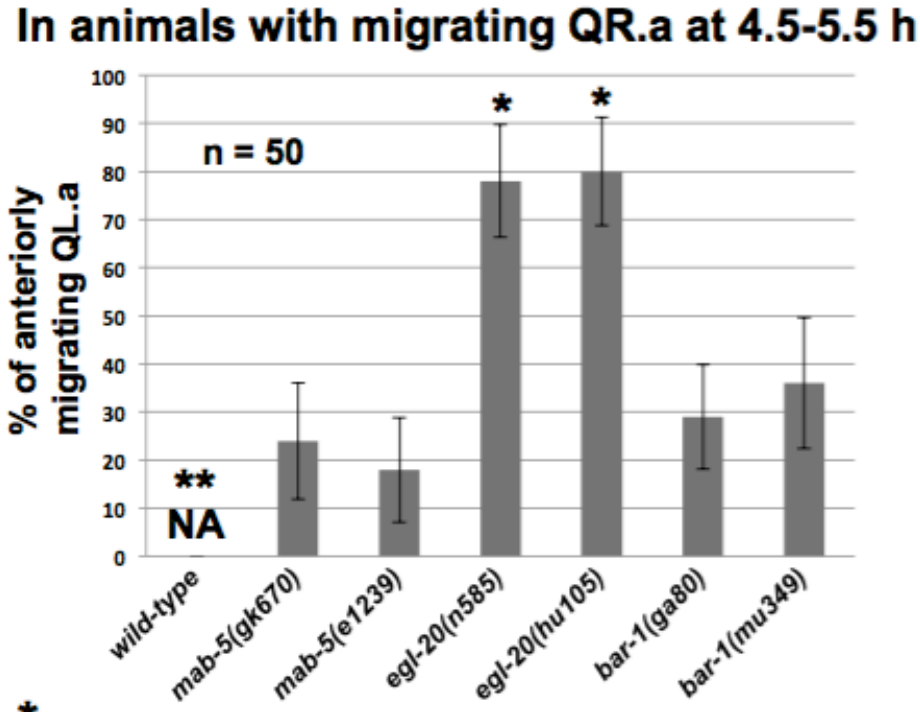

*$p < 0.0001$ compared to *mab-5(e1239* and *gk670)*, and to *bar-1(ga80* and *mu349)*

**QLa does not migrate anteriorly in *wild-type*, but 4% had started posterior migration.

Figure 3.10 QL.a/p migrate anteriorly sooner in *egl-20* than in *mab-5*. Animals from the 4.5-5.5h timepoint with migrating QR.a were analyzed for QL.a anterior migration. The percentage of animals with anteriorly-migrating QL.a (Y axis) is indicated for each genotype (X axis). In wild-type, QL.a migrated posteriorly (4%). Error bars represent 2x standard error of the proportion, and *p* values were determined using Fisher's exact test.

Figure 3.11

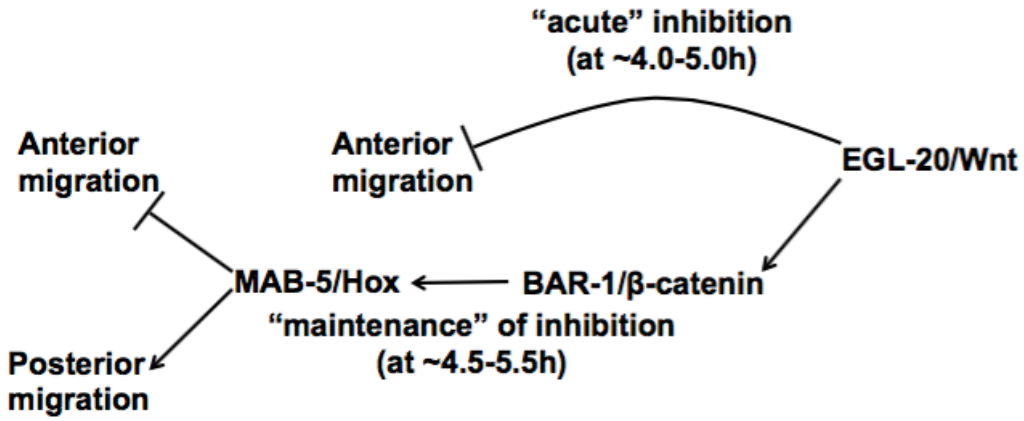
"acute" inhibition
(at ~4.0-5.0h)
Anterior
migration
Anterior
migration
EGL-20/Wnt
MAB-5/Hox
BAR-1/β-catenin
"maintenance" of inhibition
(at ~4.5-5.5h)
Posterior
migration

Figure 3.11 A model of EGL-20/Wnt and MAB-5/Hox function in QL migration. Data presented here indicate that both EGL-20/Wnt and MAB-5/Hox are required to inhibit anterior migration of QL.a/p. EGL-20 might immediately inhibit QL.a/p anterior migration via an "acute" mechanisms independent of BAR-1/β-catenin and MAB-5/Hox, as well as through a later "maintenance" phase that requires BAR-1 and MAB-5 and might require changes in gene expression. MAB-5 might also promote posterior migration.

Figure 3.S1

3.S1 File

http://journals.plos.org/plosone/article?id=10.1371/journal.pone.0148658#sec022

Division and migration of QR.a/p in wild-type. *casIs330*[*Pegl-17::myr::mCherry, Pegl-17::HIS-24::mCherry, Pegl-17:: MOEabd::GFP]* was used to image QR division and QR.a/p migrations. mCherry labeled cell membranes and chromatin (red), and GFP labeled F-actin (green). Images were acquired every 2 minutes using a spinning disk confocal microscope (Zeiss Axio Observer Z1, with Yokogawa CSU-X1 Spinning Disk Unit). Total imaging time was 200 minutes. Time-lapse imaging with *casIs330* resulted in an approximately 2-fold delay in events relative to *ayIs9* in timepoint analysis. Anterior is left, and dorsal is up.

Figure 3.S2

3.S2 File

http://journals.plos.org/plosone/article?id=10.1371/journal.pone.0148658#sec022

Division and migration of QL.a/p in wild-type. *casIs330*[*Pegl-17::myr::mCherry, Pegl-17::HIS-24::mCherry, Pegl-17:: MOEabd::GFP]* was used to image QL division and QL.a/p migrations. mCherry labels cell membranes and chromatin (red) and GFP labels F-actin (green). Images were acquired every 2 minutes using a spinning disk confocal microscope (Zeiss Axio Observer Z1, with Yokogawa CSU-X1 Spinning Disk Unit). Total imaging time was 250 minutes. Time-lapse imaging with *casIs330* resulted in an approximately 2-fold delay in events relative to *ayIs9* in timepoint analysis. Anterior is left, and dorsal is up.

Chapter IV:

The *C. elegans Neurofibromatosis Type II* homolog *nfm-1* is Non-Autonomously Required for Q neuroblast migration

4.1 Abstract

During central nervous system development, many neurons and their progenitors migrate to reach their destinations. In *Caenorhabditis elegans* the Q neuroblasts and their descendants migrate long distances in opposite directions despite being born in the same region and exposed to similar extracellular environments. QR on the right side migrates anteriorly giving rise to AQR near the head. QL migrates posteriorly giving rise to PQR near the tail. In a screen for genes required for AQR and PQR migration we identified an allele of *nfm-1* that disrupted AQR and PQR migration. *nfm-1* is homologous to vertebrate *NF2/Merlin* an important tumor suppressor in humans. Mutations in *NF2* leads to the Neurofibromatosis Type II disease, which is characterized by benign tumors of glial tissues. NFM-1/NF2 is a Four-point-one Ezrin Radixin Moesin (FERM) domain containing protein, and in vertebrates NF2 is required for epidermal integrity, and can regulate several transcriptional pathways including the Hippo pathway. Here we demonstrate that in *C. elegans, nfm-1* is required non-autonomously for complete migration of AQR and PQR. RNAi against *nfm-1* is reported as embryonic lethal, and we find that strong loss of *nfm-1* results in larval arrest consistent with *nfm-1* being required for viability. In vertebrates, *NF2* can control *Slit2* mRNA levels through the hippo pathway. We show here a genetic interaction between *nfm-1* and the *C. elegans Slit2* homolog *slt-1*. *slt-1* appears to act in parallel with *nfm-1* to promote migration of the Q descendants. Although *NF2* has been well-studied in vertebrates, this represents the first characterization of the *nfm-1/NF2* in *C. elegans*. This is also the first implication of SLT-1/Slit in controlling Q descendant migration in the anterior-posterior axis.

4.2 Introduction

A critical process in nervous system development is the directed migration of neurons to precise destinations. Directed migration is a complex process that requires integration of extracellular cues into cytoskeletal changes which guide the cell to a specific location. In *C. elegans* the Q neuroblasts are an established system to study directed cell migrations. The QR and QL neuroblasts are born in the posterior region of the worm yet migrate in opposite directions(Sulston and Horvitz 1977, Salser and Kenyon 1992, Salser, Loer et al. 1993). QL is born on the left side of the animal and migrates posteriorly over the seam cell V5 before dividing. During this initial migration QL detects a posteriorly derived EGL-20/Wnt signal which through canonical Wnt signaling initiates transcription of *mab-5/Hox* (Salser and Kenyon 1992). MAB-5 drives further posterior migration of the QL lineage, resulting in the QL.a descendant PQR migrating to the tail near the anus and posterior phasmid ganglion. QR is born on the right side of the animal and migrates anteriorly over the seam cell V5 and away from the EGL-20/Wnt signal (Salser, Loer et al. 1993, Harris, Honigberg et al. 1996, Salser and Kenyon 1996). QR does not initiate *mab-5* expression in response to Wnt and continues to migrate anteriorly. After division on top of V5, QR.a undergoes an identical pattern of cell divisions and cell death as QL.a while migrating anteriorly, with AQR completing migration near the posterior pharyngeal bulb in the head(Maloof, Whangbo et al. 1999, Whangbo and Kenyon 1999).

A forward genetic screen was previously performed in our lab to elucidate genes required for proper AQR and PQR migration. AQR and PQR because of their long distance migrations in opposite directions, with their precursors QR and QL being born in similar regions of the worm. This screen identified an allele of the *C. elegans Neurofibromatosis Type II (NF2)/Merlin*

homolog *nfm-1* that disrupted AQR and PQR migration. In *C. elegans nfm-1* has not been well studied, but RNAi against *nfm-1* results in embryonic lethality, and an *nfm-1::gfp* transgene is reported as being localized to the basolateral region of gut epithelium (Skop, Liu et al. 2004, Zhang, Abraham et al. 2011). *NF2* acts as a tumor suppressor in humans, and mutations in the gene lead to development of neurofibromatosis type II (Gusella, Ramesh et al. 1996, Gutmann, Giordano et al. 1997). Neurofibromatosis type II patients exhibit formation of benign tumors of Schwann cells that produce the myelin sheath of neurons in various parts of the brain that must be removed surgically. Genetically, neurofibromatosis type II is an autosomal dominant disorder where about half of the patients inherit mutations, and the other half contain somatic mutations (Evans, Huson et al. 1992, Narod, Parry et al. 1992, Gutmann, Giordano et al. 1997). Unlike many autosomal dominant disorders in which one mutant copy causes disease, almost all patients who inherit one mutated copy of *NF2* develop somatic *NF2* mutations in Schwann cells leading to tumor formation(Martuza and Eldridge 1988, Evans, Huson et al. 1992, Narod, Parry et al. 1992). NF2/Merlin is involved in many pathways including the hippo, mTOR and PI3K-Akt (Zhao, Wei et al. 2007, Striedinger, VandenBerg et al. 2008, James, Han et al. 2009, Okada, Wang et al. 2009). Additionally, NF2 is involved in nervous system maintenance, corpus callosum development, and axon guidance (Schulz, Baader et al. 2013, Lavado, Ware et al. 2014, Schulz, Zoch et al. 2014). In corpus callosum development *NF2* inhibits the hippo pathway, activating the transcriptional activator Yap-Taz. In mutants this inhibition is relieved and expression of SLIT2 in increased, leading to defects in midline guidance of several axons in the developing forebrain (Lavado, Ware et al. 2014).

In *C. elegans* several guidance cues have been found that control Q cell migration, and here we investigate the secreted guidance cue *slt-1/Slit*, in Q descendant migration (Hao, Yu et al. 2001, Zinovyeva, Yamamoto et al. 2008, Josephson, Chai et al. 2016). In vertebrates the *slt-1* homologs, *Slit1* and S*lit2* are required for guidance of many axons, acting through the Robo family receptors (Nguyen Ba-Charvet, Brose et al. 1999, Piper, Georgas et al. 2000, Bagri, Marin et al. 2002, Unni, Piper et al. 2012, Kim, Farmer et al. 2014). The *Slit Robo* guidance pathway is conserved in *C. elegans* where *slt-1* acts as a guidance cue for several neurons through its *Robo* receptor homolog, *sax-3/Robo(Hao, Yu et al. 2001, Chang, Adler et al. 2006, Quinn, Pfeil et al. 2006, Xu and Quinn 2012).* In general, detection of extracellular guidance cues such as *Slit* cause cytoskeletal changes that result in directed migration of cells and axonal growth cones, most typically repulsion.

Here we demonstrate that *nfm-1* is required for proper Q neuroblast descendant migrations. Furthermore we show that *nfm-1* is required non-autonomously for Q descendant migrations. We report *nfm-1* expression in the gut and posterior cells of *C. elegans*. We speculate that NFM-1 regulates the production of secreted or transmembrane cues that guide Q migrations. Additionally we identify genetic interactions between *nfm-1,* and *slt-1*. *slt-1* mutants enhance *nfm-1* mutants suggesting they may act in parallel pathways to control cell migration.

4.3 Materials and Methods

Nematode Strains and genetics

C. elegans were grown under standard conditions at 20°C on Nematode Growth Media (NGM) plates(Sulston and Brenner 1974). N2 Bristol was the wild-type strain. Some strains provided by the *Caenorhabditis* Genetics Center. Alleles used include LG III: *nfm-1(ok754), nfm-1(lq132),* LG X: *sax-3(ky123), slt-1(ok255), slt-1(eh15).* Standard gonadal injection was used to create the following extrachromosomal arrays: *lqEx773*[*nfm-1::gfp* fosmid (5ng/µL), *Pgcy::32::yfp* (50ng/µL)], *lqEx782* [*Pnfm-1::gfp* (10ng/µL), *Pgcy-32::cfp* (25ng/µL)]. Ultraviolet Trimethylpsoralen (UV/TMP) techniques (Mello and Fire 1995) were used to integrate extrachromosomal arrays to generate the following transgenes: LGII: *lqIs244* [*lqEx737, Pgcy-32::cfp* (25ng/µL)], unknown chromosomal location *lqIs247* [*lqEx773, nfm-1::gfp*], *lqIs274* [*lqEx834, Pegl-17::myr-mCherry* (20ng/µL) *Pegl-l7::mCherry::his-24* (20ng/µL)]. *nfm-1::gfp* fosmid obtained from the TransgeneOme project, clone 7039520022144752 D02 (Sarov, Schneider et al. 2006). *nfm-1(ok754)* was maintained as heterozygotes over the *hT2* balancer because homozygous animals arrest during larval stages, some animals with maternal contribution *of spon*-1 lived past the time of Q cell migration and were scored. Genotypes with M+ had maternal contribution from the *hT2* balancer.

Scoring migration of AQR and PQR

AQR and PQR migrate further than the other Q descendants. AQR migrates into the head near the posterior pharyngeal bulb, and PQR migrates posteriorly to a position near the phasmid just posterior to the anus. We used a method as described previously to score AQR and PQR position using *Pgcy-32* to drive expression of fluorophores (Shakir, Gill et al. 2006, Chapman, Li et al.

2008). We divide the worm into 5 positions. Position 1 is the wild-type position of AQR and is the region around the posterior pharyngeal bulb. Neurons anterior to the posterior pharyngeal bulb were not observed. Position 2 is posterior to position 1, but anterior to the vulva. Position 3 is the region around the vulva, position 4 is the birthplace of Q cells, and position 5 is anything posterior to the anus, the wild-type position of PQR, see Fig. 2D. A Leica DM550 equipped with YFP, CFP, GFP, and mCherry filters, was used to acquire all micrographs, and for visualization of A/PQR for scoring. Micrographs were acquired using a Qimaging Retiga camera.

Mosaic analysis.

Mosaic analysis was carried out as previously described (Chapman, Li et al. 2008, Sundararajan, Norris et al. 2014). A rescuing array was made by injecting wild-type *nfm-1* using the *nfm-1::gfp* fosmid with a *Pgcy-32::yfp* marker. This array was crossed into *nfm-1(ok754)/hT2; lqIs58 (Pgcy-32::cfp)* to create the rescuing array *lqEx773,* referred to as *nfm-1(+). nfm-1(ok754)III; nfm-1(+)* animals were viable and used for mosaic analysis. Presence of YFP in AQR or PQR indicated *nfm-1(+)* was present in those cells during their migrations. *Pgcy-32* is also expressed in URX, and presence of YFP in the URX neurons indicates other tissues have inherited *nfm-1(+).* Additionally, *nfm-1(+)* mosaic animals contained a stably inherited integrated *Pgcy-32::cfp* transgene *lqIs58*, that enabled consistent visualization of AQR and PQR regardless of presence of *nfm-1(+)* transgene. Animals that lost *nfm-1(+)* in AQR or PQR, and retained *nfm-1(+)* in the other Q descendant (PQR and AQR respectively) and URX were scored for AQR and PQR position.

Synchronization of L1 larvae for expression analysis.

L1 Animals carrying *Pnfm-1::gfp* or *nfm-1::gfp* fosmid were synchronized as described previously to the time of Q cell migration (3-5h post hatching)(Chapman, Li et al. 2008, Sundararajan and Lundquist 2012). Gravid adults were allowed to lay eggs overnight. Plates were washed with M9 buffer, and eggs remained attached to plate. Collection of hatched larvae was done every half hour using M9 washes and put onto clean NGM plates for later imaging. *Pegl-17::mCherry* was used as a Q cell marker to determine overlapping expression of *nfm-1* expression constructs.

4.4 Results

nfm-1 mutants have defective anterior migration of AQR.

To determine genes required for AQR and PQR migration an unbiased EMS forward genetic screen was previously carried out. This screen identified a new mutation with defective AQR and PQR migration, *lq132*. *lq132* animals had significant ($p<0.05$, Fisher's exact test) shortened migrations of AQR, and PQR migration (Fig. 4.2 E, F). After whole genome sequencing the *lq132* bearing line, we pursued a candidate gene approach to identify which mutation was causative for the migration phenotype of *lq132.* We found that *lq132* contained a splice-donor mutation after the fifth exon in the *nfm-1* gene (Fig. 4.2A). The *C. elegans* knock-out consortium allele *ok754* contains an in-frame 1042-bp deletion that removes exons 4,5,6, and part of exons 3 and 7, of all *nfm-1* isoforms (Fig. 4.2A,B). We find that *ok754* is maternal affect lethal with homozygous animals arresting during various larval stages, but after Q descendant migration (data not shown). *ok754* animals from a heterozygous parent had strong AQR defects, with 88% of AQR failing to migrate to the head, and occasional (1%) posterior AQR migration (Fig. 4.2C,E). *ok754* had significant PQR defects, with 15% of PQR failing to migrate into the wild-type position 5 posterior to the anus (Fig. 4.2F). To determine if *lq132* and *ok754* defects were due to *nfm-1* mutations we restored wild-type *nfm-1* using a *nfm-1* fosmid. Extrachromosomal arrays generated from this fosmid rescued *lq132* and *ok754* migration defects of AQR and PQR, indicating that mutations in *nfm-1* are likely causative for the migration deficiencies of *lq132* and *ok754* (Fig. 4.2E,F). This represents the first implication of *nfm-1* in cell migration.

nfm-1 encodes a protein similar to human NF2/Merlin (43% identity), and contains Four-Point-One Ezrin Radixin and Moesin (FERM) domains (Fig. 4.2B). The *lq132* splice donor mutation occurs after the conserved ERM domains, and may not strongly affect NFM-1 function,

explaining the weak defects of *lq132,* whereas the *ok754* in-frame deletion removes the entire FERM C domain, including the actin-binding site.

Mosaic analysis indicates *nfm-1* anterior AQR migration defects rescued through expression of *nfm-1* outside of Q cells.

Using mosaic analysis we tested whether or not *nfm-1* was required cell-autonomously. In *C. elegans,* extrachromosomal arrays are not stably inherited, and can be lost during cell divisions, creating genetically mosaic animals. We used an established strategy to score mosaic animals that had lost a *nfm-1(+)* rescuing transgene in AQR or PQR lineage (see methods, Chapman et al. 2008, and Sundararajan et. al. 2014). This strategy uses a stable *Pgcy-32::cfp* integrated transgene to visualize AQR and PQR in all animals, and an unstable array *nfm-1(+),* carrying the rescuing *nfm-1::gfp* fosmid and *Pgcy-32::yfp* (Fig. 4.3). Animals that had the *nfm-1(+)* array in AQR and PQR significantly rescued AQR and PQR (Fig. 4.2). We analyzed 89 mosaics where the *nfm-1(+)* array was lost from the AQR lineage, but retained in PQR lineage as shown in Fig. 4.3C. In these animals AQR migration defects were again rescued, suggesting that *nfm-1* is required non-autonomously for anterior AQR migration (Figs. 4.3, 4.4). o*k754* PQR migration defects were rescued in 75 mosaic animals where PQR that had lost the *nfm-1(+)* array (Fig. 4.4). Animals mosaic for *nfm-1(+)* in AQR or PQR rescued *nfm-1(ok754)* defects to a similar level as non mosaics (*nfm-1(+)* in AQR and PQR)(Fig. 4.4). Using this method there is no way to determine exactly which tissues the *nfm-1* array is present in, but based on cell lineages presence of *nfm-1(+)* array in URX and either AQR or PQR suggests it is present in many tissues (Fig 4.3A). Because there are two divisions during A/PQR migration (Fig. 4.3A), it is possible

that the *nfm-1(+)* array was present in some of A/PQR precursors during their migration. We think this is unlikely because this array was relatively stable, but we accounted for this by scoring at least 70 animals in each situation. Overall, mosaic analysis suggests that *nfm-1* acts non-autonomously in AQR and PQR migration, as loss of the rescuing array in AQR or PQR does not correlate with mutant phenotype.

***nfm-1::gfp* transcriptional and translational reporter constructs not expressed in Q cells.**

To further determine the location of function for *nfm-1* we analyzed various reporter constructs for *nfm-1.* A *Pnfm-1::gfp* transcriptional reporter was created by using the 2.1kb region upstream of *nfm-1* to drive expression of GFP. This 2.1kb region is the entire upstream region before encountering the next gene. This construct showed expression in the posterior cells near the anus, and variable expression in the hypodermis (Fig. 4.5 A-C). To examine *Pnfm-1::gfp* expression at the time of Q cell migration, *Pnfm-1* was crossed into a *Pegl-17::mCherry* line which shows cell specific expression in the Q neuroblasts. Animals carrying *Pnfm-1::gfp* and *Pegl-17::mCherry* had no overlap of mCherry and GFP fluorescence, consistent with *nfm-1* not being expressed in the Q neuroblasts during their migrations (Fig. 4.5). To determine the location of functional NFM-1 protein we visualized location of the rescuing *nfm-1::gfp* lines. When this line is crossed with the *Pegl-17::mCherry*, there is no observable GFP in the Q cells during their migration (Fig. 4.6). Some GFP signal was detected in a small region of the posterior gut near the anus, similar to the expression of *Pnfm-1::gfp*, and previous reports of gut epithelial expression of *nfm-1*(Zhang, Abraham et al. 2011). Overall the expression analysis suggests nfm-*1* being normally expressed in posterior cells, and excluded from the Q neuroblasts.

***slt-1* mutations enhance defects of *nfm-1* in anterior Q descendant migration.**

Previous work on mammalian *NF2/Merlin* has suggested that *NF2* can non-autonomously affect axon guidance in the developing mouse brain (Lavado, Ware et al. 2014). This guidance mechanism occurs through regulation of *Slit2* mRNA levels, suggesting a transcriptional role of *NF2* (Lavado, Ware et al. 2014). *Slit2* is a secreted guidance cue for developing neurons, and is detected by the Robo receptor. Because of interactions between *Slit2* and *NF2* we investigated the interaction of *nfm-1* and the *C. elegans Slit2* homolog *slt-1* in Q descendant migration. In this study we used one null allele *slt-1(eh15),* and one strong loss of function in frame deletion allele *slt-1(ok255)*(Hao, Yu et al. 2001, Steimel, Suh et al. 2013). *slt-1* had no effect on AQR and PQR migration on their own, but did show an interaction with *nfm-1*(Fig. 4.7). *nfm-1(lq132); slt-1(eh15)* double mutants displayed an enhancement of the *nfm-1(lq132)* AQR migration defects (Fig. 4.7), suggesting they work in parallel pathways to control migration. Interestingly *slt-1(eh15)* rescued the PQR migration defects of *nfm-1(lq132),* which may indicate a difference in how *slt-1* controls anterior vs posterior migration (Fig. 4.7). Next we examined the stronger *nfm-1(ok754)* allele with *slt-1*. *nfm-1(ok754) slt-1* double mutants showed a significant ($p<.05$, Fishers exact test) increase in AQR defects, from 88% AQR failing to migrate completely, to 99% and 96 % in *slt-1(eh15)* and *ok255* respectively (Fig. 4.7). This is again consistent with *slt-1* and *nfm-1* acting in parallel to guide AQR migration. Because we saw *slt-1* affected Q neuroblast migration we tested the SLT-1 receptor *sax-3/Robo.* We analyzed the strong loss of function allele *sax-3* allele *ky123* for AQR and PQR migration defects (Zallen, Yi et al. 1998). This allele showed shortened migration of AQR and PQR, with no directional defects, consistent with SAX-3 promoting migration of the Q lineages (Fig. 4.7).

4.5 Discussion

The ERM domain containing protein NFM-1 non-autonomously promotes migration of QR and QL descendants.

Complete migration of the QR and QL descendants AQR and PQR requires the coordination of many genes. Although numerous genes have been identified that act in the Q cells to promote migration, fewer have been identified that act outside the Q cells to control their migration. Of the non-autonomous genes that have been implicated in Q descendant migration, most are secreted molecules such as Wnts (Hunter, Harris et al. 1999, Whangbo and Kenyon 1999, Korswagen 2002, Pan, Howell et al. 2006), although some transmembrane genes such as CDH-4 have been demonstrated to non-autonomously affect Q cell migration (Sundararajan, Norris et al. 2014). Here we present data identifying a non-autonomous role for the ERM domain-containing gene *nfm-1* in promoting Q migration. Strong loss of *nfm-1* function results in severe AQR defects, and to a lesser extent PQR defects. These defects typically manifest as incomplete migrations, suggesting *nfm-1* does not play a role in directed migration along the anterior/posterior axis, but rather promotes the migratory capacity of these cells. NFM-1 is likely is able to bind actin through its FERM domain. Intriguingly, we see that n*fm-1* is expressed in posterior tissues including the gut, and absent from the Q cells suggesting a non-autonomous role for *nfm-1*. Using a functional *nfm-1::gfp* transgene, GFP was not observed in the Q cells, but was observed in the posterior region of the gut similar to where *Pnfm-1::gfp* was seen. Further mosaic analysis confirms that in Q cell migration, *nfm-1* acts through expression in tissues outside the Q cells. Presence of the translational reporter in the gut suggests the gut tissue may be important for Q cell migration. How *nfm-1* controls Q cell migration from other tissues, and

whether it is required specifically in the gut is quite intriguing and should be investigated in the future.

In *Drosophila,* the single FERM member *moesin* is required for maintenance of epithelial tissues during morphogenesis, and loss of FERM function results in lethality (Speck, Hughes et al. 2003). Loss of the FERM containing gene *NF2/Merlin* function in either mouse or *Drosophila* results in embryonic lethality (Fehon, Oren et al. 1997, McClatchey, Saotome et al. 1997). In *C. elegans, nfm-1* appears to be required in embryonic development similar to other animals, as RNAi against *nfm-1* is reported as embryonic lethal, no null alleles of *nfm-1* have been found, and strong loss of NFM-1 function causes larval arrest (Skop, Liu et al. 2004). Whether *nfm-1* is required for epithelial organization and gastrulation is unclear and warrants further study.

nfm-1 and _slt-1_ interact genetically to promote anterior AQR migration.

We used a candidate gene approach to determine genetic partners of *nfm-1* in *C. elegans.* Because *nfm-1* had not been characterized in *C. elegans* we turned to previous studies done in other systems. In *Drosophila* and mice, *NF2/Merlin* is known to regulate several signaling pathways, including stimulating the Hippo pathway to inhibit the Yorkie transcription cofactor (Hamaratoglu, Willecke et al. 2006, Moroishi, Park et al. 2015). In mice it has been demonstrated that loss of *NF2* in neural progenitor cells results in upregulation of Yap (Lavado, Ware et al. 2014). High Yap activity leads to ectopic levels of the secreted guidance cue *Slit2* which causes defects in midline axon guidance (Lavado, Ware et al. 2014). Interestingly this role of *NF2* is required non-autonomously for guidance, similar to our observation of *nfm-1* in *C. elegans.* The Hippo pathway in *C. elegans* is poorly conserved, and the *C. elegans* genome does

not encode a clear Yap homolog (Hilman and Gat 2011). Despite absence of Hippo family genes in *C. elegans,* we tested the *Slit2* homolog *slt-1.* Although no migration defects were detected in *slt-1* mutants, we noticed an enhancement of defects in AQR migration compared to *nfm-1(lq132)* alone. *nfm-1(lq132)* is a weak loss-of-function allele, and enhancement of *nfm-1(lq132)* defects could represent *slt-1* acts in either the same pathway, or a parallel pathway. To address this we analyzed the stronger loss-of-function *nfm-1* allele, *ok754. slt-1; nfm-1(ok754)* double mutants still showed enhancement of AQR defects compared to *nfm-1(ok754)* single mutants, consistent with *slt-1* acting in a parallel pathway to control migration. It cannot be ruled out that they act in the same pathway because *ok754* and *lq132* are both hypomorphic alleles. Complete knock-out of *nfm-1* is embryonic lethal by RNAi suggesting some function is required to reach the L1 larval stage. Complete knockout of *nfm-1* may cause defects similar to the *ok754; slt-1* doubles, which would be consistent with *slt-1* and *nfm-1* acting in the same pathway. Interestingly no enhancement of *nfm-1* PQR migration defects was seen in *slt-1; nfm-1* double mutants, and *slt-1* mutations rescued *nfm-1(lq132)* PQR defects. This suggests that *slt-1* and *nfm-1* interactions may act differently in anterior AQR migration, and posterior PQR migration. This is of note because *nfm-1* is expressed primarily in posterior tissues where PQR migrates, and away from which AQR migrates. We also tested the *slt-1* receptor *sax-3/Robo* and find that it can affect both AQR and PQR migration. Because *slt-1* null mutants alone did not disrupt migration, it is possible that SLT-1 and another unidentified molecule acts through the SAX-3 receptor to promote guidance. Alternatively SAX-3 may be important in other tissues for migration. This will be the focus of future studies.

Overall these results find a role for the tumor suppressor *nfm-1/NF2/Merlin* in migration of the *C. elegans* Q neuroblasts. Additionally this role comes from expression in tissues outside the Q cells, possibly the gut. Whether *nfm-1* can control pathways that regulate transcription like it does in vertebrates, or maintains epidermal integrity to control migration is unclear and should be investigated further. *NF2* has been well studied in vertebrates for its role in tumor suppression and epidermal integrity, and the lack of *C. elegans nfm-1* studies has been noted as a significant gap in the FERM research (McClatchey 2007). Our results demonstrate the first characterization of this gene in *C. elegans,* and suggest that NFM-1 is involved in the production of cues that guide Q migrations.

4.6 Figures

Figure 4.1

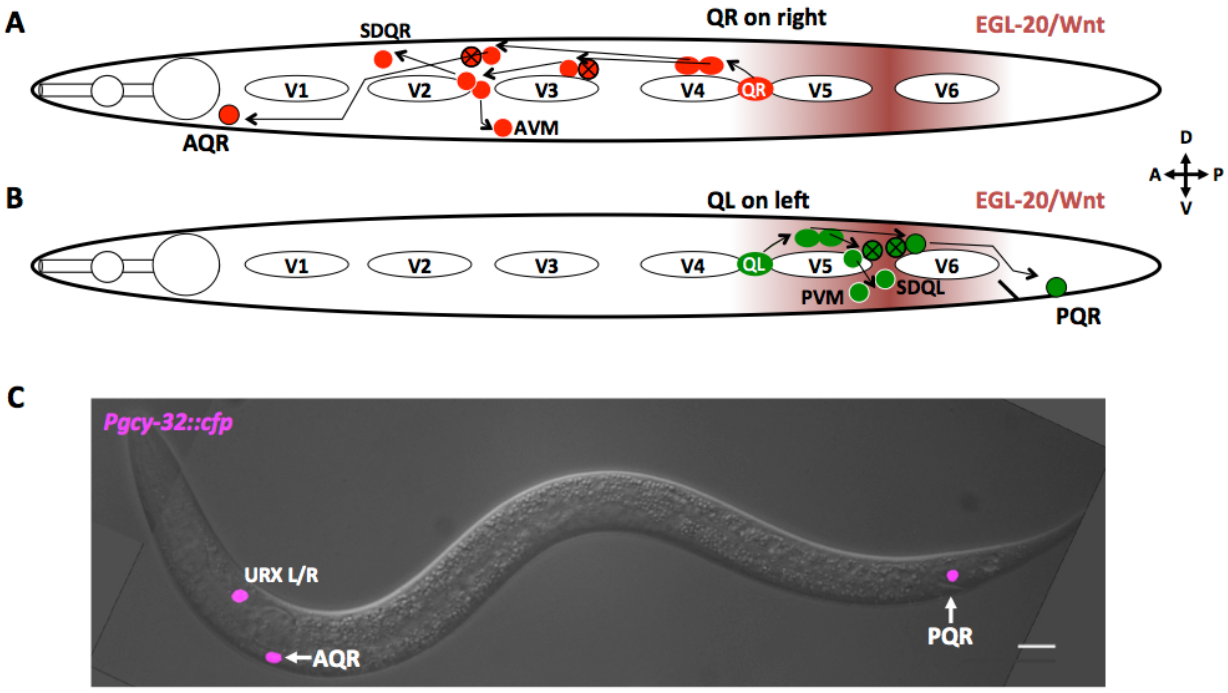

Figure 4.1 Migration of QR and QL, and position of Q descendants. A-B) Diagram representing Migration and cell division pattern of QR on the right side (A) and QL on the left side (B) in the L1 animal, showing birthplace of the Q neuroblasts, and approximate locations of the Q descendants. Maroon shading represents the posteriorly derived EGL-20/Wnt signal. White ovals are hypodermal seam cells V1-V6. Circles with black x indicate cells that undergo programmed cell death after cell division. Dorsal is up, anterior to the left. C) Merged DIC and fluorescent micrograph showing location of Q descendants AQR and PQR in adult wild-type animal. *Pgcy-32::cfp* is expressed in AQR, PQR and URXL/R. scale bar represents 10μM.

Figure 4.2

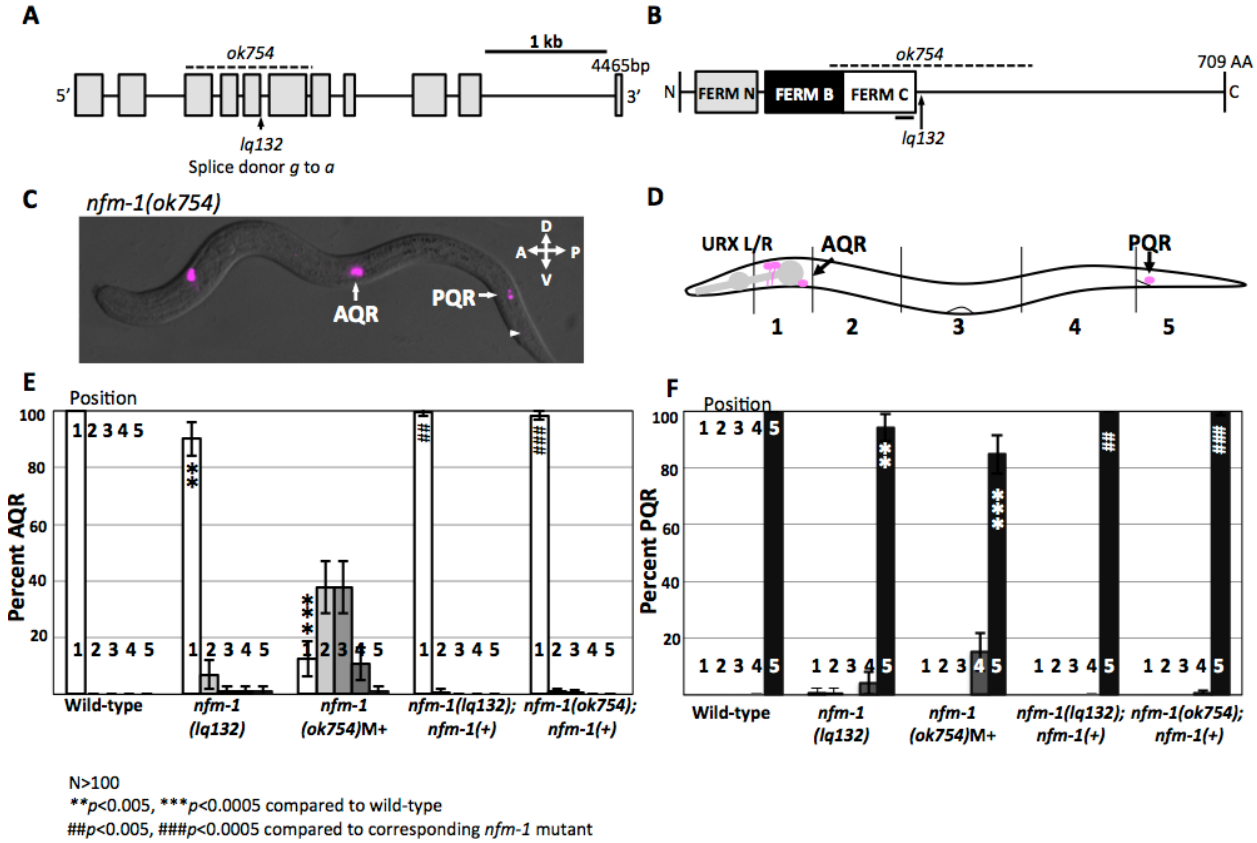

N>100
**p<0.005, ***p<0.0005 compared to wild-type
##p<0.005, ###p<0.0005 compared to corresponding *nfm-1* mutant

Figure 4.2 Position of Q descendants AQR and PQR in *nfm-1* mutants. A) *nfm-1* locus and alleles used. Drawn to scale with exons (gray squares), *ok754* deletion (dashed line), and *lq132* (arrow) noted. Scale bar represents 1kb. B) NFM-1 isoform A domain structure and allele locations. The FERM domain lobes N (gray), B (black), and C (white) are shown. Black bar under FERM C represents predicted actin-binding motif. Dashed line is *ok754* in frame deletion, and *lq132* splice donor mutation location marked by arrow. C) Merged DIC and fluorescent micrograph of *nfm-1(ok754)* mutant animal. AQR location is posterior to wild-type position, and PQR is anterior to wild-type position. PQR wild-type position noted by arrowhead. Scale bar represents 10μM. D) Diagram of scoring positions in L4 animal, with Wild-type locations of AQR and PQR shown as magenta circles. E-F) Chart showing percent of AQR (E) or PQR (F) in positions 1-5 in the adult animal. All animals unless otherwise noted were scored using *lqIs58 (Pgcy-32::cfp).* M+ indicates animals scored heterozygous parent that may have maternal contribution of *nfm-1. nfm-1(+)* animals have wild-type *nfm-1* from an array containing *nfm-1::gfp* fosmid. Asterisks indicate significant (N>100 *$p<0.05$, **$p<0.005$, ***$p<0.0005$ Fisher's exact test) difference from wild-type. Pound signs indicate, for that position, a significant (N>100 #$p<0.05$, ##$p<0.005$, ###$p<0.0005$, Fisher's exact test) rescue of corresponding *nfm-1* mutant. Error bars are 2 times the standard error of the proportion in each direction.

Figure 4.3

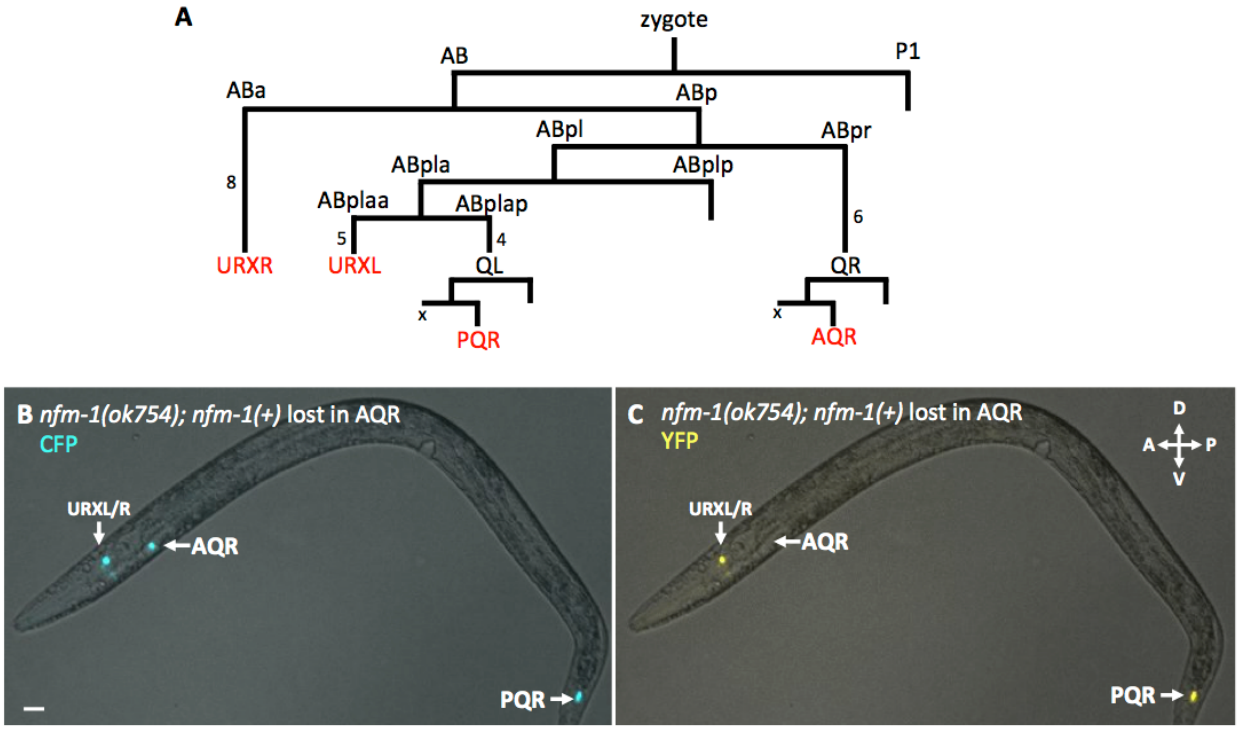
A
zygote
AB
P1
ABa
ABp
ABpl
ABpr
ABpla
ABplp
ABplaa
ABplap
8
5
4
6
URXR
URXL
QL
QR
x
x
PQR
AQR
B nfm-1(ok754); nfm-1(+) lost in AQR
CFP
URXL/R
AQR
PQR
C nfm-1(ok754); nfm-1(+) lost in AQR
YFP
URXL/R
AQR
PQR
D
A
P
V

Figure 4.3 Generation of mosaic animals for analysis. A) Lineage of cells that express *Pgcy-32.* Red names indicate cells that express *Pgcy-32.* URXL/R, QR, QL are all born in the embryo before hatching. Numbers next to lines indicate number of cell divisions not shown. X next to AQR and PQR indicates the sister of A/PQR (QL/R.aa) undergoes programmed cell death. B) Fluorescent micrograph taken with CFP filter of *nfm-1(ok754); nfm-1(+), Pgcy-32::cfp* mosaic animal with correct placement of AQR and PQR. C) Fluorescent micrograph of the same animal from B using a YFP filter. AQR is not visible in this animal indicating that somewhere in AQR lineage *nfm-1(+)* was lost. YFP is detected in URXL/R, and PQR indicating many tissues retained *nfm-1(+).* Scale bar represent 10μM.

Figure 4.4

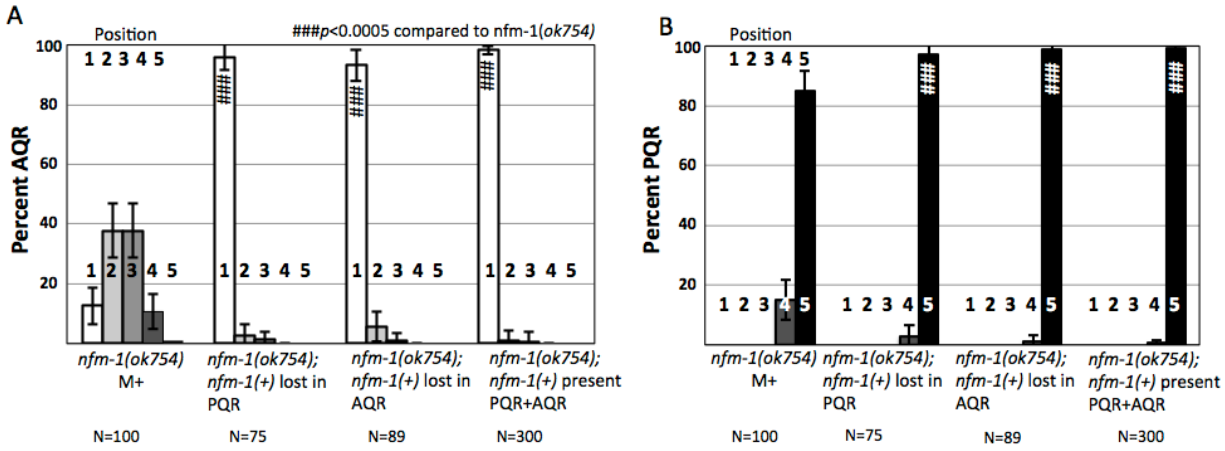
A
Position
###p<0.0005 compared to nfm-1(ok754)
Percent AQR
100
80
60
40
20
1 2 3 4 5
nfm-1(ok754) M+
nfm-1(ok754); nfm-1(+) lost in PQR
nfm-1(ok754); nfm-1(+) lost in AQR
nfm-1(ok754); nfm-1(+) present PQR+AQR
N=100
N=75
N=89
N=300
B
Position
Percent PQR
100
80
60
40
20
1 2 3 4 5
nfm-1(ok754) M+
nfm-1(ok754); nfm-1(+) lost in PQR
nfm-1(ok754); nfm-1(+) lost in AQR
nfm-1(ok754); nfm-1(+) present PQR+AQR
N=100
N=75
N=89
N=300

Figure 4.4 Analysis of *nfm-1(+)* mosaic animals. Quantification of AQR (A), and PQR (B) migration as in figure 4.2 with *nfm-1(+)* mosaic animals. *nfm-1(+)* represents presence of *nfm-1* rescuing fosmid. *nfm-1(+)* rescued *ok754* lethality, and animals were maintained as rescued homozygous *ok754* mutants. Mosaic animals have *nfm-1(+)* in URX but have lost *nfm-1(+)* in either AQR or PQR (see fig. 4.3). Pound signs indicate, for that position, a significant (N>100 #$p<0.05$, ##$p<0.005$, ###$p<0.0005$, Fisher's exact test) rescue of corresponding *nfm-1* mutant. Error bars are 2 times the standard error of the proportion in each direction.

Figure 4.5

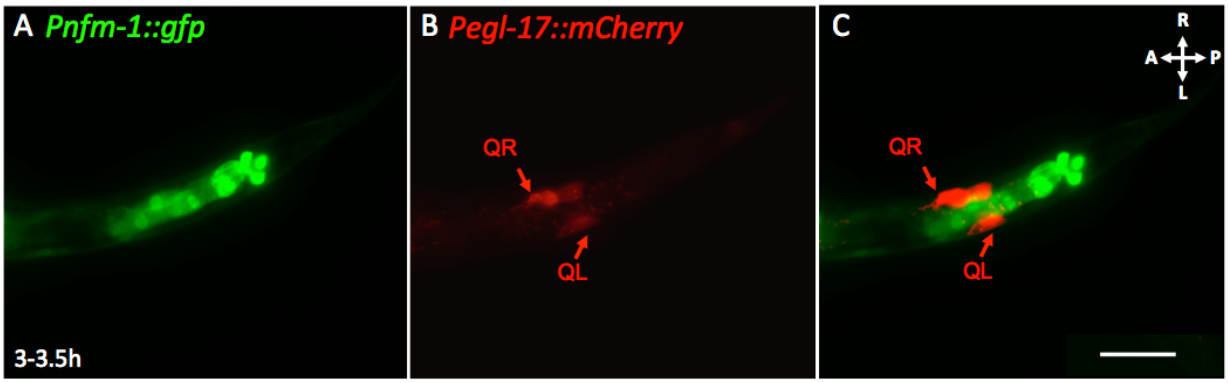

Figure 4.5 *nfm-1* transcriptional reporter not expressed in Q cells during their early migrations. A-C) *Pnfm-1::gfp; Pegl-17::mCherry* animal staged to 3-3.5h post hatching. A) GFP Micrograph showing expression of *Pnfm-1::gfp*. Expression seen in several posterior cells. B) mCherry micrograph shows Q cell specific expression during their migrations. C) merged micrograph of A and B. GFP is not observed in Q cells, but is expressed in neighboring tissues and posterior cells. Scale bar is 10μm, anterior is to the left, right is up.

Figure 4.6

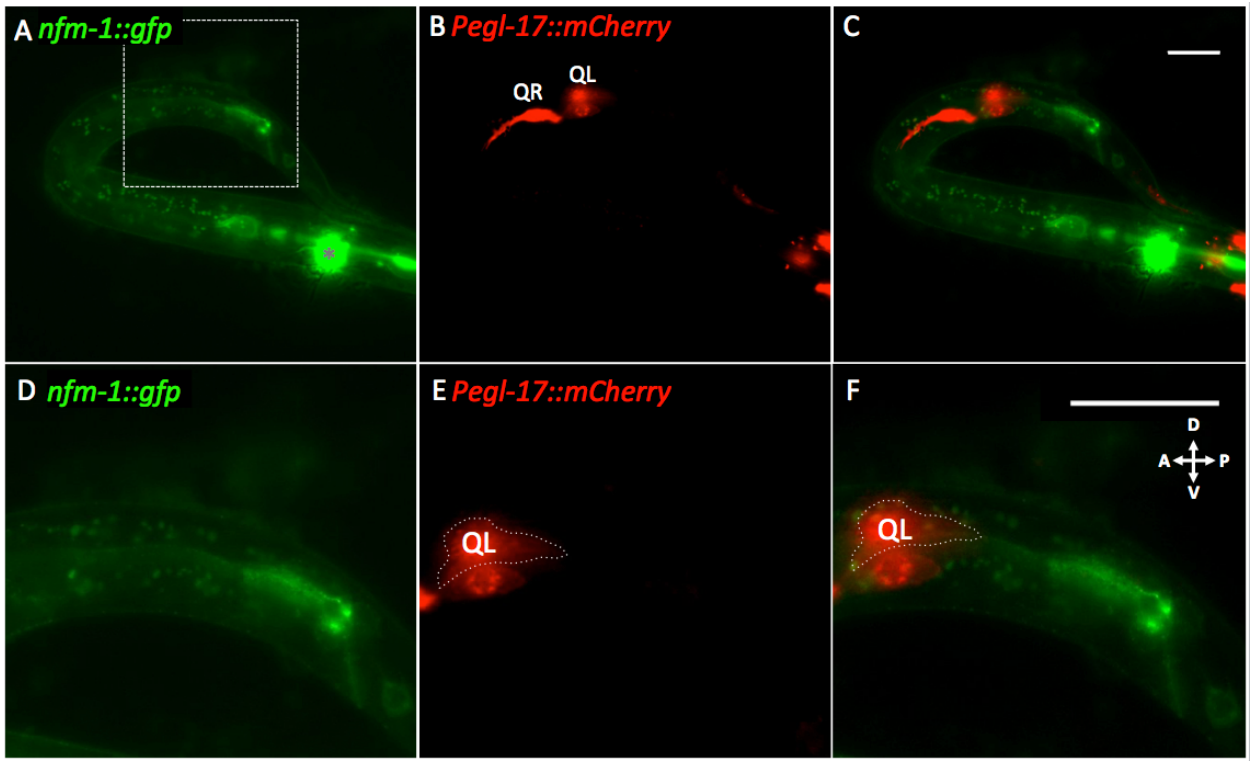
A nfm-1::gfp
B Pegl-17::mCherry
QR
QL
C
D nfm-1::gfp
E Pegl-17::mCherry
QL
F
D
A
P
V
QL

Figure 4.6 *nfm-1::gfp* translational reporter expressed in posterior and anterior gut, and excluded from Q cells. A-C) Staged 3-3-5h post hatching L1 *nfm-1::gfp; Pegl-17::mCherry* animal. A) Fluorescent micrograph of GFP expression from *nfm-1::gfp* rescuing fosmid. Asterisk marks URX expression of *Pgcy-32::yfp* that is not excluded by GFP filter. Dashed rectangle indicates enlarged section for D-F. B) *Pegl-17::mCherry*, fluorsecent micrograph showing location of early Q neuroblasts. QL is out of focus because QL and QR are on different planes, QR on the right side, and QL on left side of the animal. C) Merge of A and B. No overlap of mCherry and GFP is seen. D-F) Enlarged posterior section of A-C. Anterior is left, dorsal is up. D) Enlargement of A to show *nfm-1::gfp* present in posterior gut near the anus. E) Enlargement of B. QL outlined to distinguish it from the V5 seam cell that transiently expresses *Pegl-17.* F) Enlargement of C. Scale bars in C and F are 10 μm.

Figure 4.7

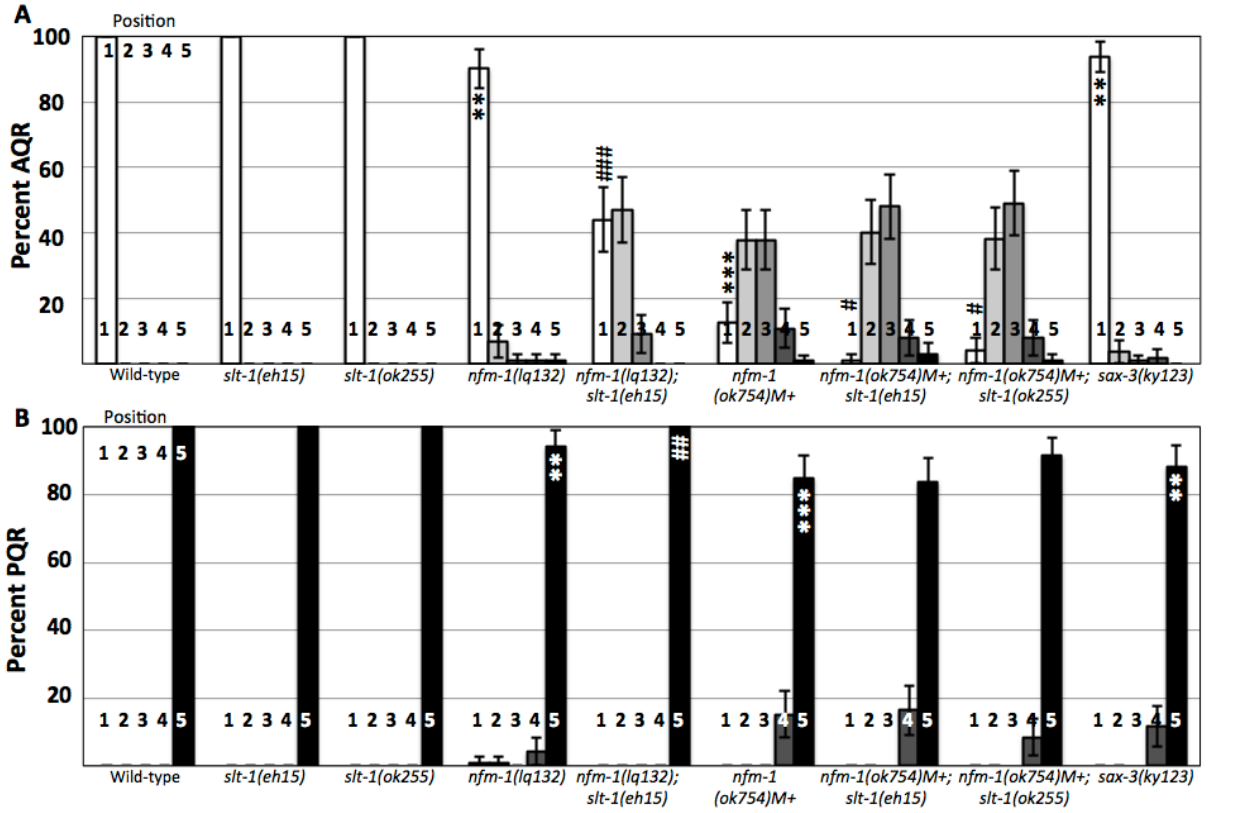

N≥100
*p<0.05, **p<0.005,***p<0.0005 compared to wild-type
#p<0.05, ##p<0.005, ###p<0.0005 compared to corresponding *nfm-1* mutant

Figure 4.7 *slt-1* enhances *nfm-1* AQR migration defects, and *slt-1* receptor *sax-3* shows defects in AQR and PQR migration. A) Percentage of AQR in each position, quantified as in Fig-2. B) Same as A, but for PQR positioning. Asterisks indicate significant (N>100 *$p<0.05$, **$p<0.005$, ***$p<0.0005$ Fisher's exact test) difference from wild-type. Pound signs indicate, for that position, a significant (N>100 #$p<0.05$, ##$p<0.005$, ###$p<0.0005$, Fisher's exact test) rescue of corresponding *nfm-1* mutant. Error bars are 2 times the standard error of the proportion in each direction..

Chapter V:

Concluding Remarks

5.1 Concluding remarks

In this dissertation I specifically examined the genes and gene networks that control migration of the Q descendants AQR and PQR. We found many genes that act outside the Q cells to control migration, and new roles for Wnt and Hox factors in migration

I began in chapter II by describing new roles for Hox factors in cell migration. I identified that the Hox factors *egl-5* and *mab-5* can promote Q neuroblast migration through expression in posterior body wall muscle. This represents a shift in how Hox genes should be considered in future studies. *mab-5* has previously been thought of as a switch in Q cell migration: Q cells that express *mab-5* go to the posterior, and those that do not express *mab-5* migrate to the anterior. Going forward I suggest that Hox genes be considered for more than their opposing autonomous roles in controlling cell fate, but also their overlapping roles in other tissues where they are expressed. Here I find that *mab-5* and other Hox genes can regulate the environment which the Q cells migrate through non-autonomous roles, and how the Q cells respond to that environment through established autonomous mechanisms. Previously an RNA-seq experiment found that MAB-5 regulates a large amount of secreted and transmembrane molecules (Tamayo, Gujar et al. 2013). I suspect that many of these secreted and transmembrane molecules are controlled by MAB-5 in posterior body wall muscle to pattern the extracellular environment to create an environment that promotes Q descendant migration.

I identify one such candidate SPON-1/F-spondin. I demonstrate that *spon-1* is required in body wall muscles for migration, and that *spon-1* promoter activity can be driven by MAB-5 in muscle cells. I suspect that the suite of extracellular genes regulated by *mab-5* and other hox genes *lin-39* and *egl-5* pattern the posterior region of the worm to promote migration. In the absence of these genes very little if any migration occurs, demonstrating their importance in this

process. I also show that *egl-5* acts non-autonomously through body wall expression to promote migration, consistent with a patterning role for EGL-5. It is likely that many genes which these transcription factors regulate are important in embryogenesis, as they have not been identified by classical genetic screens. *spon-1* is required during larval hatching and null alleles do not survive past the first larval stage, consistent with this theory. My work validates that RNA-seq experiments are an effective method to identify new genes in migration that may be required for early developmental processes, and later for migration or other developmental events. Future studies with RNA-seq could identify more of the genes regulated by Hox genes for migration and other processes.

In chapter III I find a new roles for MAB-5 and EGL-20/Wnt in inhibiting anterior migration. These roles were identified through analyzing the timing of the Q descendant migrations. In *egl-20* mutants, QL descendants begin anterior migration immediately after QL division, where in *mab-5* mutants the anterior migration of QL descendants is delayed. I show evidence that EGL-20 initially can acutely inhibit anterior migration, likely through a non-canonical, β-catenin independent mechanism, and also later promote posterior migration through canonical Wnt pathway activation of *mab-5* expression. I further characterize this to show that EGL-20/Wnt has MAB-5 dependent, and MAB-5 independent roles in inhibiting anterior migration and promoting posterior migration.

The acute MAB-5-independent role for EGL-20/Wnt in inhibiting anterior migration is immediate, and I suspect it serves as a stop signal for the QL descendants while waiting for the slower MAB-5 dependent pathway to mature. While QL descendants are stopped, canonical Wnt pathway is activated leading to expression and translation of *mab-5.* Once MAB-5 is present, it might regulate transcription of target genes which in turn must be translated and perform their

functions to promote further posterior migration of the QL lineage. In the absence of the acute EGL-20/Wnt role, QL descendants begin anterior migration immediately and fail to express MAB-5 later. Future intricate studies may be able to separate the roles of *egl-20* and determine if this hypothesis is correct. How EGL-20 acutely inhibits anterior migration is unclear, but it may bind receptors that inhibit cytoskeletal rearrangements and cellular protrusions involved in migration, processes later inhibited by MAB-5.

Chapter IV contains my investigation into the role of *nfm-1/NF2* in promoting Q cell migration. Through a forward genetic screen the Lundquist lab found an allele of *nfm-1* that was required for Q descendant migrations. Further analysis determined that *nfm-1* is required through expression outside of the Q cells, possibly the gut, for Q migration, and that *nfm-1* can interact genetically with the secreted guidance cue *slt-1/Slit. nfm-1* is homologous to human tumor suppressor *Neurofibromatosis Type II(NF2)/Merlin.* NF2 is a classic tumor suppressor that has been well studied in many systems, but this report is the first characterization of *nfm-1* in *C. elegans* (Evans, Huson et al. 1992, Gusella, Ramesh et al. 1996, Gutmann, Giordano et al. 1997, Willecke, Hamaratoglu et al. 2006, Zhao, Wei et al. 2007, Lavado, Ware et al. 2014).

I initially suspected NFM-1 would be able to regulate actin dynamics through its actin binding FERM domain to promote migration cell autonomously, however my results refute this hypothesis. How NFM-1 can regulate migration through expression in other tissues is quite intriguing, and might involve the production of cues that guide Q migrations. If NFM-1 in *C. elegans* acts similar to NF2 in other systems, NFM-1 may promote migration through regulation of a transcriptional pathway such as Hippo, mTOR, or PI3K (Schulz, Baader et al. 2013, Lavado, Ware et al. 2014, Schulz, Zoch et al. 2014, Moroishi, Park et al. 2015). The Hippo Pathway is poorly conserved or absent in *C. elegans* making this unlikely, but mTOR and PI3K pathways

are present and may be regulated by NFM-1. Alternatively NFM-1 could act to maintain epidermal integrity similar to NF2, to provide a consistent structure for cells to migrate over (Fehon, Oren et al. 1997, McClatchey, Saotome et al. 1997, Speck, Hughes et al. 2003). Studies aimed at determining the role of *nfm-1* are ongoing and are aimed at determining both the location of NFM-1 function, and the mechanism of NFM-1 in cell migration. This study should also provide valuable information to other researchers to begin study of this important molecule in *C. elegans*.

The results and discussion detailed above highlights new roles of established genes, and characterizes new genes in *C. elegans* Q cell migration. New roles for Hox and Wnt demonstrate that advances in technologies continue to facilitate genetic research, and highlight the complexities of development. We also find multiple mechanisms that act outside the Q cells to control migration. This is an important part of cell migration that often remains unstudied, what type of molecules are present in the extracellular matrix that allow for migration? Here we identify several genes important in this process and provide groundwork for studying other genes that act outside of the Q cells to create an environment amenable to migration.

References

Arenkiel, B. R., P. Tvrdik, G. O. Gaufo and M. R. Capecchi (2004). "Hoxb1 functions in both motoneurons and in tissues of the periphery to establish and maintain the proper neuronal circuitry." Genes Dev **18**(13): 1539-1552.

Azevedo, F. A., L. R. Carvalho, L. T. Grinberg, J. M. Farfel, R. E. Ferretti, R. E. Leite, W. Jacob Filho, R. Lent and S. Herculano-Houzel (2009). "Equal numbers of neuronal and nonneuronal cells make the human brain an isometrically scaled-up primate brain." J Comp Neurol **513**(5): 532-541.

Bagri, A., O. Marin, A. S. Plump, J. Mak, S. J. Pleasure, J. L. Rubenstein and M. Tessier-Lavigne (2002). "Slit proteins prevent midline crossing and determine the dorsoventral position of major axonal pathways in the mammalian forebrain." Neuron **33**(2): 233-248.

Bernadskaya, Y. Y., A. Wallace, J. Nguyen, W. A. Mohler and M. C. Soto (2012). "UNC-40/DCC, SAX-3/Robo, and VAB-1/Eph polarize F-actin during embryonic morphogenesis by regulating the WAVE/SCAR actin nucleation complex." PLoS Genet **8**(8): e1002863.

Berry, M. and A. W. Rogers (1965). "The migration of neuroblasts in the developing cerebral cortex." J Anat **99**(Pt 4): 691-709.

Boitard, M., R. Bocchi, K. Egervari, V. Petrenko, B. Viale, S. Gremaud, E. Zgraggen, P. Salmon and J. Z. Kiss (2015). "Wnt signaling regulates multipolar-to-bipolar transition of migrating neurons in the cerebral cortex." Cell Rep **10**(8): 1349-1361.

Branda, C. S. and M. J. Stern (2000). "Mechanisms controlling sex myoblast migration in Caenorhabditis elegans hermaphrodites." Dev Biol **226**(1): 137-151.

Brenner, S. (1974). "The genetics of Caenorhabditis elegans." Genetics **77**(1): 71-94.

Burstyn-Cohen, T., A. Frumkin, Y. T. Xu, S. S. Scherer and A. Klar (1998). "Accumulation of F-spondin in injured peripheral nerve promotes the outgrowth of sensory axons." J Neurosci **18**(21): 8875-8885.

Burstyn-Cohen, T., V. Tzarfaty, A. Frumkin, Y. Feinstein, E. Stoeckli and A. Klar (1999). "F-Spondin is required for accurate pathfinding of commissural axons at the floor plate." Neuron **23**(2): 233-246.

Calixto, A., D. Chelur, I. Topalidou, X. Chen and M. Chalfie (2010). "Enhanced neuronal RNAi in C. elegans using SID-1." Nat Methods **7**(7): 554-559.

Chalfie, M. and J. Sulston (1981). "Developmental genetics of the mechanosensory neurons of Caenorhabditis elegans." Dev Biol **82**(2): 358-370.

Chalfie, M., J. N. Thomson and J. E. Sulston (1983). "Induction of neuronal branching in Caenorhabditis elegans." Science **221**(4605): 61-63.

Chang, C., C. E. Adler, M. Krause, S. G. Clark, F. B. Gertler, M. Tessier-Lavigne and C. I. Bargmann (2006). "MIG-10/lamellipodin and AGE-1/PI3K promote axon guidance and outgrowth in response to slit and netrin." Curr Biol **16**(9): 854-862.

Chapman, J. O., H. Li and E. A. Lundquist (2008). "The MIG-15 NIK kinase acts cell-autonomously in neuroblast polarization and migration in C. elegans." Dev Biol **324**(2): 245-257.

Chen, L., M. Krause, B. Draper, H. Weintraub and A. Fire (1992). "Body-wall muscle formation in Caenorhabditis elegans embryos that lack the MyoD homolog hlh-1." Science **256**(5054): 240-243.

Chen, L., M. Krause, M. Sepanski and A. Fire (1994). "The Caenorhabditis elegans MYOD homologue HLH-1 is essential for proper muscle function and complete morphogenesis." Development **120**(6): 1631-1641.
Chisholm, A. (1991). "Control of cell fate in the tail region of C. elegans by the gene egl-5." Development **111**(4): 921-932.
Chow, K. L. and S. W. Emmons (1994). "HOM-C/Hox genes and four interacting loci determine the morphogenetic properties of single cells in the nematode male tail." Development **120**(9): 2579-2592.
Clandinin, T. R., W. S. Katz and P. W. Sternberg (1997). "Caenorhabditis elegans HOM-C genes regulate the response of vulval precursor cells to inductive signal." Dev Biol **182**(1): 150-161.
Clark, S. G., A. D. Chisholm and H. R. Horvitz (1993). "Control of cell fates in the central body region of C. elegans by the homeobox gene lin-39." Cell **74**(1): 43-55.
Cordes, S., C. A. Frank and G. Garriga (2006). "The C. elegans MELK ortholog PIG-1 regulates cell size asymmetry and daughter cell fate in asymmetric neuroblast divisions." Development **133**(14): 2747-2756.
Coudreuse, D. Y., G. Roel, M. C. Betist, O. Destree and H. C. Korswagen (2006). "Wnt gradient formation requires retromer function in Wnt-producing cells." Science **312**(5775): 921-924.
Cowing, D. W. and C. Kenyon (1992). "Expression of the homeotic gene mab-5 during Caenorhabditis elegans embryogenesis." Development **116**(2): 481-490.
Debby-Brafman, A., T. Burstyn-Cohen, A. Klar and C. Kalcheim (1999). "F-Spondin, expressed in somite regions avoided by neural crest cells, mediates inhibition of distinct somite domains to neural crest migration." Neuron **22**(3): 475-488.
Desai, C. and H. R. Horvitz (1989). "Caenorhabditis elegans mutants defective in the functioning of the motor neurons responsible for egg laying." Genetics **121**(4): 703-721.
Dyer, J. O., R. S. Demarco and E. A. Lundquist (2010). "Distinct roles of Rac GTPases and the UNC-73/Trio and PIX-1 Rac GTP exchange factors in neuroblast protrusion and migration in C. elegans." Small GTPases **1**(1): 44-61.
Eisenmann, D. M. (2005). "Wnt signaling." WormBook: 1-17.
Esposito, G., E. Di Schiavi, C. Bergamasco and P. Bazzicalupo (2007). "Efficient and cell specific knock-down of gene function in targeted C. elegans neurons." Gene **395**(1-2): 170-176.
Evans, D. G., S. M. Huson, D. Donnai, W. Neary, V. Blair, D. Teare, V. Newton, T. Strachan, R. Ramsden and R. Harris (1992). "A genetic study of type 2 neurofibromatosis in the United Kingdom. I. Prevalence, mutation rate, fitness, and confirmation of maternal transmission effect on severity." J Med Genet **29**(12): 841-846.
Fehon, R. G., T. Oren, D. R. LaJeunesse, T. E. Melby and B. M. McCartney (1997). "Isolation of mutations in the Drosophila homologues of the human Neurofibromatosis 2 and yeast CDC42 genes using a simple and efficient reverse-genetic method." Genetics **146**(1): 245-252.
Ferreira, H. B., Y. Zhang, C. Zhao and S. W. Emmons (1999). "Patterning of Caenorhabditis elegans posterior structures by the Abdominal-B homolog, egl-5." Dev Biol **207**(1): 215-228.
Freese, J. L., D. Pino and S. J. Pleasure (2010). "Wnt signaling in development and disease." Neurobiol Dis **38**(2): 148-153.

Gavalas, A., M. Davenne, A. Lumsden, P. Chambon and F. M. Rijli (1997). "Role of Hoxa-2 in axon pathfinding and rostral hindbrain patterning." Development **124**(19): 3693-3702.
Gleason, J. E., H. C. Korswagen and D. M. Eisenmann (2002). "Activation of Wnt signaling bypasses the requirement for RTK/Ras signaling during C. elegans vulval induction." Genes Dev **16**(10): 1281-1290.
Guo, J. and E. S. Anton (2014). "Decision making during interneuron migration in the developing cerebral cortex." Trends Cell Biol **24**(6): 342-351.
Gusella, J. F., V. Ramesh, M. MacCollin and L. B. Jacoby (1996). "Neurofibromatosis 2: loss of merlin's protective spell." Curr Opin Genet Dev **6**(1): 87-92.
Gutmann, D. H., M. J. Giordano, A. S. Fishback and A. Guha (1997). "Loss of merlin expression in sporadic meningiomas, ependymomas and schwannomas." Neurology **49**(1): 267-270.
Hafez, D. M., J. Y. Huang, J. C. Richardson, E. Masliah, D. A. Peterson and R. A. Marr (2012). "F-spondin gene transfer improves memory performance and reduces amyloid-beta levels in mice." Neuroscience **223**: 465-472.
Hamaratoglu, F., M. Willecke, M. Kango-Singh, R. Nolo, E. Hyun, C. Tao, H. Jafar-Nejad and G. Halder (2006). "The tumour-suppressor genes NF2/Merlin and Expanded act through Hippo signalling to regulate cell proliferation and apoptosis." Nat Cell Biol **8**(1): 27-36.
Hao, J. C., T. W. Yu, K. Fujisawa, J. G. Culotti, K. Gengyo-Ando, S. Mitani, G. Moulder, R. Barstead, M. Tessier-Lavigne and C. I. Bargmann (2001). "C. elegans slit acts in midline, dorsal-ventral, and anterior-posterior guidance via the SAX-3/Robo receptor." Neuron **32**(1): 25-38.
Harfe, B. D., C. S. Branda, M. Krause, M. J. Stern and A. Fire (1998). "MyoD and the specification of muscle and non-muscle fates during postembryonic development of the C. elegans mesoderm." Development **125**(13): 2479-2488.
Harris, J., L. Honigberg, N. Robinson and C. Kenyon (1996). "Neuronal cell migration in C. elegans: regulation of Hox gene expression and cell position." Development **122**(10): 3117-3131.
Herman, M. A. (2003). Wnt signaling in C. elegans. In *Wnt signaling in Development* (ed. M. Kühl), pp. 187-212. Georgetown, TX, Landes Biosciences.
Higashijima, S., A. Nose, G. Eguchi, Y. Hotta and H. Okamoto (1997). "Mindin/F-spondin family: novel ECM proteins expressed in the zebrafish embryonic axis." Dev Biol **192**(2): 211-227.
Hilman, D. and U. Gat (2011). "The evolutionary history of YAP and the hippo/YAP pathway." Mol Biol Evol **28**(8): 2403-2417.
Ho, A. and T. C. Sudhof (2004). "Binding of F-spondin to amyloid-beta precursor protein: a candidate amyloid-beta precursor protein ligand that modulates amyloid-beta precursor protein cleavage." Proc Natl Acad Sci U S A **101**(8): 2548-2553.
Hoe, H. S., D. Wessner, U. Beffert, A. G. Becker, Y. Matsuoka and G. W. Rebeck (2005). "F-spondin interaction with the apolipoprotein E receptor ApoEr2 affects processing of amyloid precursor protein." Mol Cell Biol **25**(21): 9259-9268.
Honigberg, L. and C. Kenyon (2000). "Establishment of left/right asymmetry in neuroblast migration by UNC-40/DCC, UNC-73/Trio and DPY-19 proteins in C. elegans." Development **127**(21): 4655-4668.

Hu, H., N. Xin, J. Liu, M. Liu, Z. Wang, W. Wang, Q. Zhang and J. Qi (2016). "Characterization of F-spondin in Japanese flounder (Paralichthys olivaceus) and its role in the nervous system development of teleosts." Gene **575**(2 Pt 3): 623-631.
Hunter, C. P., J. M. Harris, J. N. Maloof and C. Kenyon (1999). "Hox gene expression in a single Caenorhabditis elegans cell is regulated by a caudal homolog and intercellular signals that inhibit wnt signaling." Development **126**(4): 805-814.
James, M. F., S. Han, C. Polizzano, S. R. Plotkin, B. D. Manning, A. O. Stemmer-Rachamimov, J. F. Gusella and V. Ramesh (2009). "NF2/merlin is a novel negative regulator of mTOR complex 1, and activation of mTORC1 is associated with meningioma and schwannoma growth." Mol Cell Biol **29**(15): 4250-4261.
Ji, N., T. C. Middelkoop, R. A. Mentink, M. C. Betist, S. Tonegawa, D. Mooijman, H. C. Korswagen and A. van Oudenaarden (2013). "Feedback control of gene expression variability in the Caenorhabditis elegans Wnt pathway." Cell **155**(4): 869-880.
Josephson, M. P., Y. Chai, G. Ou and E. A. Lundquist (2016). "EGL-20/Wnt and MAB-5/Hox Act Sequentially to Inhibit Anterior Migration of Neuroblasts in C. elegans." PLoS One **11**(2): e0148658.
Kalis, A. K., D. U. Kissiov, E. S. Kolenbrander, Z. Palchick, S. Raghavan, B. J. Tetreault, E. Williams, C. M. Loer and J. R. Wolff (2014). "Patterning of sexually dimorphic neurogenesis in the caenorhabditis elegans ventral cord by Hox and TALE homeodomain transcription factors." Dev Dyn **243**(1): 159-171.
Kenyon, C. (1986). "A gene involved in the development of the posterior body region of C. elegans." Cell **46**(3): 477-487.
Kim, M., W. T. Farmer, B. Bjorke, S. A. McMahon, P. J. Fabre, F. Charron and G. S. Mastick (2014). "Pioneer midbrain longitudinal axons navigate using a balance of Netrin attraction and Slit repulsion." Neural Dev **9**: 17.
Klar, A., M. Baldassare and T. M. Jessell (1992). "F-spondin: a gene expressed at high levels in the floor plate encodes a secreted protein that promotes neural cell adhesion and neurite extension." Cell **69**(1): 95-110.
Korswagen, H. C. (2002). "Canonical and non-canonical Wnt signaling pathways in Caenorhabditis elegans: variations on a common signaling theme." Bioessays **24**(9): 801-810.
Korswagen, H. C., M. A. Herman and H. C. Clevers (2000). "Distinct beta-catenins mediate adhesion and signalling functions in C. elegans." Nature **406**(6795): 527-532.
Lavado, A., M. Ware, J. Pare and X. Cao (2014). "The tumor suppressor Nf2 regulates corpus callosum development by inhibiting the transcriptional coactivator Yap." Development **141**(21): 4182-4193.
Lei, H., T. Fukushige, W. Niu, M. Sarov, V. Reinke and M. Krause (2010). "A widespread distribution of genomic CeMyoD binding sites revealed and cross validated by ChIP-Chip and ChIP-Seq techniques." PLoS One **5**(12): e15898.
Li, X., R. P. Kulkarni, R. J. Hill and H. M. Chamberlin (2009). "HOM-C genes, Wnt signaling and axial patterning in the C. elegans posterior ventral epidermis." Dev Biol **332**(1): 156-165.
Maloof, J. N., J. Whangbo, J. M. Harris, G. D. Jongeward and C. Kenyon (1999). "A Wnt signaling pathway controls hox gene expression and neuroblast migration in C. elegans." Development **126**(1): 37-49.

Martuza, R. L. and R. Eldridge (1988). "Neurofibromatosis 2 (bilateral acoustic neurofibromatosis)." N Engl J Med **318**(11): 684-688.
McClatchey, A. I. (2007). "Neurofibromatosis." Annu Rev Pathol **2**: 191-216.
McClatchey, A. I., I. Saotome, V. Ramesh, J. F. Gusella and T. Jacks (1997). "The Nf2 tumor suppressor gene product is essential for extraembryonic development immediately prior to gastrulation." Genes Dev **11**(10): 1253-1265.
Mello, C. and A. Fire (1995). "DNA transformation." Methods Cell Biol **48**: 451-482.
Mentink, R. A., T. C. Middelkoop, L. Rella, N. Ji, C. Y. Tang, M. C. Betist, A. van Oudenaarden and H. C. Korswagen (2014). "Cell intrinsic modulation of Wnt signaling controls neuroblast migration in C. elegans." Dev Cell **31**(2): 188-201.
Middelkoop, T. C. and H. C. Korswagen (2014). "Development and migration of the C. elegans Q neuroblasts and their descendants." WormBook: 1-23.
Minevich, G., D. S. Park, D. Blankenberg, R. J. Poole and O. Hobert (2012). "CloudMap: a cloud-based pipeline for analysis of mutant genome sequences." Genetics **192**(4): 1249-1269.
Moroishi, T., H. W. Park, B. Qin, Q. Chen, Z. Meng, S. W. Plouffe, K. Taniguchi, F. X. Yu, M. Karin, D. Pan and K. L. Guan (2015). "A YAP/TAZ-induced feedback mechanism regulates Hippo pathway homeostasis." Genes Dev **29**(12): 1271-1284.
Narod, S. A., D. M. Parry, J. Parboosingh, G. M. Lenoir, M. Ruttledge, G. Fischer, R. Eldridge, R. L. Martuza, M. Frontali, J. Haines and et al. (1992). "Neurofibromatosis type 2 appears to be a genetically homogeneous disease." Am J Hum Genet **51**(3): 486-496.
Nguyen Ba-Charvet, K. T., K. Brose, V. Marillat, T. Kidd, C. S. Goodman, M. Tessier-Lavigne, C. Sotelo and A. Chedotal (1999). "Slit2-Mediated chemorepulsion and collapse of developing forebrain axons." Neuron **22**(3): 463-473.
Niu, W., Z. J. Lu, M. Zhong, M. Sarov, J. I. Murray, C. M. Brdlik, J. Janette, C. Chen, P. Alves, E. Preston, C. Slightham, L. Jiang, A. A. Hyman, S. K. Kim, R. H. Waterston, M. Gerstein, M. Snyder and V. Reinke (2011). "Diverse transcription factor binding features revealed by genome-wide ChIP-seq in C. elegans." Genome Res **21**(2): 245-254.
Okada, M., Y. Wang, S. W. Jang, X. Tang, L. M. Neri and K. Ye (2009). "Akt phosphorylation of merlin enhances its binding to phosphatidylinositols and inhibits the tumor-suppressive activities of merlin." Cancer Res **69**(9): 4043-4051.
Ou, G., N. Stuurman, M. D'Ambrosio and R. D. Vale (2010). "Polarized myosin produces unequal-size daughters during asymmetric cell division." Science **330**(6004): 677-680.
Ou, G. and R. D. Vale (2009). "Molecular signatures of cell migration in C. elegans Q neuroblasts." J Cell Biol **185**(1): 77-85.
Pan, C. L., J. E. Howell, S. G. Clark, M. Hilliard, S. Cordes, C. I. Bargmann and G. Garriga (2006). "Multiple Wnts and frizzled receptors regulate anteriorly directed cell and growth cone migrations in Caenorhabditis elegans." Dev Cell **10**(3): 367-377.
Penigault, J. B. and M. A. Felix (2011). "High sensitivity of C. elegans vulval precursor cells to the dose of posterior Wnts." Dev Biol **357**(2): 428-438.
Peterziel, H., T. Sackmann, J. Strelau, P. H. Kuhn, S. F. Lichtenthaler, K. Marom, A. Klar and K. Unsicker (2011). "F-spondin regulates neuronal survival through activation of disabled-1 in the chicken ciliary ganglion." Mol Cell Neurosci **46**(2): 483-497.
Piper, M., K. Georgas, T. Yamada and M. Little (2000). "Expression of the vertebrate Slit gene family and their putative receptors, the Robo genes, in the developing murine kidney." Mech Dev **94**(1-2): 213-217.

Quinn, C. C., D. S. Pfeil, E. Chen, E. L. Stovall, M. V. Harden, M. K. Gavin, W. C. Forrester, E. F. Ryder, M. C. Soto and W. G. Wadsworth (2006). "UNC-6/netrin and SLT-1/slit guidance cues orient axon outgrowth mediated by MIG-10/RIAM/lamellipodin." Curr Biol **16**(9): 845-853.
Rakic, P. (1972). "Mode of cell migration to the superficial layers of fetal monkey neocortex." J Comp Neurol **145**(1): 61-83.
Ruiz i Altaba, A., C. Cox, T. M. Jessell and A. Klar (1993). "Ectopic neural expression of a floor plate marker in frog embryos injected with the midline transcription factor Pintallavis." Proc Natl Acad Sci U S A **90**(17): 8268-8272.
Salser, S. J. and C. Kenyon (1992). "Activation of a C. elegans Antennapedia homologue in migrating cells controls their direction of migration." Nature **355**(6357): 255-258.
Salser, S. J. and C. Kenyon (1996). "A C. elegans Hox gene switches on, off, on and off again to regulate proliferation, differentiation and morphogenesis." Development **122**(5): 1651-1661.
Salser, S. J., C. M. Loer and C. Kenyon (1993). "Multiple HOM-C gene interactions specify cell fates in the nematode central nervous system." Genes Dev **7**(9): 1714-1724.
Sarov, M., S. Schneider, A. Pozniakovski, A. Roguev, S. Ernst, Y. Zhang, A. A. Hyman and A. F. Stewart (2006). "A recombineering pipeline for functional genomics applied to Caenorhabditis elegans." Nat Methods **3**(10): 839-844.
Schafer, S. T., J. Han, M. Pena, O. von Bohlen Und Halbach, J. Peters and F. H. Gage (2015). "The Wnt adaptor protein ATP6AP2 regulates multiple stages of adult hippocampal neurogenesis." J Neurosci **35**(12): 4983-4998.
Schulz, A., S. L. Baader, M. Niwa-Kawakita, M. J. Jung, R. Bauer, C. Garcia, A. Zoch, S. Schacke, C. Hagel, V. F. Mautner, C. O. Hanemann, X. P. Dun, D. B. Parkinson, J. Weis, J. M. Schroder, D. H. Gutmann, M. Giovannini and H. Morrison (2013). "Merlin isoform 2 in neurofibromatosis type 2-associated polyneuropathy." Nat Neurosci **16**(4): 426-433.
Schulz, A., A. Zoch and H. Morrison (2014). "A neuronal function of the tumor suppressor protein merlin." Acta Neuropathol Commun **2**: 82.
Shakir, M. A., J. S. Gill and E. A. Lundquist (2006). "Interactions of UNC-34 Enabled with Rac GTPases and the NIK kinase MIG-15 in Caenorhabditis elegans axon pathfinding and neuronal migration." Genetics **172**(2): 893-913.
Shen, Z., X. Zhang, Y. Chai, Z. Zhu, P. Yi, G. Feng, W. Li and G. Ou (2014). "Conditional knockouts generated by engineered CRISPR-Cas9 endonuclease reveal the roles of coronin in C. elegans neural development." Dev Cell **30**(5): 625-636.
Skop, A. R., H. Liu, J. Yates, 3rd, B. J. Meyer and R. Heald (2004). "Dissection of the mammalian midbody proteome reveals conserved cytokinesis mechanisms." Science **305**(5680): 61-66.
Smalley, M. J. and T. C. Dale (1999). "Wnt signalling in mammalian development and cancer." Cancer Metastasis Rev **18**(2): 215-230.
Speck, O., S. C. Hughes, N. K. Noren, R. M. Kulikauskas and R. G. Fehon (2003). "Moesin functions antagonistically to the Rho pathway to maintain epithelial integrity." Nature **421**(6918): 83-87.
Steimel, A., J. Suh, A. Hussainkhel, S. Deheshi, J. M. Grants, R. Zapf, D. G. Moerman, S. Taubert and H. Hutter (2013). "The C. elegans CDK8 Mediator module regulates axon guidance decisions in the ventral nerve cord and during dorsal axon navigation." Dev Biol **377**(2): 385-398.

Striedinger, K., S. R. VandenBerg, G. S. Baia, M. W. McDermott, D. H. Gutmann and A. Lal (2008). "The neurofibromatosis 2 tumor suppressor gene product, merlin, regulates human meningioma cell growth by signaling through YAP." Neoplasia **10**(11): 1204-1212.
Studer, M., A. Lumsden, L. Ariza-McNaughton, A. Bradley and R. Krumlauf (1996). "Altered segmental identity and abnormal migration of motor neurons in mice lacking Hoxb-1." Nature **384**(6610): 630-634.
Sulston, J. E. and S. Brenner (1974). "The DNA of Caenorhabditis elegans." Genetics **77**(1): 95-104.
Sulston, J. E. and H. R. Horvitz (1977). "Post-embryonic cell lineages of the nematode, Caenorhabditis elegans." Dev Biol **56**(1): 110-156.
Sundararajan, L. and E. A. Lundquist (2012). "Transmembrane proteins UNC-40/DCC, PTP-3/LAR, and MIG-21 control anterior-posterior neuroblast migration with left-right functional asymmetry in Caenorhabditis elegans." Genetics **192**(4): 1373-1388.
Sundararajan, L., M. L. Norris and E. A. Lundquist (2015). "SDN-1/Syndecan Acts in Parallel to the Transmembrane Molecule MIG-13 to Promote Anterior Neuroblast Migration." G3 (Bethesda).
Sundararajan, L., M. L. Norris and E. A. Lundquist (2015). "SDN-1/Syndecan Acts in Parallel to the Transmembrane Molecule MIG-13 to Promote Anterior Neuroblast Migration." G3 (Bethesda) **5**(8): 1567-1574.
Sundararajan, L., M. L. Norris, S. Schoneich, B. D. Ackley and E. A. Lundquist (2014). "The fat-like cadherin CDH-4 acts cell-non-autonomously in anterior-posterior neuroblast migration." Dev Biol **392**(2): 141-152.
Tamayo, J. V., M. Gujar, S. J. Macdonald and E. A. Lundquist (2013). "Functional transcriptomic analysis of the role of MAB-5/Hox in Q neuroblast migration in Caenorhabditis elegans." BMC Genomics **14**: 304.
Thompson, O., M. Edgley, P. Strasbourger, S. Flibotte, B. Ewing, R. Adair, V. Au, I. Chaudhry, L. Fernando, H. Hutter, A. Kieffer, J. Lau, N. Lee, A. Miller, G. Raymant, B. Shen, J. Shendure, J. Taylor, E. H. Turner, L. W. Hillier, D. G. Moerman and R. H. Waterston (2013). "The million mutation project: a new approach to genetics in Caenorhabditis elegans." Genome Res **23**(10): 1749-1762.
Tian, D., M. Diao, Y. Jiang, L. Sun, Y. Zhang, Z. Chen, S. Huang and G. Ou (2015). "Anillin Regulates Neuronal Migration and Neurite Growth by Linking RhoG to the Actin Cytoskeleton." Curr Biol **25**(9): 1135-1145.
Tzarfaty-Majar, V., R. Lopez-Alemany, Y. Feinstein, L. Gombau, O. Goldshmidt, E. Soriano, P. Munoz-Canoves and A. Klar (2001). "Plasmin-mediated release of the guidance molecule F-spondin from the extracellular matrix." J Biol Chem **276**(30): 28233-28241.
Unni, D. K., M. Piper, R. X. Moldrich, I. Gobius, S. Liu, T. Fothergill, A. L. Donahoo, J. M. Baisden, H. M. Cooper and L. J. Richards (2012). "Multiple Slits regulate the development of midline glial populations and the corpus callosum." Dev Biol **365**(1): 36-49.
Van Auken, K., D. C. Weaver, L. G. Edgar and W. B. Wood (2000). "Caenorhabditis elegans embryonic axial patterning requires two recently discovered posterior-group Hox genes." Proc Natl Acad Sci U S A **97**(9): 4499-4503.
Wagmaister, J. A., J. E. Gleason and D. M. Eisenmann (2006). "Transcriptional upregulation of the C. elegans Hox gene lin-39 during vulval cell fate specification." Mech Dev **123**(2): 135-150.

Wagmaister, J. A., G. R. Miley, C. A. Morris, J. E. Gleason, L. M. Miller, K. Kornfeld and D. M. Eisenmann (2006). "Identification of cis-regulatory elements from the C. elegans Hox gene lin-39 required for embryonic expression and for regulation by the transcription factors LIN-1, LIN-31 and LIN-39." Dev Biol **297**(2): 550-565.
Wang, B. B., M. M. Muller-Immergluck, J. Austin, N. T. Robinson, A. Chisholm and C. Kenyon (1993). "A homeotic gene cluster patterns the anteroposterior body axis of C. elegans." Cell **74**(1): 29-42.
Wang, X., F. Zhou, S. Lv, P. Yi, Z. Zhu, Y. Yang, G. Feng, W. Li and G. Ou (2013). "Transmembrane protein MIG-13 links the Wnt signaling and Hox genes to the cell polarity in neuronal migration." Proc Natl Acad Sci U S A **110**(27): 11175-11180.
Whangbo, J. and C. Kenyon (1999). "A Wnt signaling system that specifies two patterns of cell migration in C. elegans." Mol Cell **4**(5): 851-858.
White, J. G., E. Southgate, J. N. Thomson and S. Brenner (1986). "The structure of the nervous system of the nematode *Caenorhabditis elegans*." Philos. Trans. R. Soc. Lond. **314**: 1-340.
White, J. G., E. Southgate, J. N. Thomson and S. Brenner (1986). "The structure of the nervous system of the nematode Caenorhabditis elegans." Philos Trans R Soc Lond B Biol Sci **314**(1165): 1-340.
Willecke, M., F. Hamaratoglu, M. Kango-Singh, R. Udan, C. L. Chen, C. Tao, X. Zhang and G. Halder (2006). "The fat cadherin acts through the hippo tumor-suppressor pathway to regulate tissue size." Curr Biol **16**(21): 2090-2100.
Winston, W. M., C. Molodowitch and C. P. Hunter (2002). "Systemic RNAi in C. elegans requires the putative transmembrane protein SID-1." Science **295**(5564): 2456-2459.
Woo, W. M., E. C. Berry, M. L. Hudson, R. E. Swale, A. Goncharov and A. D. Chisholm (2008). "The C. elegans F-spondin family protein SPON-1 maintains cell adhesion in neural and non-neural tissues." Development **135**(16): 2747-2756.
Xu, Y. and C. C. Quinn (2012). "MIG-10 functions with ABI-1 to mediate the UNC-6 and SLT-1 axon guidance signaling pathways." PLoS Genet **8**(11): e1003054.
Yang, L., M. Sym and C. Kenyon (2005). "The roles of two C. elegans HOX co-factor orthologs in cell migration and vulva development." Development **132**(6): 1413-1428.
Yang, P. T., M. J. Lorenowicz, M. Silhankova, D. Y. Coudreuse, M. C. Betist and H. C. Korswagen (2008). "Wnt signaling requires retromer-dependent recycling of MIG-14/Wntless in Wnt-producing cells." Dev Cell **14**(1): 140-147.
Zallen, J. A., B. A. Yi and C. I. Bargmann (1998). "The conserved immunoglobulin superfamily member SAX-3/Robo directs multiple aspects of axon guidance in C. elegans." Cell **92**(2): 217-227.
Zhang, H., N. Abraham, L. A. Khan, D. H. Hall, J. T. Fleming and V. Gobel (2011). "Apicobasal domain identities of expanding tubular membranes depend on glycosphingolipid biosynthesis." Nat Cell Biol **13**(10): 1189-1201.
Zhao, B., X. Wei, W. Li, R. S. Udan, Q. Yang, J. Kim, J. Xie, T. Ikenoue, J. Yu, L. Li, P. Zheng, K. Ye, A. Chinnaiyan, G. Halder, Z. C. Lai and K. L. Guan (2007). "Inactivation of YAP oncoprotein by the Hippo pathway is involved in cell contact inhibition and tissue growth control." Genes Dev **21**(21): 2747-2761.
Zinovyeva, A. Y., Y. Yamamoto, H. Sawa and W. C. Forrester (2008). "Complex network of Wnt signaling regulates neuronal migrations during Caenorhabditis elegans development." Genetics **179**(3): 1357-1371.

Zisman, S., K. Marom, O. Avraham, L. Rinsky-Halivni, U. Gai, G. Kligun, V. Tzarfaty-Majar, T. Suzuki and A. Klar (2007). "Proteolysis and membrane capture of F-spondin generates combinatorial guidance cues from a single molecule." J Cell Biol **178**(7): 1237-1249.